NOTICE

CERTAIN DATA CONTAINED IN THIS DOCUMENT MAY BE DIFFICULT TO READ IN MICROFICHE PRODUCTS.

106
12-18-90 JS (2)

Y/DZ-687

Y-12

APPLICATION OF SEDIMENTATION MODEL TO UNIFORM AND SEGREGATED FLUIDIZED BEDS

OAK RIDGE Y-12 PLANT

MARTIN MARIETTA

James Lee Shippy, III
Development Division
Oak Ridge Y-12 Plant

Jack S. Watson
Chemical Technology Division
Oak Ridge National Laboratory

October 24, 1990

Prepared by the
Oak Ridge Y-12 Plant
Oak Ridge, Tennessee 37831
managed by
Martin Marietta Energy Systems, Inc.
for the
U. S. DEPARTMENT OF ENERGY
under contract DE-AC05-84OR21400

OPERATED BY
MARTIN MARIETTA ENERGY SYSTEMS, INC.
FOR THE UNITED STATES
DEPARTMENT OF ENERGY

Y/DZ--687

DE91 004932

ABSTRACT

Similarities between fluidization and sedimentation have been recognized for decades, and it is even common practice to estimate the solids holdup in the particulate regions of the fluidization beds using expressions developed for describing rates of particulate sedimentation. The most frequently used expression is that of Richardson and Zaki. This equation has a simple form and predicts for suspensions of uniform particles sedimentation rates that are proportional to the Stokes settling velocities at infinite dilution and proportional to the void fraction raised to an exponent between 2 and 5. The value of the exponent depends upon the Reynold's number for the settling particles. However, recent measurements have shown that this relation does not always give an accurate description of the slip velocities or the solid holdup in particulate fluidized beds. The Richardson and Zaki equation predicts slip velocities between the fluid and the particles that are usually too high; this means that the predicted solids holdup is often lower than those measured experimentally.

This paper incorporates concepts of unimodal and bimodal sedimentation to develop a model that accurately predicts bed expansion during particulate fluidization. During bed expansion a particle is considered to be fluidized not by the pure fluid, but by a slurry consisting of the pure fluid and other surrounding particles. The contributions of the other surrounding particles to the additional buoyant and drag forces are accounted for with the use of effective fluid or slurry properties, density and viscosity. As bed expansion proceeds, influences of the surrounding particles decrease; therefore, these effective properties are functions of the changing void fraction of the suspension. Furthermore, the expansion index, which empirically represents the degree to which viscous and inertial forces are present, is traditionally a function of a constant terminal Reynold's number. Because the effective fluid properties are considered to be changing as fluidization proceeds, the degree to which viscous and inertial forces also changes; therefore, the expansion index is written as a function of a local or intermediate Reynold's number. These concepts are further extended to bimodal fluidization in which small or light particles aid in the fluidization of the large or heavy particles. The results indicate that the proposed model more accurately predicts particulate bed expansion for a wider range of systems (gas - liquid, low Reynold's number - high Reynold's number) than other analytical or empirical models.

CONTENTS

LIST OF FIGURES

FIGURE PAGE

LIST OF SYMBOLS

GENERAL

C_D	drag coefficient
D_p, d	particle diameter
D	column diameter
F_g	gravitational force
g	gravitational acceleration
n	expansion index
Re	Reynold's number
V	velocity

Subscripts

f	fluid
t	terminal

SEDIMENTATION

C	solids concentration
C′	solids concentration to be used in the Ting and Luebbers equation of Shor and Watson sedimentation
K	constant
V	velocity

Subscripts

a	large particles
b	small particles
d	displacement
o	superficial

Subscripts (Continued).

s	slip
t	terminal

FLUIDIZATION

Ar	Archimedes number
a	constant used in the Al-Dibouni correlation
m	parameter in Zhang Fan correlation
n	expansion index
U	velocity
U'	bimodal fluidization step one velocity

Subscripts

eff	effective
L	large particle
LR	laminar region
mf	minimum fluidization
o	superficial
s	small particle
t	terminal
TR	turbulent region
1	lower region in Zhang Fan correlation
2	upper region in Zhang Fan correlation

GREEK

ρ	density
μ	viscosity
ε	void fraction
ϕ	sphericity

Subscripts

a,s	small particle
b,L	large particle
c	inflection point for Zhang Fan correlation
eff	effective
f	fluid
mf	minimum fluidization
p	particle
sus	suspension

Superscript

$'$	bimodal fluidization step one
$''$	bimodal fluidization step two

CHAPTER I

INTRODUCTION

Charles E. Robinson pioneered the technique of fluidization and sedimentation more than a century ago.[1] Researchers in petroleum refining, waste water treatment, chemical separations, mineral ore mining, etc. have elaborated on his efforts. Fluidizing technology has been used on a large scale since 1942. Early applications were applied to the catalytic cracking of high boiling petroleum fractions. Currently, fluidization and sedimentation technologies are being applied to an increasing number of new application; however, process design is based on past experience and a limited understanding of the fundamental relationships.[2] This study investigates one promising path to a better unified understanding of fluidization and sedimentation phenomena which are very important in much of the same process industries.

Fluidization and sedimentation both involve drag and gravitational forces acting on particles within a suspension. During fluidization of a suspension with a constant fluid flow, particles exhibit a random motion with a net vertical velocity of zero. Particles produce an additional drag on other particles and result in an apparent viscosity of the suspension greater than the viscosity of the fluid. Conversely, during sedimentation of a unimodal (uniform particle size) suspension with no applied fluid flow, the downward movement of particles has been observed to be uniform and constant.[3] Particle - particle interactions are thus limited to restrictions in flow between particles, drag effects are not influenced by direct particle - particle interactions, and the apparent viscosity affecting particles of the suspension is that of the fluid. For a multimodal suspension, this does not appear to be true.[3] Particle - particle interactions do occur as larger particles settle past the slower settling smaller particles and thus the smaller particles contribute to the apparent slurry viscosity as "seen" by the larger particles. As in fluidization, these particle interactions produce an additional drag and result in an apparent viscosity affecting particles of the suspension greater than the viscosity of the fluid.

Although fluidization and sedimentation have some differences, they can be described by similar relationships. Investigators in the past have developed models that apply to both fluidization and sedimentation; however, these models usually ignored some differences between the two phenomena. Attempts have been made by Richardson and Zaki,[4] Zhang Fan,[5] Steinour,[6] Foscolo[7] and others to model fluidized bed expansion and settling; however, their models have limited applications and are subject to error. Much of the errors exist due to a failure to account for the difference between sedimentation and fluidization.

Problems associated with the previously developed models are indicated when they under-predict fluidization velocities for liquid - solid systems[5] and over-predict fluidization velocities for gas - solid systems[8] at given void fractions. Although these models may be accurate for select cases, they do not apply over a range of systems (gas - solid, liquid - solid) and a large range of flow regimes (Reynold's Number).

The goal of this study was to extend a sedimentation model for application to fluidization. A theoretical model for sedimentation of bimodal suspensions developed by Shor and Watson[3] is used as the foundation of the research. The Shor and Watson relationship accounts for the previously mentioned apparent fluid properties and accurately predicts sedimentation velocities for bimodal suspensions. In this paper, the Shor and Watson relationship is altered to describe fluidization of unimodal suspensions. The relationship is then extended to describe fluidization of bimodal suspensions.

CHAPTER II

LITERATURE REVIEW

This study investigates both fluidization and sedimentation, and literature for both topics is reviewed. Some relationships for predicting voidages and velocities have been derived by the incorporation of effective fluid / particle properties into traditional fluidization or sedimentation equations. Others models have been derived by strictly empirical means. Both sedimentation and fluidization relationships, empirical and analytical, have contributed to the development of models that predict voidage and fluidization velocities in unimodal, as well as multimodal, beds.

TERMINAL VELOCITY

"Terminal velocity" is the rate at which a single particle will settle in a large body of quiescent fluid. A particle allowed to free fall will accelerate and reach its terminal velocity when the drag forces exerted on the particle by the fluid (gas or liquid) are balanced by the gravitational/buoyant forces.

$$\text{effective gravitational force} = \text{drag} + \text{buoyancy forces}$$

Settling of a single particle can be categorized by three regions: Stokes (or creeping flow), intermediate (or transition), and inertial. The region which best describes a particle's settling phenomena depends on the Reynold's number, the ratio of the inertial to the viscous forces. Particles in the Stokes region are characterized by relatively low or creeping flow conditions. Inertial effects from the fluid accelerating around the particle are not significant and viscous forces predominate. Particles in the inertial region are characterized by relatively high settling rates and large particle diameters. In this region the fluid accelerates rapidly around the particle's outer surface contributing to inertial effects. Viscous forces are less significant. Particles in the intermediate region, as expected, exhibit both inertial and viscous effects, characterizing the transition between the Stokes and inertial region. A plot of drag coefficient versus Reynold's number shows that the Stokes region exists below a Reynold's number of 0.3, the intermediate region exists between Reynold's numbers of 0.3 and 1000, and the inertial region exists above a Reynold's number of 1000.[9]

Because different fluid dynamic forces are more important in certain regions than in others, there must exist three separate relationships to describe the terminal velocity. These three relationships have been developed to describe settling in the separate regions in terms of the drag coefficient for spherical particles.[9]

$$V_t = [4gD_p(\rho_p-\rho_f)/(3\rho_f C_D)]^{1/2} \tag{1}$$

where

g = gravitational acceleration

D_p = particle diameter

ρ_p = particle density

ρ_f = fluid density

C_D = drag coefficient

The drag coefficient for the Stokes region is given by

$$C_D = 24/Re_t \tag{2}$$

Substituting equation 2 into 1 results in the terminal velocity for a particle in the Stokes region.

$$V_t = D_p^2(\rho_p-\rho_f)g/(18\mu_f) \tag{3}$$

where

μ_f = fluid viscosity

Similarly, for the intermediate region, the drag coefficient is approximately

$$C_D = 18.5/Re_t^{0.6} \tag{4}$$

Substitution of equation 4 into 1 yields the terminal settling velocity for a single particle in the intermediate or transition region.

$$V_t = (0.0721gD_p^{1.6}(\rho_p-\rho_f)/(\mu_f^{0.6}\rho_f^{0.4}))^{0.7143} \qquad (5)$$

Finally, the drag coefficient for the inertial region remains approximately constant at 0.44. As a result the terminal velocity in this region is defined as

$$V_t = 1.74(gD_p(\rho_p-\rho_f)/\rho_f)^{1/2} \qquad (6)$$

SEDIMENTATION

Sedimentation is characterized by the downward movement of particles of a suspension relative to a stationary container. In dilute systems, the settling rate will approach the terminal velocity. Settling rates in more concentrated systems will be slowed by the presence of other particles; this is often called "hindered settling." The "hindering" in concentrated systems results from two effects. First, the drag is increased because near-by particles constrict the flow field around a particle and increase the velocity gradient. Second, the settling particles displace fluid, and there is a net upward fluid velocity equivalent to the volumetric downward flow of the settling particles. Unimodal suspensions appear to settle with little particle - particle contact.[3] The settling particles are affected by the upward fluid flow, the density of the suspension, and the hindered flow between particles. In most difficult sedimentation cases inertial effects are more likely to be negligible and viscous effects are more likely to be predominate. During sedimentation of bimodal suspension, the faster settling particles descend past other slower settling particles as well as displace fluid. As a result, these faster settling particles are affected by both the fluid and the presence of the smaller particles.

Unimodal Sedimentation

Robinson, in 1926, investigated settling velocities of suspensions of very small particles in a viscous fluid.[10] He modified Stoke's Law[11] to predict the settling rate, V_o, of fine uniformly sized particles.

$$V_o = D_p^2 K(\rho_p - \rho_{sus}) g / \mu_{sus} \qquad (7)$$

where

K = constant

ρ_{sus} = average density of suspension

μ_{sus} = viscosity of suspension

This equation yields a settling rate as a function of the suspension viscosity and density. He assumed that the settling particles are affected more by a slurry of particles than by the pure fluid; therefore, the driving force for settling is not the difference between the particle and fluid specific gravity, but the difference between the particle and slurry specific gravity.

Steinour, in 1944, adapted the equation for the effective gravitational force of a single particle in an infinite medium to compensate for the effects of concentration in a suspension.[6]

$$F_g = \pi D_p^3(\rho_p - \rho_{sus})g\phi\varepsilon/6 \tag{8}$$

where

ε = void fraction

ϕ = sphericity

Phi (ϕ) was inserted into the equation to account for the geometry and size of the spaces available for fluid flow. Inserting this relation into Stoke's Law yields the following slip velocity, or, the velocity of the particle relative to the fluid.

$$V_s = D_p^2(\rho_p - \rho_{sus})g\phi\varepsilon/(18\mu_f) \tag{9}$$

Since the free space available for flow is ε, the fluid velocity around the particles relative to the wall is:

$$V_o(1-\varepsilon)/\varepsilon$$

$$V_s = V_o + V_o(1-\varepsilon)/\varepsilon = V_o/\varepsilon \tag{10}$$

$$\rho_p - \rho_{sus} = \rho_p - (\rho_p(1-\varepsilon) + \rho_f\varepsilon) = \varepsilon(\rho_p - \rho_f) \tag{11}$$

Steinour performed experiments with tapioca in oil, applied the above relationships, and arrived at the following conclusion.

$$\phi\varepsilon = 10^{-1.82(1-\varepsilon)} \tag{12}$$

Therefore,

$$V_o = \varepsilon^2 D_p^2(\rho_p - \rho_f) g 10^{-1.82(1-\varepsilon)}/(18\mu_f) \tag{13}$$

where

V_c = superficial settling velocity

Although Steinour's approach has logic, his expression for $\phi\varepsilon$ is largely empirical. It applies only to sedimentation and is limited to unimodal suspensions.

In 1954 Richardson and Zaki derived a relationship for superficial fluid velocity which has been applied to both fluidization and sedimentation.[4]

$$V_o = V_t \varepsilon^n \tag{14}$$

where

V_t = terminal settling velocity

$n = 4.65 + 19.5d/D$	$Re_t < 0.2$	(15)
$n = (4.35 + 17.5d/D)Re_t^{-0.03}$	$0.2 < Re_t < 1.0$	(16)
$n = (4.45 + 18d/D)Re_t^{-0.1}$	$1.0 < Re_t < 200$	(17)
$n = 4.45Re_t^{-0.1}$	$200 < Re_t < 500$	(18)
$n = 2.39$	$500 < Re_t$	(19)

This equation can be easily manipulated and substituted into material balance relations to yield various other useful forms of the Richardson and Zaki model. Slip velocity is defined as the velocity of the particle relative to the fluid. Therefore, if the particle's net movement is zero, then the slip velocity is the sum of the superficial inlet fluid velocity (V_o) and the displaced fluid velocity (V_d).

$$V_s = V_o + V_d \tag{20}$$

Substituting the Richardson and Zaki equation into equation 20 yields the following.

$$V_s = V_t \varepsilon^n + V_d \tag{21}$$

Solving a material balance on a finite section of a fluidization column,

$$V_d \varepsilon = (1-\varepsilon) V_o \tag{22}$$

$$V_d = (1-\varepsilon) V_o / \varepsilon \tag{23}$$

Substituting the original form Richardson and Zaki equation into equation 18,

$$V_d = (1-\varepsilon) \varepsilon^n V_t / \varepsilon \tag{24}$$

Finally, substituting equation 24 into equation 21, and rearranging results in an equation for slip velocity as a function of void fraction and terminal settling velocity.

$$V_s = V_t\varepsilon^n + V_t\varepsilon^n(1-\varepsilon)/\varepsilon \qquad (25)$$

$$V_s = V_t\varepsilon^n(1+(1-\varepsilon)/\varepsilon) \qquad (26)$$

$$V_s/V_t = \varepsilon^n(1/\varepsilon) \qquad (27)$$

$$V_s/V_t = \varepsilon^{(n-1)} \qquad (28)$$

Equations 14 and 28 are very effective for predicting settling rates in unimodal liquid systems. Furthermore, when combined with equations 15 - 19, equations 14 and 28 yield reasonably good predictions for a number of different unimodal systems. However, the model does not accurately predict settling velocities for bimodal systems. This is because the model was developed based on particle behavior in the presence of a pure fluid. In unimodal sedimentation, the settling particles appear to descend uniformly and without significant particle - particle interactions; therefore, the drag associated with a settling particle results from the fluid - particle contact. Significant interactions with other surrounding particles would greatly influence the drag on a suspended particle.

Bimodal Sedimentation

In 1979, Mirza and Richardson applied the Richardson and Zaki equation to bimodal suspensions and developed an equation to predict the settling velocity of the larger particles as they descend and displace smaller particles.[12]

$$V_{oa} = V_{ta}(\varepsilon^{n-1})(1-C_a) - V_{tb}(\varepsilon^{n-1})(C_b) \qquad (29)$$

where

V_{oa} = settling velocity of large particles

V_{ta} = terminal velocity of large particles

V_{tb} = terminal velocity of small particles

C_a = solid concentration of large particles

C_b = solid concentration of small particles

This relationship is a result of a material balance between the settling particles and the displaced fluid. Although this was an improvement since it took into account, by a material balance, the displaced fluid as well as the displaced smaller particles, there appear to be other factors which influence the settling rate of the larger particles. The equation tended to over-predict settling rates for the larger particles.

During sedimentation of bimodal suspensions, the settling particles appear to be influenced by their movement relative to the other particles. The drag on a settling particle is due, not only to the displaced fluid, but to the displaced particles. Consequently, the Richardson and Zaki equation applied to bimodal systems over-predicts settling velocities. That is, the Richardson and Zaki model does not account for particles - particle interaction or hinderance during settling.

In 1983, Selim modified the Mirza and Richardson equation by incorporating an effective density of a slurry to account for hindered settling.[13] The fluid density is redefined to reflect its effect on the larger settling particles; therefore, the effective density is written as a weighted volume average concentration of the fluid and the smaller particles as if the larger particles were not present.

$$\rho_{eff} = (\rho_b C_b + \rho_f \varepsilon)/(1-C_a) \tag{30}$$

where

ρ_b = density of small particles

The density of the fluid in the Stokes equation becomes the density of a slurry.

$$V_t = D_p^2(\rho_p - \rho_{eff})g/(18\mu_f) \tag{31}$$

where

ρ_p = density of the settling particle

ρ_{eff} = effective density of the settling slurry

This is a notable improvement to the original Mirza and Richardson equation and gives excellent prediction of available bimodal settling data, but its unequal account for buoyant force contributions by all the particles doesn't look theoretically sound. The pressure gradient across a suspension is equivalent to the effective density and all particles contribute to the effective pressure. In other words, all particles contribute to the effective buoyant force which oppose the gravitational force. In addition, Selim's relationship is inaccurate for bimodal suspension of closely sized particles. It does not quantitatively account for the difference in particle density or size; therefore, it treats bimodal systems with larger differences in particle sizes the same way it treats systems small differences in particle sizes. Consequently, application of the Selim relationship to a suspension of a continuous distribution would yield inaccurate results.

In 1990, Shor and Watson proposed to modify the Mirza and Richardson model in a different manner by incorporating an effective viscosity into the terminal settling velocity equation.[3] This was done as an alternative to the density correction proposed by Selim in order to account for the hindered settling of bimodal suspensions. They assumed that the effective density came from all particles and its effects were already incorporated in the Richardson and Zaki equation for unimodal systems. The resulting terminal velocity may be written as

$$V_{ta} = D_p^2(\rho_a - \rho_f)g/(18\mu_{eff}) \tag{32}$$

where

ρ_a = density of large particle

μ_{eff} = effective viscosity of slurry

In 1911 Einstein derived a equation for the viscosity of a suspension as a function of the fluid viscosity and the solids fraction.[14] Unfortunately, this relationship holds only for dilute stages of sedimentation.

$$\mu_{eff} = \mu_f(1+2.5C) \tag{33}$$

where

C = volume fraction of solids

At large void fractions ($0.9 < \varepsilon < 1.0$), the solids concentration is approximately zero and the effective viscosity of the suspension approaches the actual fluid viscosity. However, this equation indicates that the effective viscosity dependence on solids concentration is linear over the entire solid concentrations range. This is not the case for void fractions approaching minimum fluidization and ultimately at static bed conditions. At void fraction nearing the static bed voidage, the slurry appears more rigid and the viscosity should approach infinity.

Ting and Luebbers in 1957 developed a similar relationship for viscosity accurate over a much wider range of solid fractions.[15]

$$\mu_{eff} = \mu_f(0.464+0.21C)/(0.464-0.78C) \tag{34}$$

In dilute sedimentation there is little difference between this and the Einstein relationship. Both equations appear linear with a slope of 2.5. The distinction between the two relationships arises at large solid fraction. As the solid concentration approaches a value of 0.595, an approximate solids concentration for a settled bed of spheres, the denominator of the Ting and Luebbers equation approaches zero and effective viscosity approaches infinity. The result is a semiemperical equation that accurately describes the effective slurry viscosity over a much broader range of solid fractions.

Shor and Watson chose to incorporated the Ting and Luebbers correlation to represent the effective viscosity of the suspension. The large particles are expected to have little effect on the slurry viscosity, but the smaller particles are expected to have significant effects on the slurry viscosity. As a result, Shor and Watson proposed that the contribution of each size fraction is a function of the relative motion between the large and small particles. The solids concentration is thus defined to account for the relative contributions of the different size particles to the slurry viscosity; therefore, the solids concentration for use in the Ting and Luebbers equations is written as follows.

$$C_b' = C_b(1-V_{tb}/V_{ta}) \tag{35}$$

Shor and Watson incorporated the Ting and Luebbers correlation with the effective solids concentration into the equation for terminal velocity in the Stokes region to arrive at a slight modification of the Mirza and Richardson relationship.

$$V_{oa} = V_{ta}(\mu_\ell/\mu_{eff})(\varepsilon^{n-1})(1-C_a) - V_{tb}(\varepsilon^{n-1})C_b \tag{36}$$

Comparison with experimental results indicated that this equation was accurate for sedimentation of suspensions having particles of different densities, as well as different diameters. Upon analyzing new data, it was found that the terminal velocities of the large particles at infinite dilution corresponded to Reynold's numbers of approximately 30, a value well within the intermediate or transition region. Under those conditions, inertial forces are significant and the viscosity has less of an influence in the transition region ($0.3 < Re < 1000$) than in the Stokes or creeping flow region ($Re < 0.3$). Therefore, the dependency of the fluid properties on the terminal settling velocity was determined by expanding equation 5.

$$V_t = 0.1528 g^{0.7143} D_p^{1.1428} (\rho_a - \rho_f)^{0.7143} / (\mu_f^{0.4286} \rho_f^{0.2857}) \qquad (37)$$

This relationship was applied to the Mirza and Richardson equation and resulted in an equation for settling in the intermediate region.

$$V_{oa} = V_{ta}(\varepsilon^{n-1.7143})(1-C_a)(\mu_f/\mu_{eff})^{0.4286}(\rho_f/\rho_{eff})^{0.2857} \\ ((\rho_a-\rho_{eff})/(\rho_a-\rho_f))^{0.7143} - V_{tb}(\varepsilon^{n-1.7143})(C_b) \qquad (38)$$

The density ratio factor accounts for the effective density of the slurry accelerating around the settling particle's outer surface. Because the larger settling particles descend and displace the fluid and the smaller particles, the effective density is equivalent to the weighted volume average concentration of the suspension as if the larger particles were not present. That is, the density of the fluidizing media has properties of a slurry containing the pure fluid and the smaller particles. This is identical to the effective density proposed by Selim, but it is used in the inertial term.

$$\rho_{eff} = (\rho_b C_b + \rho_f \varepsilon)/(1 - C_a) \tag{30}$$

The ratio of the density differences accounts for the effective buoyancy forces of the slurry on a particle of the suspension. As described previously, the pressure gradient is equivalent to the density difference. Furthermore, all particles contribute to the effective pressure gradient across the suspension, and the settling particles are opposed by the effect pressure gradient; therefore, the buoyancy forces should include contributions from all particles of the suspension, regardless of size. Consequently, the effective density to be used in the density difference ratio is a weight volume average concentration of all the components (fluid and particles) of the suspension.

$$\rho' = C_a \rho_a + C_b \rho_b + \varepsilon \rho_f \tag{39}$$

The final Shor and Watson equation, incorporating the effective fluid properties for the buoyancy, the viscosity, and the accelerating fluid, accurately predicts settling rates of bimodal suspension as larger particles descend and displace fluid, as well as smaller particles, in both the Stokes and transition regions.

VOID FRACTION IN PARTICULATE FLUIDIZATION

Fluidization involves the suspension of particles by a fluid flowing upward. As the superficial inlet fluid velocity, U_o, is increased above the velocity required for minimum fluidization, U_{mf}, the particles begin a random motion, colliding with other surrounding particles and, for most gas - solid systems, bubbling occurs. At a constant superficial inlet velocity, all particles are fluidized in a suspension at a constant voidage. In addition, the net vertical velocity of a single particle is zero. At this point the buoyancy forces acting on the all particles of the suspension are balanced with the effective gravitational and drag forces. A continued increase in flow rate results in bed expansion. Further increases cause the bed expansion to reach a point of minimum bubbling, $U_o=U_{mb}$, and the void fraction, ε, remains relatively constant. Finally, beyond the region of constant voidage, bubbling continues, but the void fraction, ε, increases.

Systems which have a relatively large ratio of particle density to fluid density (like gases - solids systems) tend to exhibit an early onset of bubbling. This bubbling results when the particles are arranged in such a manner that a large proportion of the flow exceeding that required for minimum fluidization rises through the bed in region of large voidages (bubbles).[16] A typical bubbling system would consist of a gas flowing through a bed of dense particles (air - steel bearings). An example of this bubbling phenomena is presented in the

Jacob and Weimer data consisting of fine carbon powders fluidized by a high pressure gas.[8] This study was directed at cases when fluid flows are uniform over the width of the suspension with no bubbling.

Although most gas fluidized beds are prone to bubbling, liquid systems are less likely to bubble and can be more easily modelled. Fluidization without bubbles is called particulate fluidization. This type of fluidization, characteristic of many liquid systems, is the simplest of all fluidization in that no bubbling occurs and bed expansion is uniform. Increases in the superficial inlet fluid velocity produce increases in bed expansion. Ultimately, bed expansion reaches a point at which the particles are suspended by the fluid with no particles interaction and the superficial inlet fluid velocity is equivalent to the suspended particle's terminal velocity.

FLUIDIZATION / SEDIMENTATION COMPARISON

Fluidization and sedimentation have similarities which suggest that a single descriptive model can be derived for both processes incorporating parameters such as voidage, Reynold's number, particle diameter, etc. Each phenomena involves the suspension of particles by a fluid and can be modelled by force balances which account for suitable drag, buoyancy, and effective gravitational forces. In addition, starting points for modelling either process may be Stokes Law, the drag coefficient relationships for the transition region, and/or the

Richardson and Zaki equation.

Current relationships for fluidization do not always apply to sedimentation. This can be partially attributed to the different conditions under which each phenomena most often appears. Most fluidization occurs in the transition region where both viscous and inertial effects are important. However, most important sedimentation cases are in the Stokes region where particle inertial forces become insignificant (viscous forces predominate).

PARTICULATE FLUIDIZATION

Bed expansion relationships for particulate fluidization are essential for the design of both liquid and bubbling gaseous systems. For liquid systems, an accurate model of bed voidage as a function of fluid flow and physical properties of the fluid and particles would be useful in determining a bed height and reactor volume. For a bubbling gaseous system, such a relationship would be useful in determining a reactor residence time of relatively small particles, and possibly the gas density in the particulate phase.[17]

The linear log - log relationship between settling velocity and bed voidage proposed by Richardson and Zaki (see Equation 9) has been used to predict voidage during fluidization as well as sedimentation.[4]

$$Re = Re_t \varepsilon^n \tag{40}$$

Although this equation is accurate for predicting settling velocities of unimodal suspensions, it needs modifications to predict fluidization velocities in both gas and liquid systems. The model predicts slightly lower fluidization velocities than those observed for liquid systems; however, it predicts significantly higher fluidization velocities than those observed for high pressure gas systems.[5,8] The Richardson and Zaki exponent or expansion index, n, is a function of only the particle diameter to column diameter ratio and the particle's terminal Reynold's number at infinite dilution; therefore, the expansion index remains constant for a given particle and fluid, regardless of the superficial inlet fluid flow or the void fraction. These conditions would give a constant slope of the log (U_o/U_t) vs. $\log(\varepsilon)$ plot. It is apparent from data of several investigators that the Richardson and Zaki exponent does not remain constant for a given particle and fluid.[5]

In 1977 Garside and Al-Dibouni analyzed fluidization and sedimentation data for redefining the Richardson and Zaki equation.[18] They plotted data in the form of the superficial velocity / terminal velocity ratio vs. the terminal Reynold's number. They concluded that the shape of this plot represented a logistic curve and the Richardson and Zaki exponent should take the form of a logistic equation. The result was a new correlation for the expansion index to be used in the Richardson and Zaki equation.

$$(n_{LR}-n)/(n-n_{TR}) = aN_{Ret}^{\,b} \tag{41}$$

where

n = Richardson and Zaki expansion index.

n_{TR} = asymptotic value of n in the turbulent region.

n_{LR} = asymptotic value of n in the laminar region.

a = constant determined by slope if logistic curve.

The general shape of the curve appears to logistic; however, at the region of inflection the model does not conform to the experimental results. In addition, the model tends to become less accurate in modeling behavior at high void fractions.

Foscolo et al in 1983 derived a model which predicts bed expansion for a wider flow range and all void fractions. This equation applies to flow conditions with terminal Reynold's numbers between 0.2 and 500.

$$U_o/U_t = \{[0.0777Re_t(1+0.0194Re_t)\varepsilon^{4.8}+1]^{0.5}-1\}/(0.0388Re_t) \tag{42}$$

Under the same conditions (particle size and pressure drop) as Richardson and Zaki, the results are substantially improved (see Figures 4 and 5). Foscolo's equation was derived from an analytical model. His equation originates from the Ergun equation for pressure drop in a packed bed and, thus, incorporates the Hagen-Poiseuille equation for pressure drop through straight tubes. As expected, because the voidage is not made up of straight tubes, this alone did not model the true characteristics of fluidization. As a result, a factor to correct for the various fluid paths was added and the equation took the form of the Blake-Kozeny equation. It was then assumed that this correction factor could be replaced with a constant tortuosity factor. The results were substantially improved; however, the tortuosity factor was largely empirical.

Zhang Fan in 1985 graphically presented data on twelve unimodal suspensions and illustrated that there are instances in which the log(Re) vs. log(ϵ) relationship exhibits nonlinearity at void fractions over 0.430.[5] At a void fraction of 1, the experimental terminal velocity, U_t', is theoretically equal to U_t; however, experimental data yield slightly lower results. A plot of Log(Re) versus Log(void fraction) indicates a distinct inflection at void fractions near 0.9. Fan et al attempted to model this change in slope by making use of the classical Richardson and Zaki equation. They determined that entire curve could be modeled by two linear equations. The first equation would hold for the portion of the curve below the inflection and the second for the portion above the inflection. Therefore, through an empirical regression analysis, Fan determined the point of inflection and the relationships to be used for the new exponents of the Richardson and Zaki equation.

$$n_1 = 1.90 + 5.46\ \mathrm{Log(Ar)} - 2.96\ \mathrm{Log}^2\mathrm{(Ar)} \qquad \mathrm{Ar} < 21 \qquad (43)$$

$$n_1 = 5.72 - 1.70\ \mathrm{Log(Ar)} - 0.27\ \mathrm{Log}^2\mathrm{(Ar)} \qquad \mathrm{Ar} \geq 21 \qquad (44)$$

$$n_2 = 4.92 \qquad \mathrm{Ar} < 7.2 \qquad (45)$$

$$n_2 = 5.11 - 0.11\ \mathrm{Log(Ar)} - 0.12\ \mathrm{Log}^2\mathrm{(Ar)} \qquad \mathrm{Ar} \geq 7.2 \qquad (46)$$

$$Re_{t1} = Re_{t2}\varepsilon_c^{m} \qquad (47)$$

$$Re_{t2} = 0.0517\ Ar^{1.096-0.068\ \mathrm{Log}(Ar)} \qquad (48)$$

$$m = 3.02 - 5.46\ \mathrm{Log}(Ar) + 2.96\ \mathrm{Log}^2(Ar) \qquad 2 < Ar < 7.2 \qquad (49)$$

$$m = 3.21 - 5.57\ \mathrm{Log}(Ar) + 2.84\ \mathrm{Log}^2(Ar) \qquad 7.2 <= Ar < 21 \qquad (50)$$

$$m = 1.59\ \mathrm{Log}(Ar) - 0.39\ \mathrm{Log}^2(Ar) - 0.61 \qquad 21 <= Ar < 1600 \qquad (51)$$

$$Re_t = 0.0616\ Ar^{1.000-0.048\ \mathrm{Log}(Ar)} \qquad (52)$$

$$\varepsilon_c = 0.853 - 0.076\ \mathrm{Log}(Ar) + 0.009\ \mathrm{Log}^2(Ar) \qquad (53)$$

Values of n_1 and n_2 are the expansion indexes or exponents to be used in the Richardson and Zaki type equation for predicting the velocity vs. voidage relationship below and above the curve inflection point, respectively. Each Richardson and Zaki equation remains linear due to a constant expansion index over a range of void fractions.

CHAPTER III

THEORETICAL

Numerous models have been developed to describe the relationship between slip velocity and suspension voidage; unfortunately, most models lack the ability to incorporate both observed sedimentation and fluidization phenomena into the correlations. Restated, the goal of this investigation was to expand a model that would be applicable to both sedimentation and particulate fluidization. Because fluidization and sedimentation both involve similar fundamental fluid dynamic relationships, it is likely that a single model can explain both phenomena, but the model will also have to address the differences in the phenomena. The most common fundamental relationship to fluidization and sedimentation analysis is the Richardson and Zaki equation. This relationship accurately accounts for fluid - particle dynamics of unimodal sedimentation; however, as previously described, during fluidization and bimodal sedimentation, there are other factors that influence the particle behavior in a suspension, namely other particles. Regardless of whether the suspension is unimodal or multimodal, the apparent viscosity that affects particle behavior is not likely to be that of the fluid, but of a slurry. Therefore, the slip velocity, V_s, can be assumed a function of the physical properties of the fluid / particle combination. Consequently, other surrounding particles contribute to additional drag forces and can be accounted for in numerous ways. Mirza and Richardson described bimodal settling by performing a material balance over a finite section of a suspension. This accounted for observed displacement of the smaller particles as well as the fluid. Shor and Watson expanded the Mirza and Richardson equation and took into account the particle - particle interaction contributing to a higher effective viscosity, a characteristic very likely to be important in fluidization. Therefore, it is appropriate to examine the Shor and Watson correlation when developing a unified model for predicting sedimentation rates as well as fluidization velocities.

APPLICATION TO SHOR AND WATSON EQUATION

As mentioned previously, the Shor and Watson equation contains contributions from Richardson and Zaki, Mirza and Richardson, Ting and Luebbers, and others. Therefore, it is appropriate to reanalyze the make-up of this model before expanding it for application to fluidization.

$$V_{oa} = V_{ta}(\epsilon^{n-1.7143})(1-C_a)(\mu_f/\mu_{eff})^{0.4286}(\rho_f/\rho_{eff})^{0.2857} ((\rho_a-\rho_{eff})/(\rho_a-\rho_f))^{0.7143} - V_{tb}(\epsilon^{n-1.7143})(C_b) \tag{38}$$

The Shor and Watson equation above incorporates the two terms as described by Mirza and Richardson for the displaced fluid and smaller particles. The first term of accounts for the downward movement of the large particles. The second term accounts for the displacement of the smaller particles. The presence of these two terms suggests that segregation occurs as settling proceeds.

To modify this equation to account for fluidization of uniformly sized spheres, the settling velocity in this equation can be interpreted as the velocity of the fluid required to suspend the particles. A necessary assumption in the modification of this equation is that the fluidized portion of the bed is well mixed. That is, there is negligible segregation, and the entire bed is homogeneous. Therefore, the second term of equation 38 can be eliminated. In addition, the large particle concentration, C_a, represents the fraction of solids affected by the surrounding smaller particles. Consequently, because the modification describes unimodal systems, this term can be incorporated into the exponent of the void fraction. As a result, the modified equation can be written as follows.

$$U_o = U_t(\varepsilon^{n-.7143})(\mu_f/\mu_{eff})^{0.4286}(\rho_f/\rho_{eff})^{0.2857}((\rho_a-\rho_{eff})/(\rho_a-\rho_f))^{0.7143} \quad (54)$$

where

U_o = superficial inlet fluid velocity

U_t = terminal velocity of single particle in dilute fluid

What remains to be determined are the values to be used for the effective fluid properties. Unlike bimodal sedimentation in which only the smaller particles contribute to the effective fluid viscosity, during fluidization all particles could contribute to any effective fluid property.

The effective viscosity of the fluidizing or settling media depends primarily to the extent to which particles are present in the shear fields. Shor and Watson observed that particle collision are negligible during sedimentation of unimodal suspensions; therefore, the effective viscosity of the fluidizing media is the viscosity of the pure fluid. Shor and Watson further stated that during sedimentation of bimodal suspension, the effective viscosity of the fluid media as "seen" by the larger particles depends on the solids concentration of the small particle fraction. Consequently, during unimodal fluidization in which interactions of all particles are random and additional shear fields are created, the effective viscosity is a contribution of the total solids concentration and equation 35 can be written as follows.

$$\mu_{eff} = \mu_f(0.464-0.78(1-\varepsilon))/(0.464+0.21(1-\varepsilon)) \qquad (55)$$

The ratio of the density difference in the Shor and Watson equation accounts for the buoyancy affects of the slurry realized by a particle in a suspension. As described by Shor and Watson, the pressure gradient across the suspension results from a contribution of all particles, and a settling particle is opposed by the effective pressure gradient of the suspension; therefore, because the effective density is equivalent to the effective pressure gradient, all particles should contribute to the effective buoyancy forces of the suspension. Consequently, the effective density of this difference ratio should be a function of the total solids concentration of the suspension and may be written in terms of a weighted volume average density.

$$\rho_{eff} = (1-\varepsilon)\rho_p + \varepsilon\rho_f \qquad (56)$$

The ratio of densities in the Shor and Watson equation accounts for the effective density of fluid or slurry accelerating around a particle of the suspension. For bimodal sedimentation, the settling larger particles descend through a slurry consisting of the pure fluid and the smaller particles. Consequently, the effective density of this accelerating fluid as "seen" by the larger particles is a function of the fluid density and concentration, as well as the small particle density and concentration. However, during unimodal fluidization, all particles are in a random motion and particles interactions are frequent. Consequently, the density of the accelerating fluid as "seen" by a suspended particle is, again, that of a slurry consisting of both the fluid and other surrounding particles. Furthermore, because all particles have the same potential for frequency of interactions, the slurry accelerating around a single particle of the suspension has the density equivalent to the weighted volume average density of all the components (fluid and particles) of the suspension. Therefore, the effective density used in this ratio is the same as that used in the density difference ratio (see equation 56).

The resulting equation for fluidization accounts for the fundamental fluid dynamics as described by Richardson and Zaki as well as the effective fluid properties of the fluidizing media as described by Shor and Watson. Additional inertial and viscous forces are accounted for by the use of effective fluid properties such as density and viscosity. Furthermore, the equation is of a form that allows observed fluidization phenomena of different systems to be easily incorporated. That is, in bimodal or multimodal systems, it can be altered to account for the various extents to which smaller particles contribute to the fluidization of the larger particles.

CHAPTER IV

RESULTS AND DISCUSSION

Data used to evaluate the proposed model encompass a wide range of fluidization properties and flow regimes. Data were selected for accuracy, reliability, and coverage of a wide range of fluid and particle properties. The study was limited to particulate fluidization but sought diversity of fluid and particle properties. In addition, data sets were also selected based on negligible wall effects. That is, the particle diameter to column diameter ratio was considered small enough to neglect additional wall drag. Data from Zhang Fan,[5] Loeffler and Ruth,[19] and Richardson and Zaki[4] are presented to cover a range of liquid fluidization systems in the creeping flow and transition regions, while recent data from Jacob and Weimer represent high pressure gas fluidization systems in the transition region.

The data were analyzed to evaluate the observed fluidization expansion model of both gas and liquid systems over a wide range of flow regimes and fluid / particle properties. Parameters for previously developed relationships are discussed and used to arrive at a proposed new modified approach to describe particulate fluidization. The proposed model is compared with existing data and with previous models of other investigators. Finally, the concepts used in the proposed model are expanded to describe fluidization of bimodal suspensions.

COLLECTED DATA

Richardson and Zaki presented liquid - solid particulate fluidization data which account for fluidization in the creeping flow and early transition regions. These data were used to develop the classical Richardson and Zaki fluidization relationship and are presented in Figures 1 and 2. A slight curvature in the log(Re) vs. log(ε) is worth noting. Their data were for divinyl benzene particles fluidized in water at ambient temperatures. The same fluid and particles were used in each run; however, the difference between the two runs is the column diameter. Figure 1 represents fluidization data in a column of diameter 2.44 inches. Figure 2 represents fluidization data in a column of diameter 1.5 inches. As stated previously, the particle diameter to column diameter is considered negligible; therefore, the two runs serve as a measure of the consistency of the data and the proposed model.

In 1985 Zhang Fan presented data on twelve unimodal suspensions encompassing all three flow regimes (creeping flow region, transition region, and inertial region). Spherical particles with diameters ranging from 53.6 to 1180 microns and densities ranging from 1.045 to 2.43 g/cm^3 were fluidized with water at or near ambient temperatures. Fluidization was assumed to be particulate, and the bed expansion was

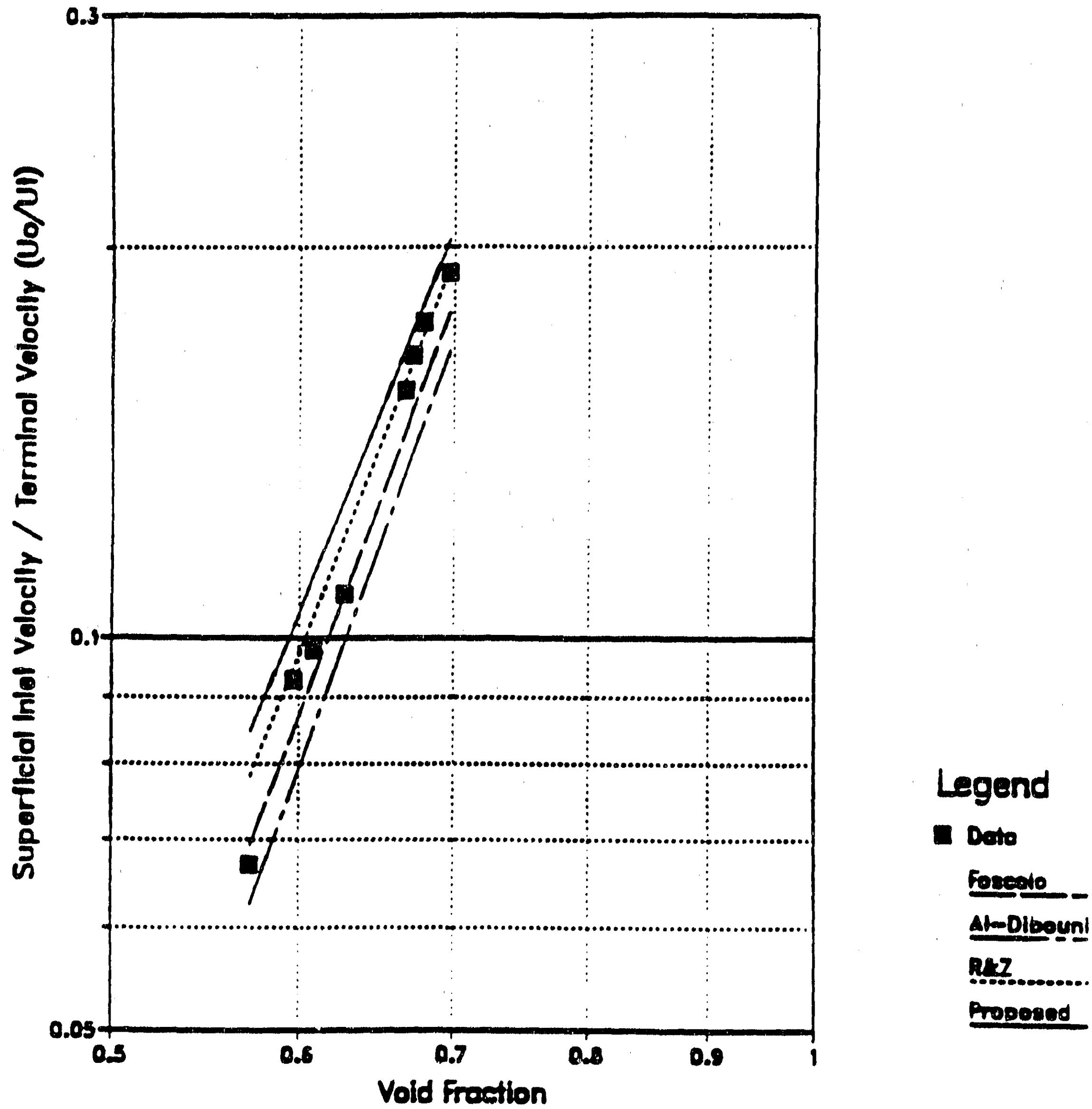

Figure 1. Richardson and Zaki data - divinyl benzene particles in water, small column.

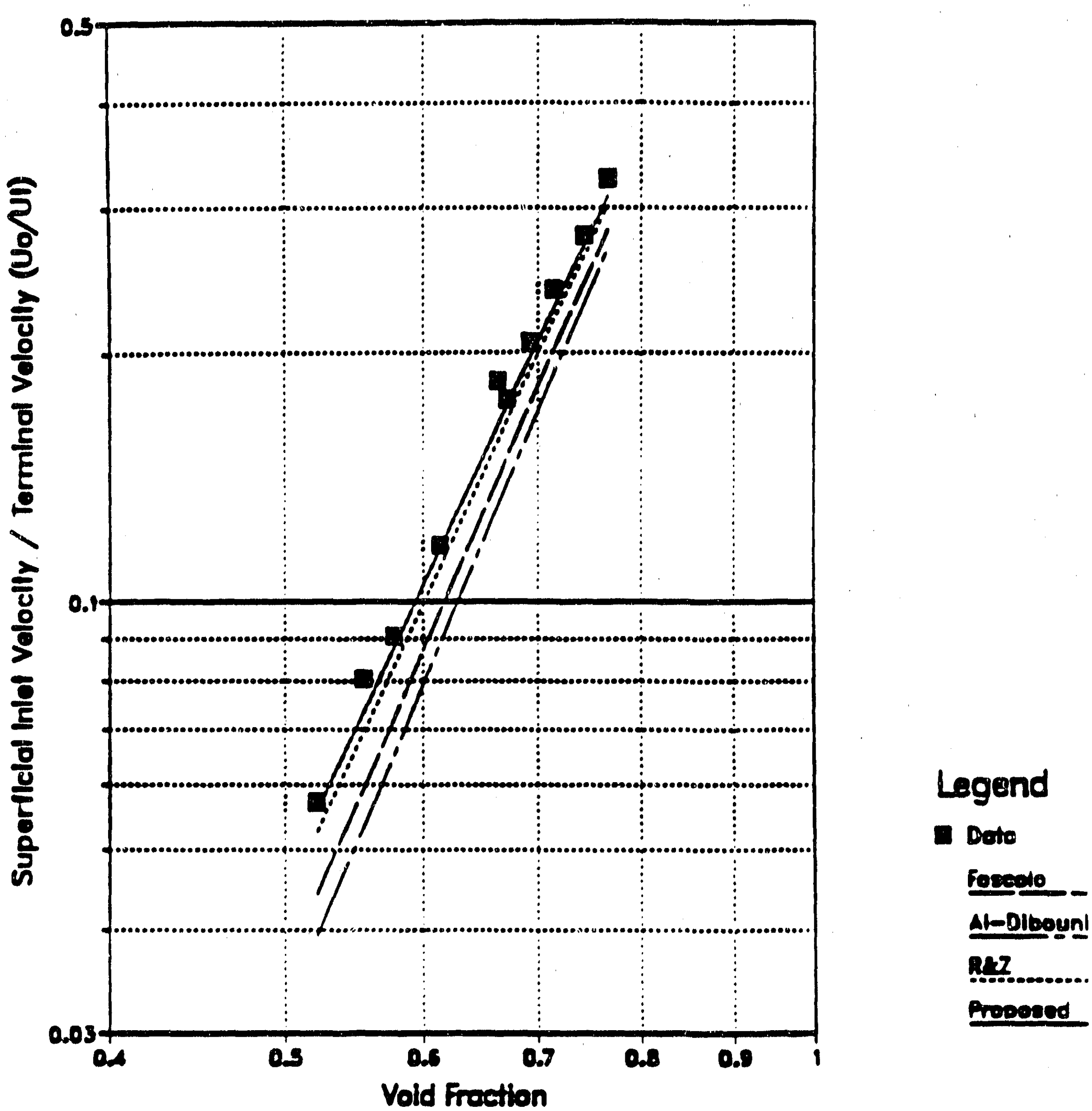

Figure 2. Richardson and Zaki data - divinyl benzene particles in water, large column.

assumed to be uniform. The particle diameter to column diameter ratio is assumed to be negligible; therefore, wall effects are not considered significant. A summary of the data is listed in Table 1. Figures 3, 4, and 5 illustrate the data in the form of $\log(U_o/U_t)$ vs. $\log(\varepsilon)$. Additional Zhang Fan data are presented in the appendix. As previously mentioned, investigations by Richardson and Zaki lead to the development of the classical fluidization equation in which this log - log dependence is considered linear; however, as evident from the Zhang Fan data, the dependence of $\log(U_o/U_t)$ vs. $\log(\varepsilon)$ appears to be slightly, but consistently, nonlinear.

Liquid fluidization data from Loeffler and Ruth are presented to account for fluidization in the transition and inertial regions and are illustrated in Figure 6. Particles of diameter 0.06586 cm and density 2.63 g/cm^3 were fluidized by water at ambient temperatures. Their data exhibit bed expansion; however, the nonlinearity is more evident than in either the Zhang Fan or the Richardson and Zaki data.

Jacob and Weimer provided new data and expanded the data base into new conditions, fluidization by high pressure gases. Their study focused on minimum bubbling characteristics in which fine carbon powders with diameters of 44 and 112 microns and densities of 850 kg/m^3 were fluidized by a CO_2/H_2 gas at pressures ranging from 2070 to 12420 kPa. The data from flow rates below bubble formation offer an unusual opportunity to study particulate fluidization. At high pressure, the gas densities are moderately high, and the initiation of bubbling is

Table 1. Fan run data.

Material	Run No.	Diameter (microns)	Density (cm)	Terminal Velocity (cm/s)
Glass Spheres	1	53.6 +/- 1.4	2.38	0.252
	4	82.3 +/- 2.8	2.38	0.498
	5	103 +/- 3.2	2.38	1.17
	9	326	2.27	3.75
	10	500	2.43	7.28
Polystyrene Spheres	11	535	1.045	0.449
	13	1020	1.045	1.085
Heavy Polystyrene Spheres	14	350 +/- 6.5	1.16	0.657
	16	488 +/- 7	1.16	1.12
Cation Exchange Resins	17	551 +/- 17	1.295	2.16
Anion Exchange Resins	20	1180 +/- 59	1.095	2.61
Heavy Exchange Resins	23	745 +/- 43	1.195	2.57

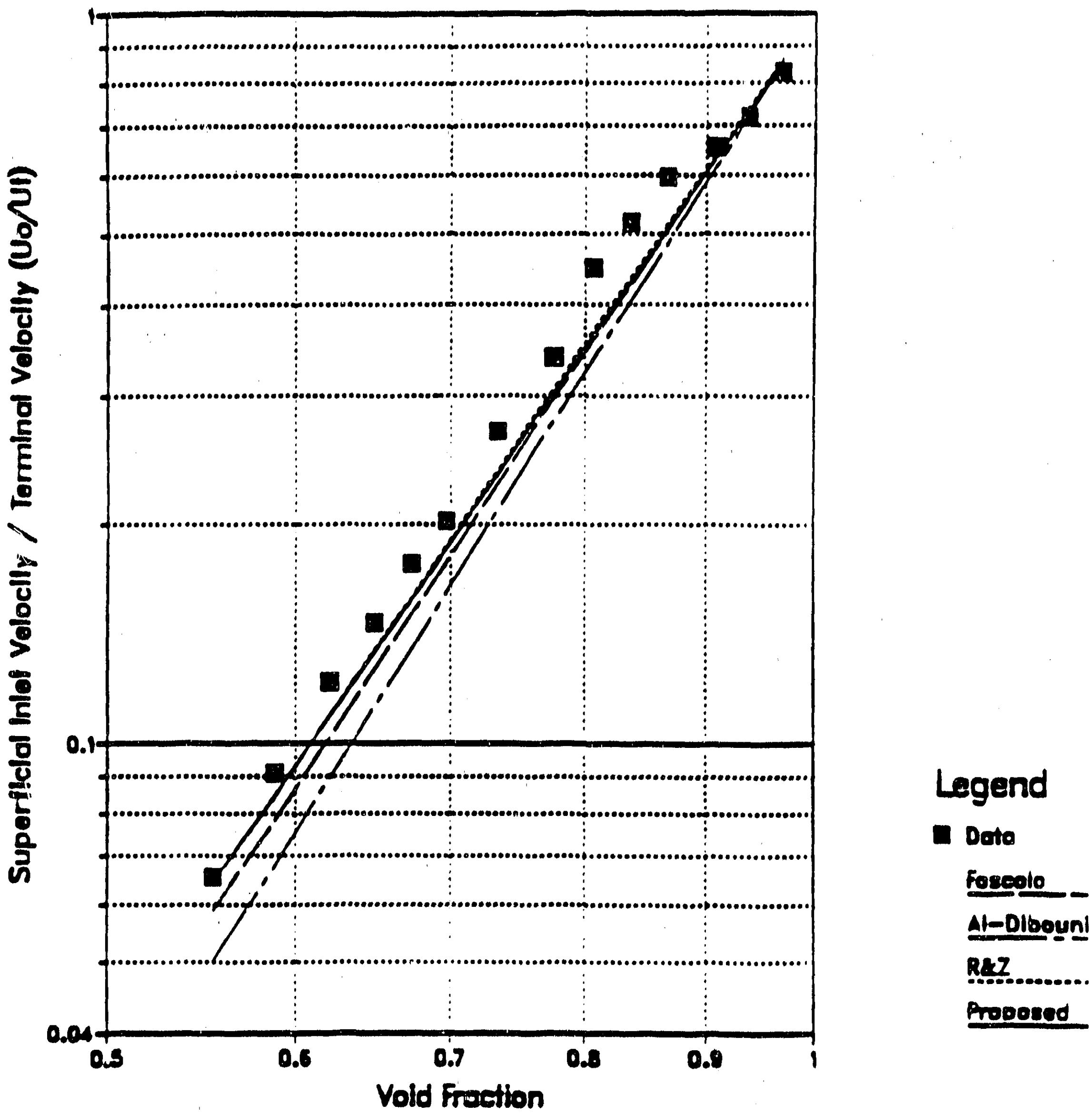

Figure 3. Fan data - Run 1, glass beads in water.

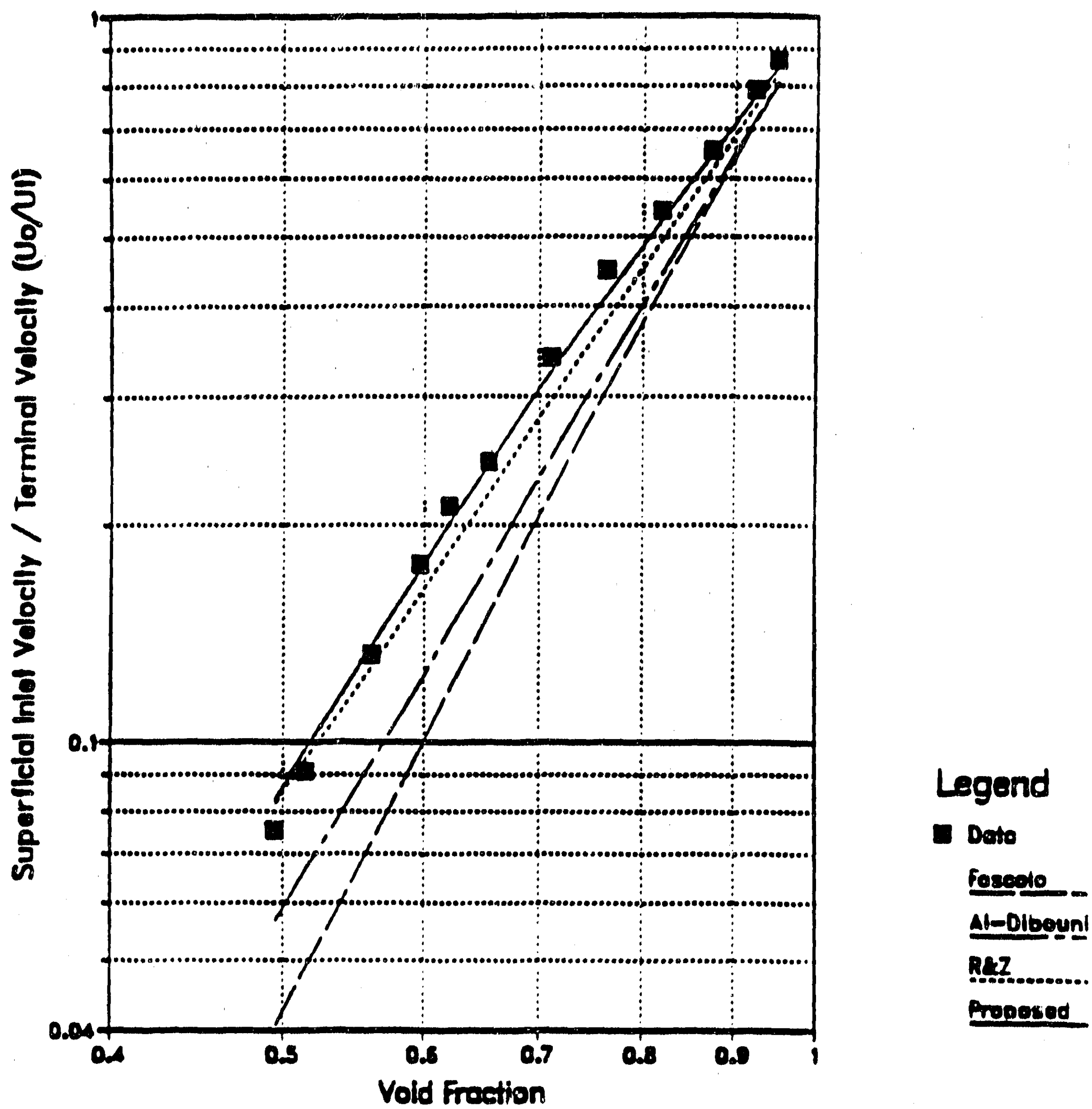

Figure 4. Fan data - Run 9, glass beads in water.

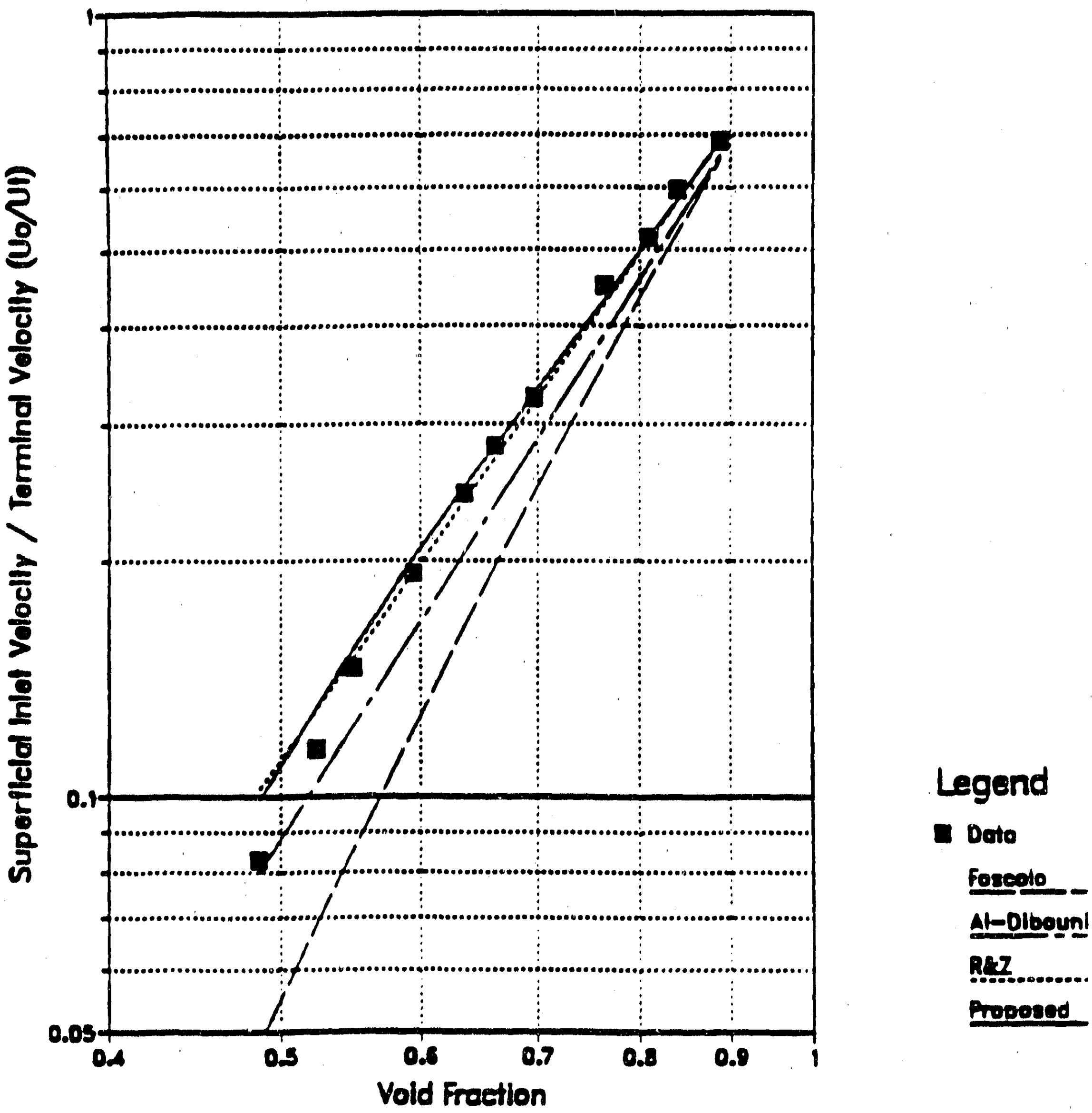

Figure 5. Fan data - Run 10, glass beads in water.

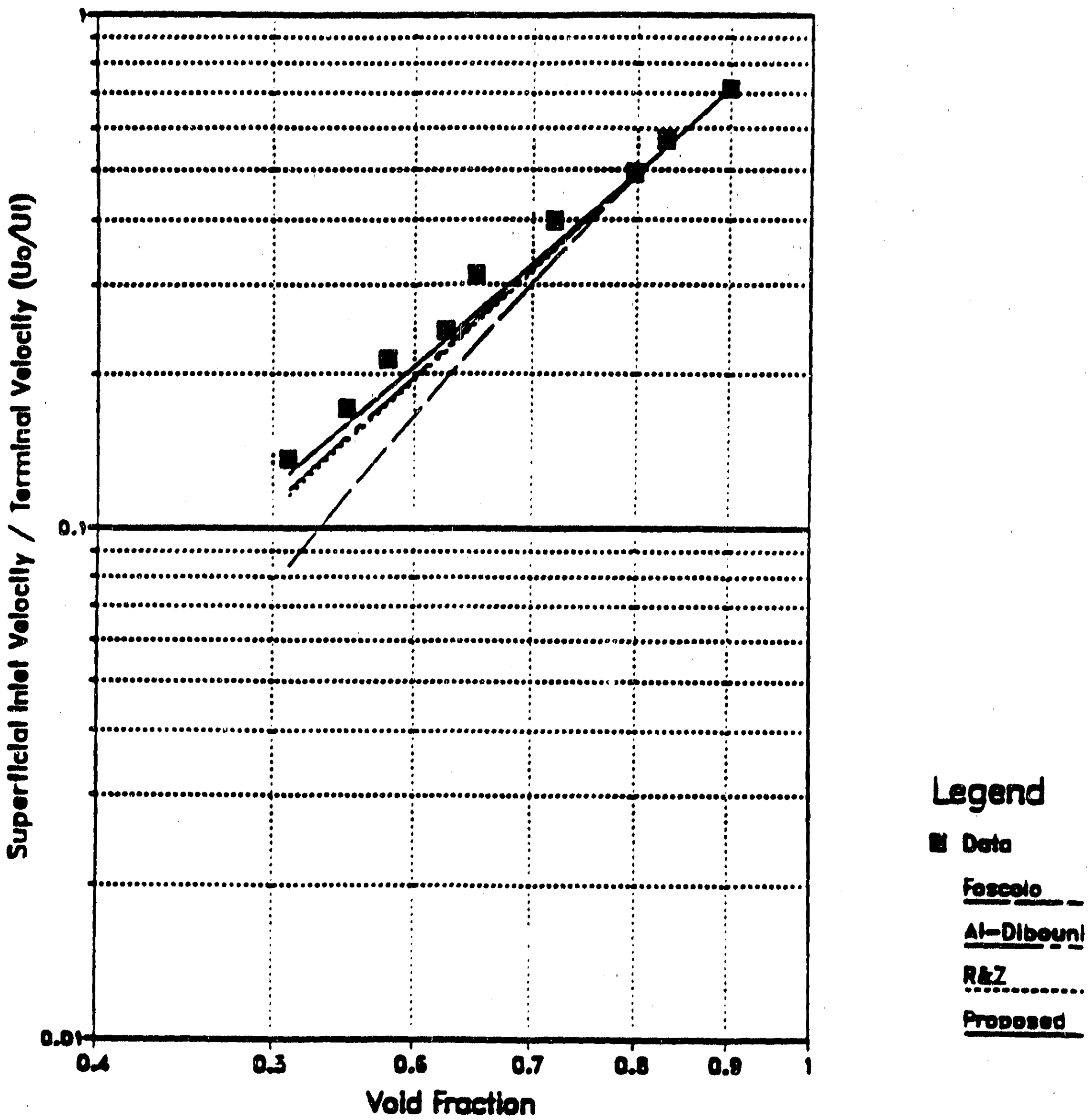

Figure 6. Loeffler and Ruth data - glass beads in water.

delayed to flow rates significantly above minimum fluidization rates. As illustrated in Figure 7 - 18, at relatively low void fractions, the bed expansion resembles particulate fluidization; however, as fluidization proceeds, the bed expansion slows and stops indicating that bubbling has begun. As stated previously, data to be used for the verification of the proposed model are assumed to be in the particulate regime; therefore, only values at relatively low void fractions are used in this study. Because only a small portion of Jacob and Weimer data are in the particulate regime, the exact limits of the particulate fluidization are not always certain; however, the extended range of conditions makes the Jacob and Weimer data especially useful for testing the validity of the proposed models and correlations.

CLASSICAL EXPANSION INDEX

A common characteristic of the Zhang Fan, Ruth, and Richardson and Zaki liquid fluidization data in the transition region is the nonlinearity of the $\log(U_o)/\log(U_t)$ plot. This nonlinearity indicates that the relationship between the fluidization velocity and the voidage is not purely exponential; that is, the velocity vs. voidage relationship can not be accurately modeled by an exponential equation with a constant expansion index or exponent as suggested by Richardson and Zaki and by several succeeding investigators.

Fluidization expansion indexes most commonly used by investigators

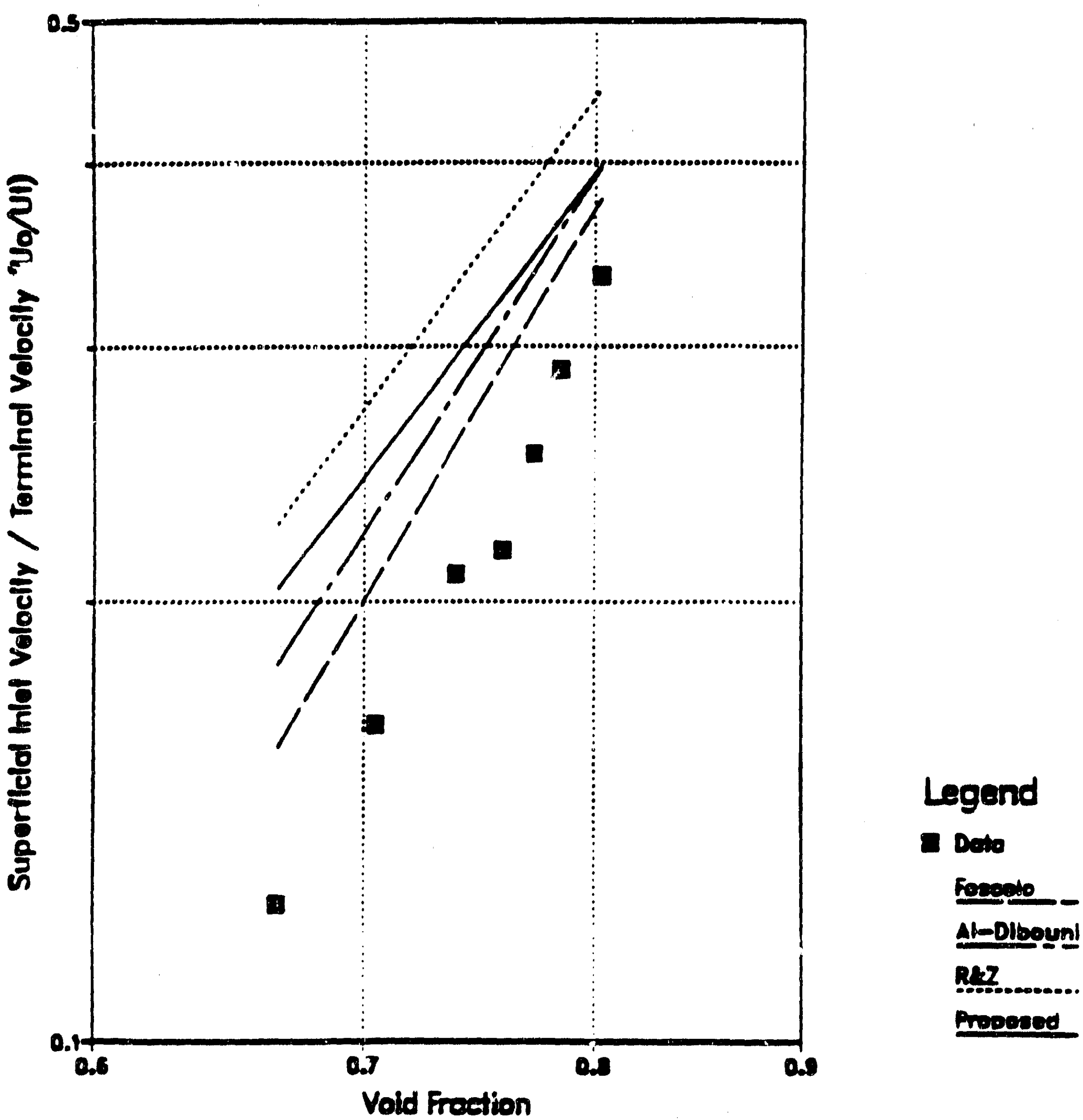

Figure 7. Jacob and Weimer data - carbon powder in gas,

P = 12420 kPa, D_p = 44 microns.

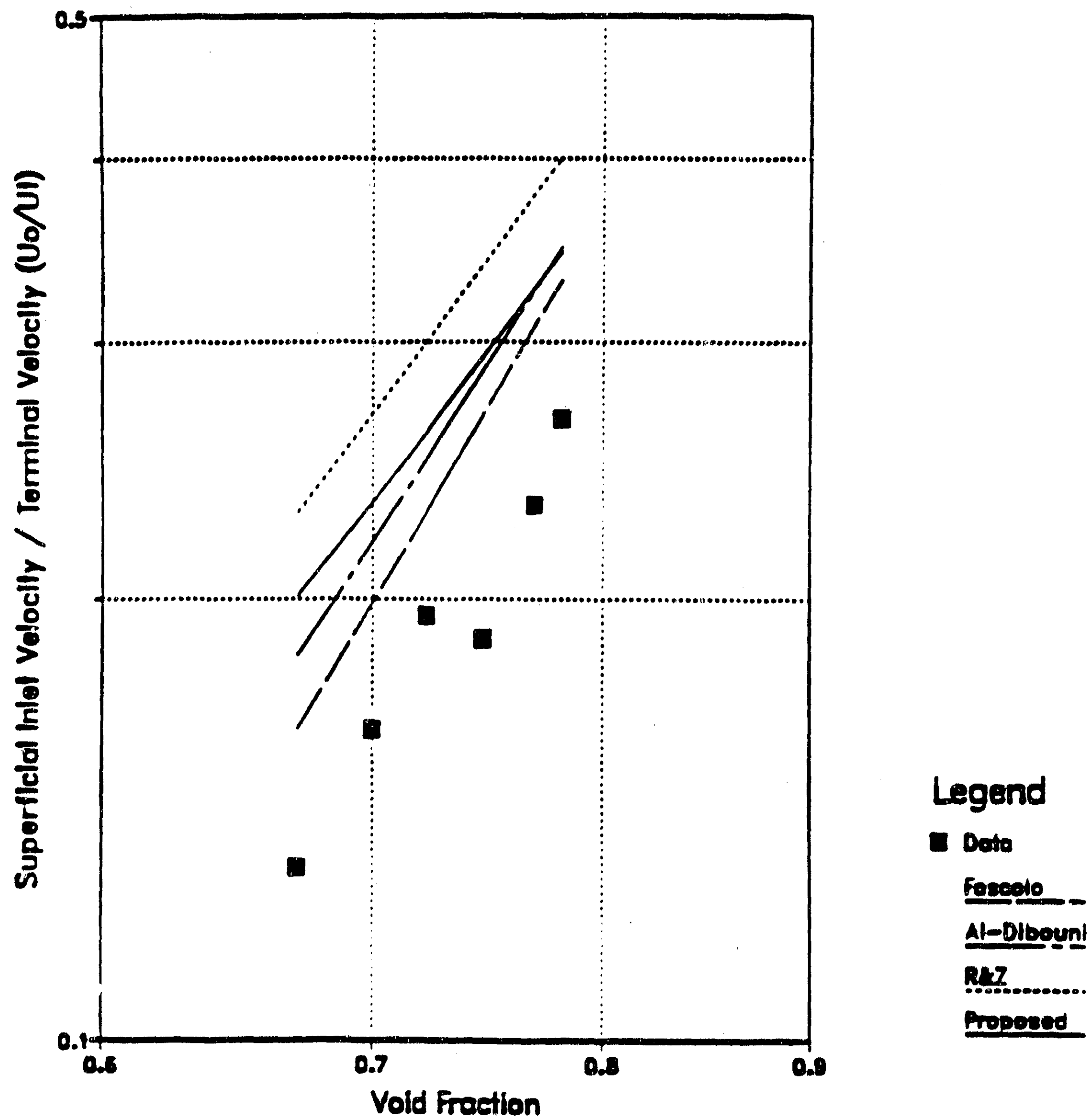

Figure 8. Jacob and Weimer data - carbon powder in gas, P = 10350 kPa, D_p = 44 microns.

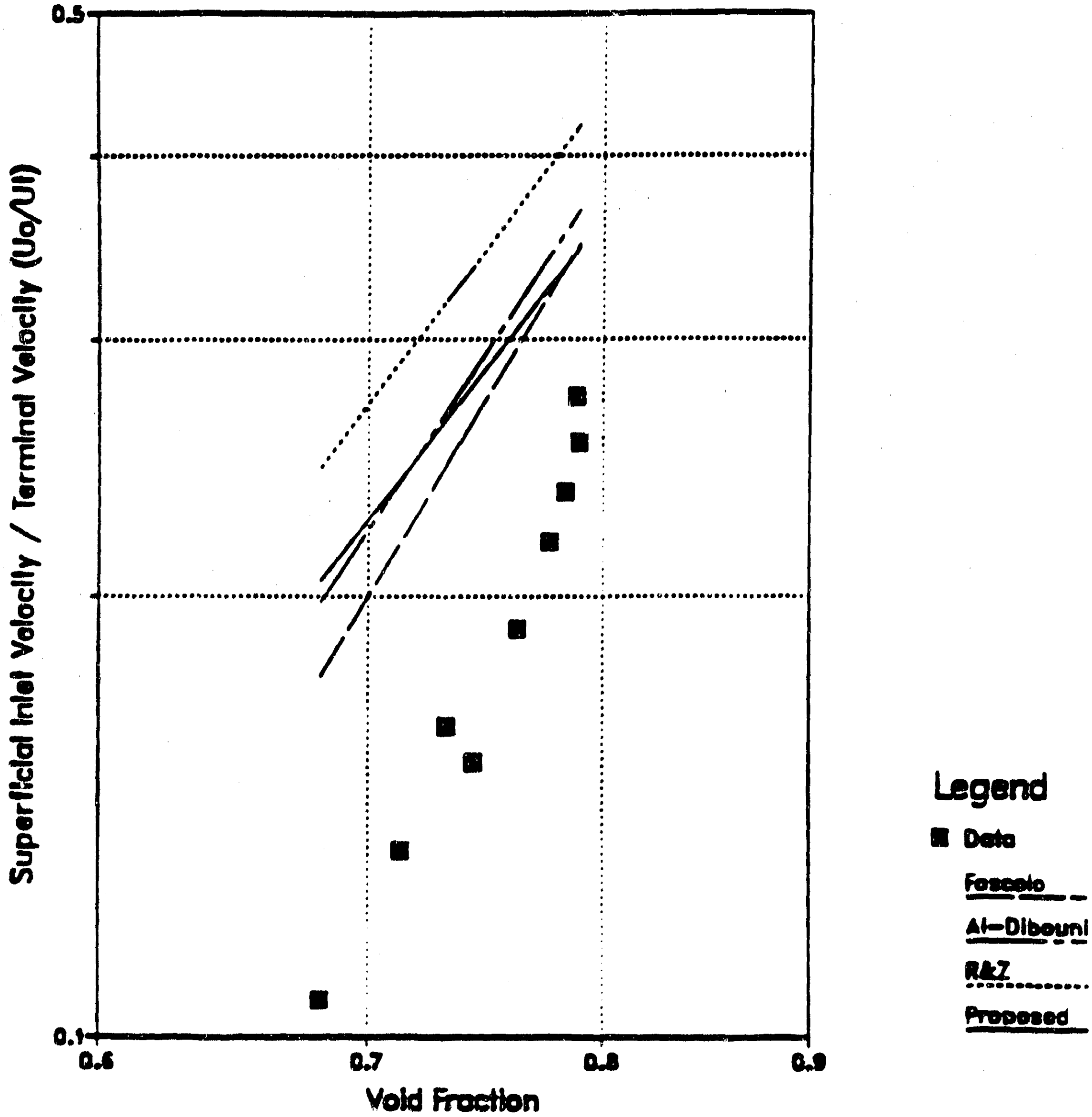

Figure 9. Jacob and Weimer data - carbon powder in gas,

P = 8280 kPa, D_p = 44 microns.

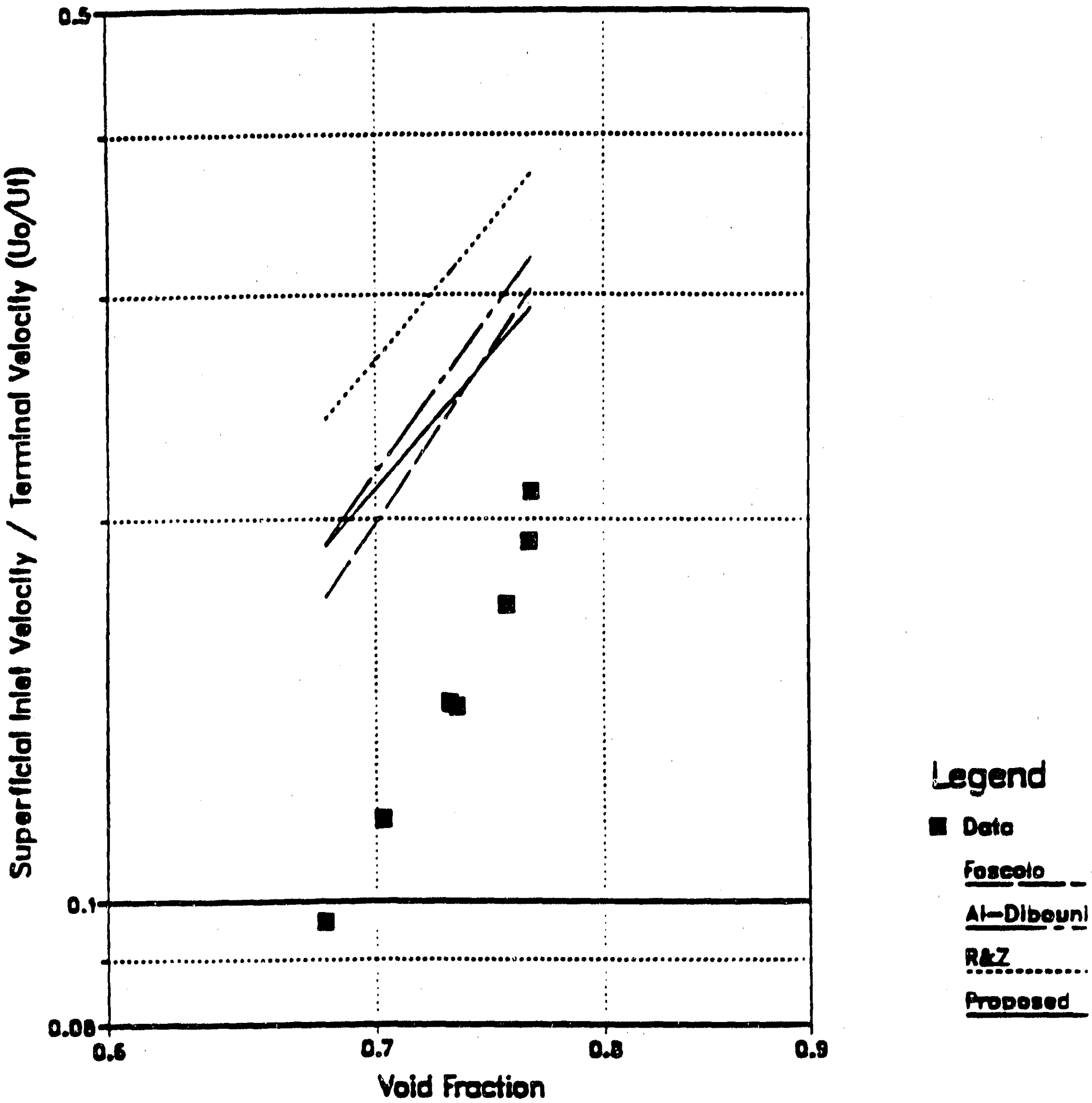

Figure 10. Jacob and Weimer data - carbon powder in gas, P = 6210 kPa, D_p = 44 microns.

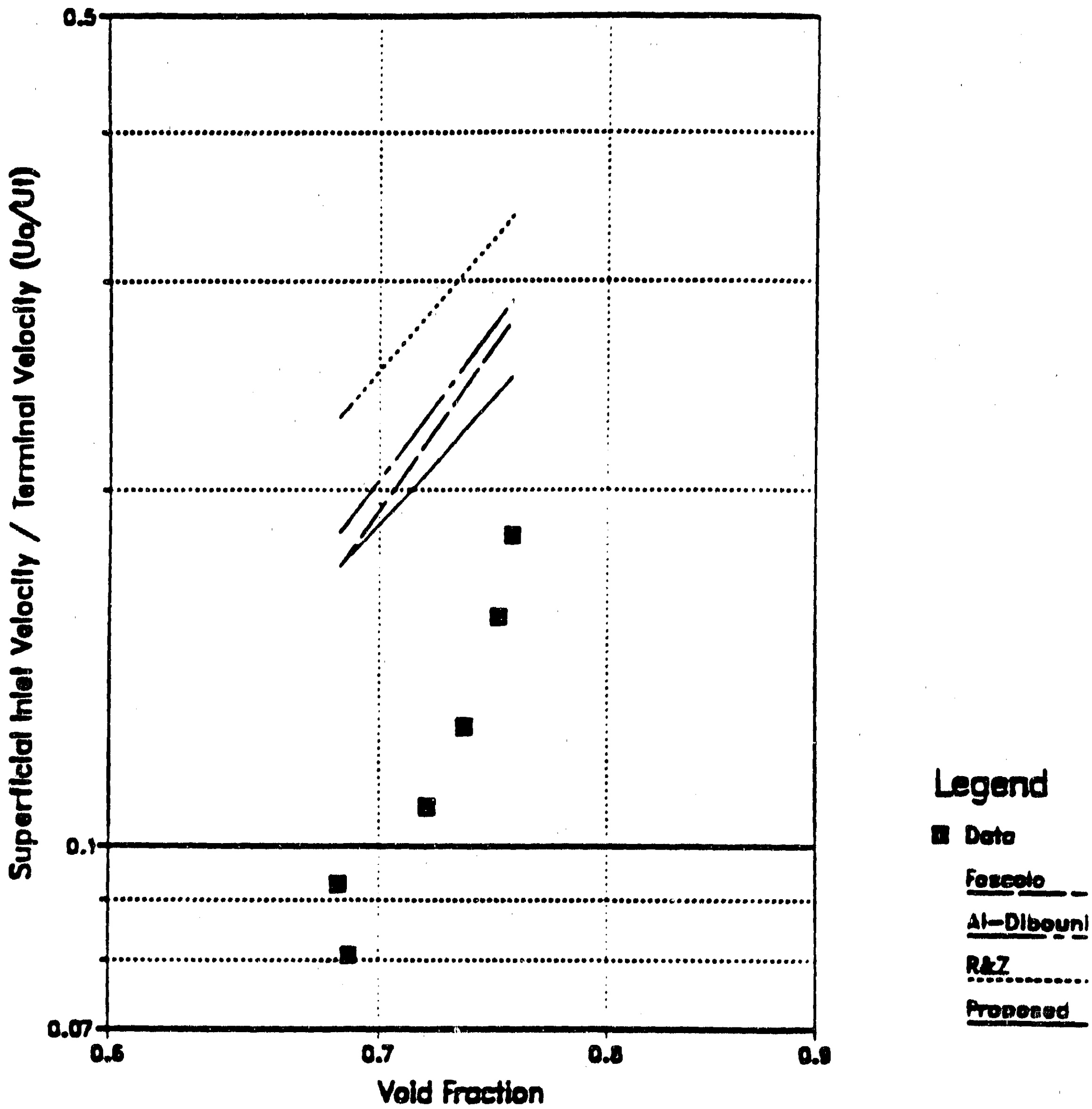

Figure 11. Jacob and Weimer data - carbon powder in gas, P = 4140 kPa, D_p = 44 microns.

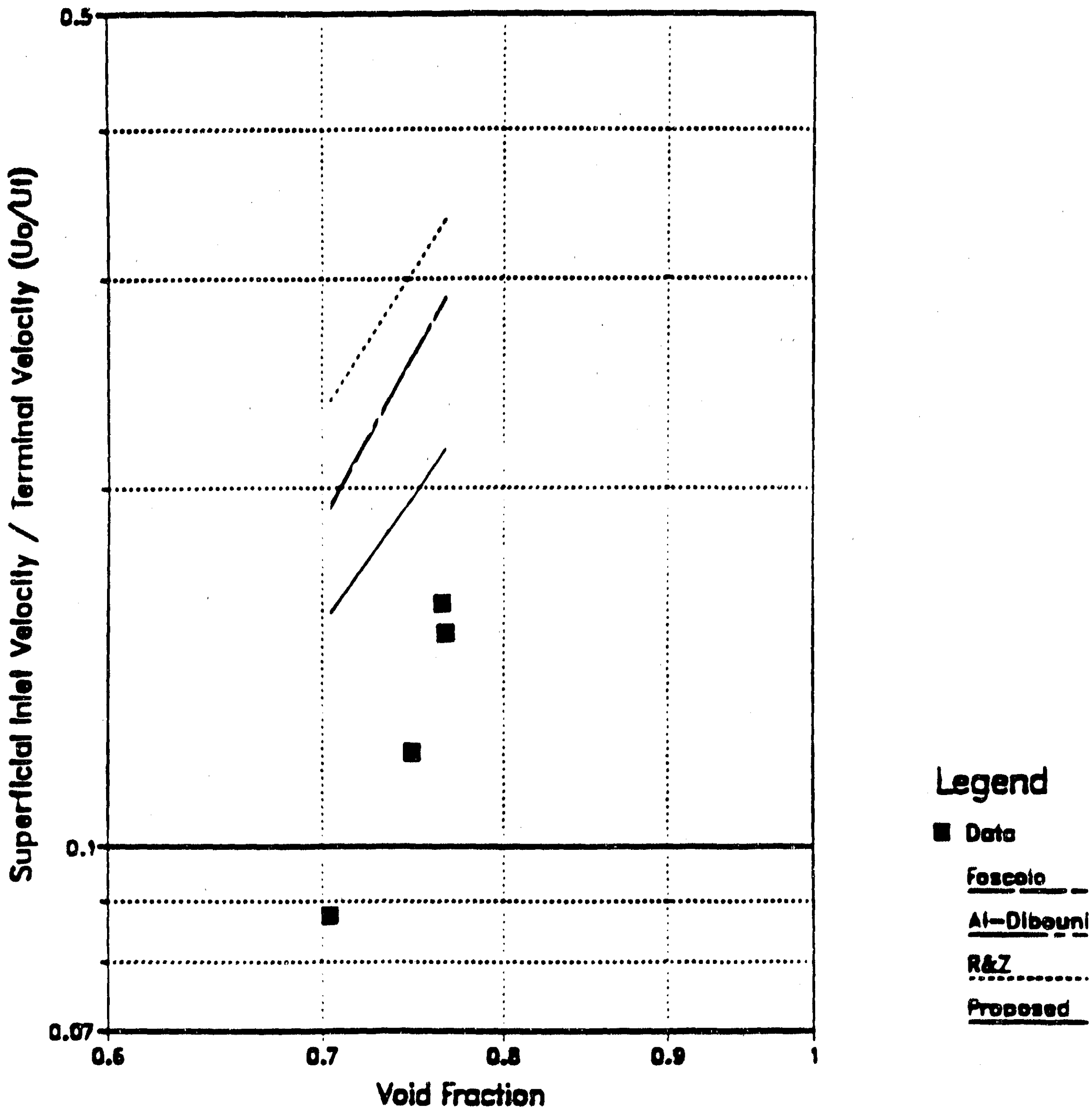

Figure 12. Jacob and Weimer data - carbon powder in gas,

P = 2070 kPa, D_p = 44 microns.

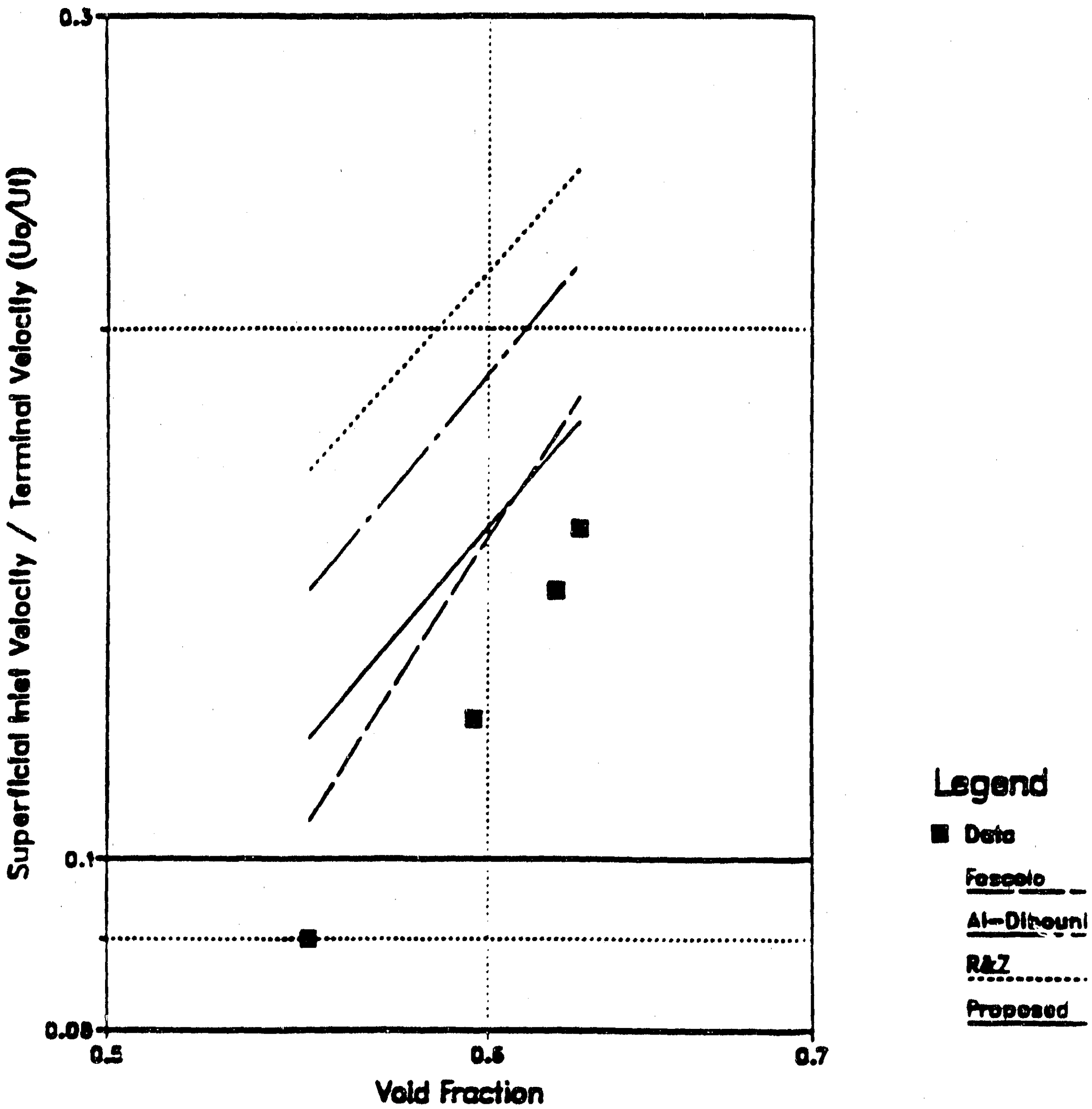

Figure 13. Jacob and Weimer data - carbon powder in gas, $P = 12420$ kPa, $D_p = 112$ microns.

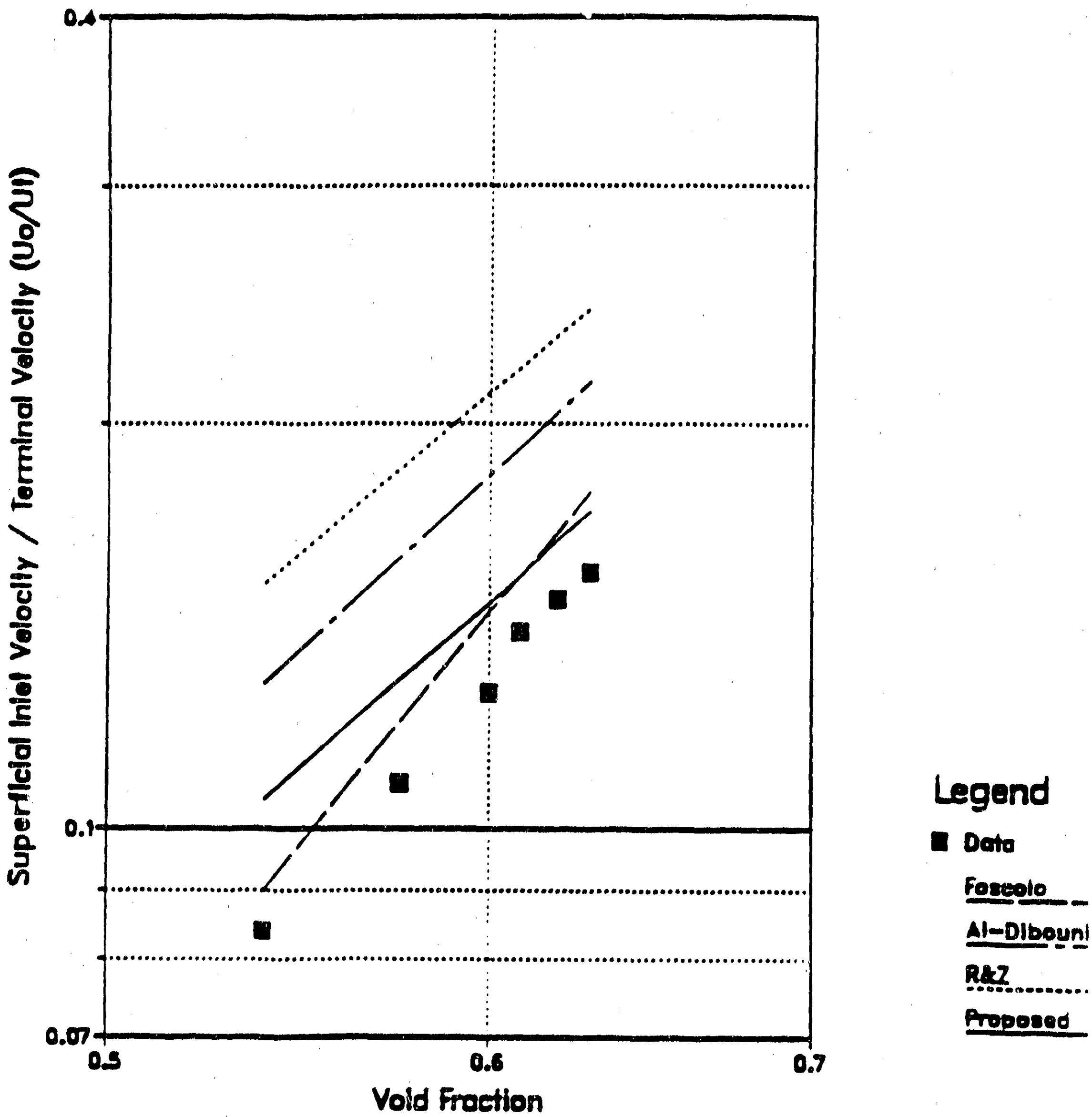

Figure 14. Jacob and Weimer data - carbon powder in gas, P = 10350 kPa, D_p = 112 microns.

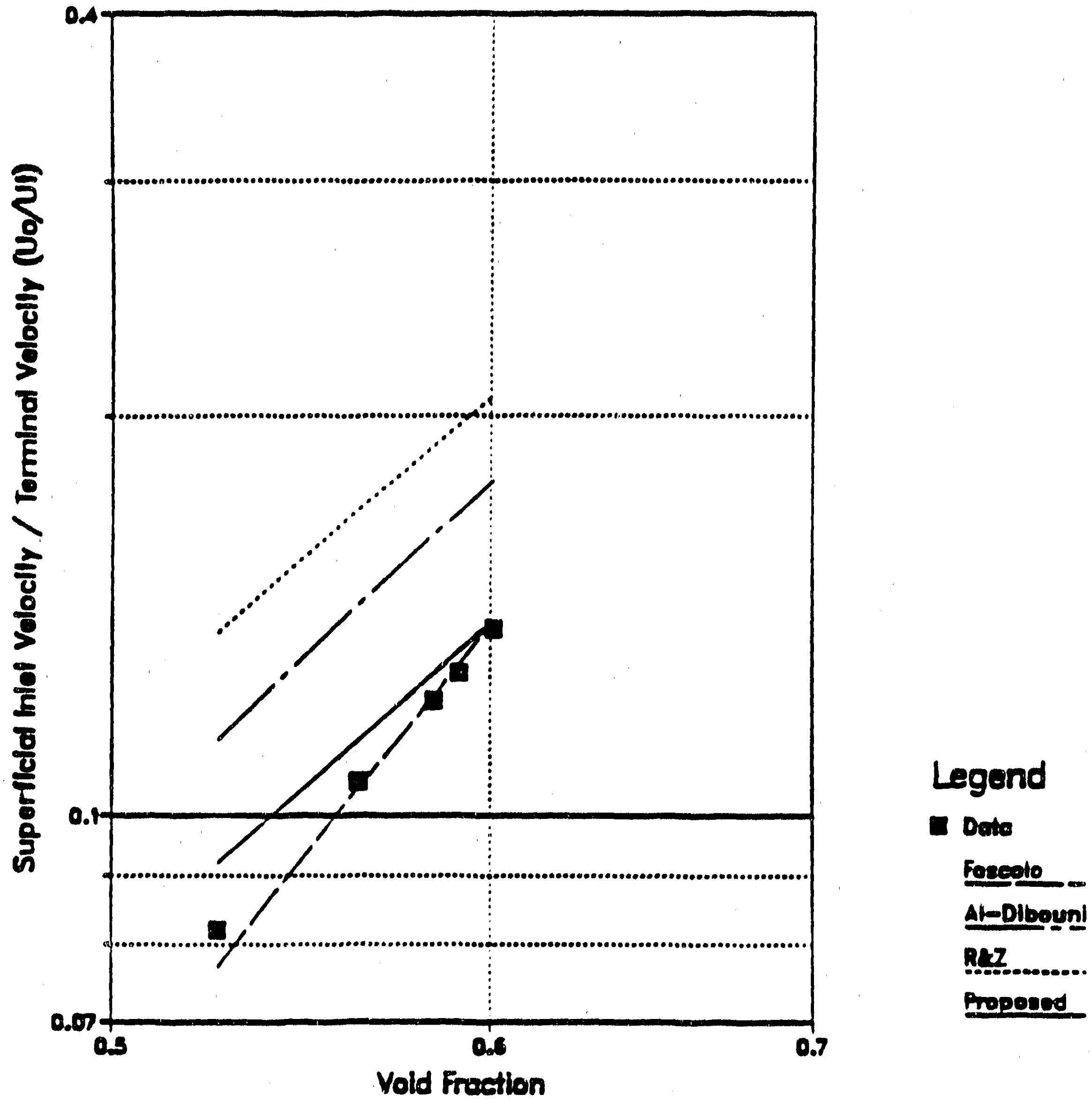

Figure 15. Jacob and Weimer data - carbon powder in gas,

P = 8280 kPa, D_p = 112 microns.

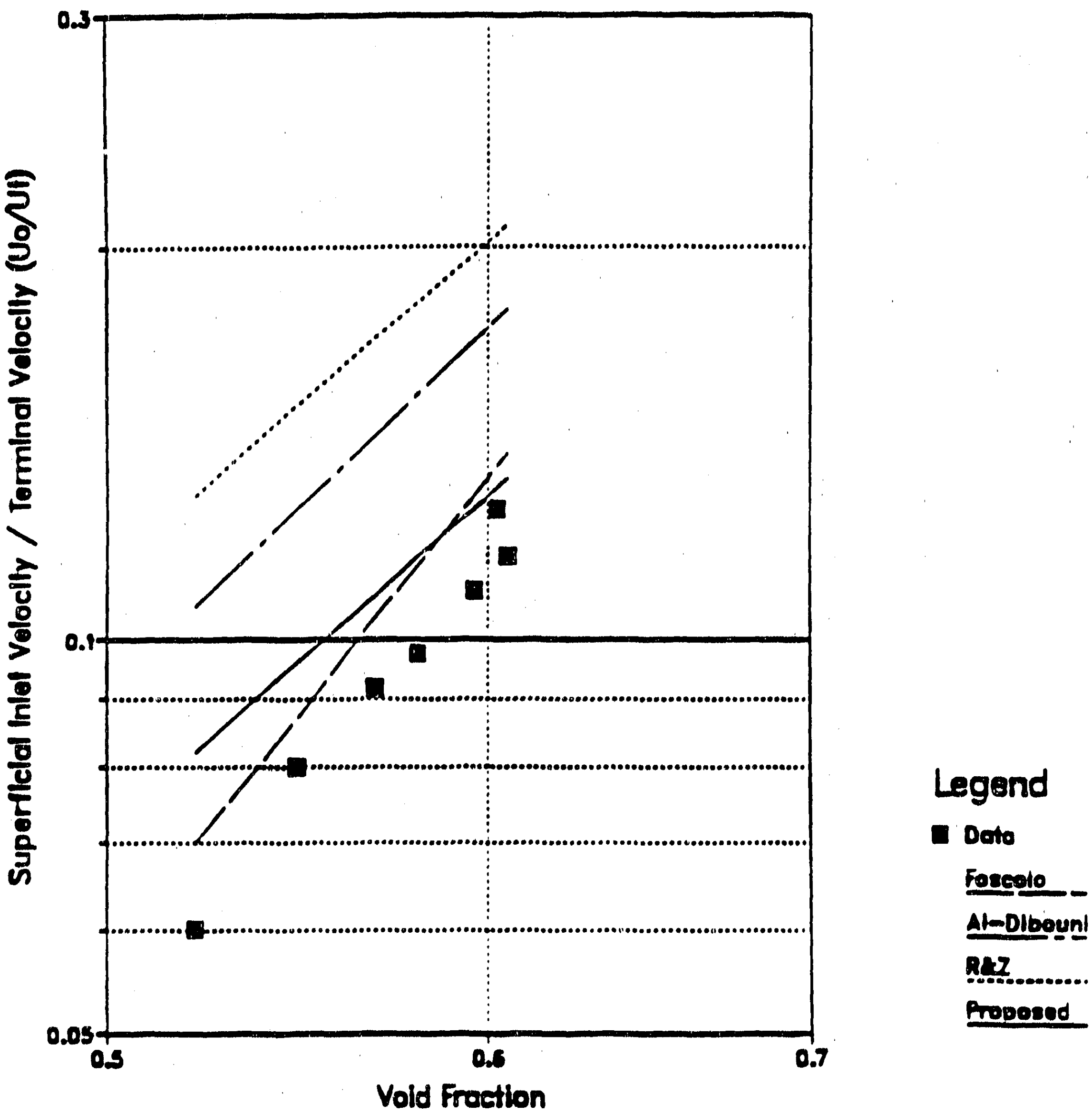

Figure 16. Jacob and Weimer data - carbon powder in gas,

P = 6210 kPa, D_p = 112 microns.

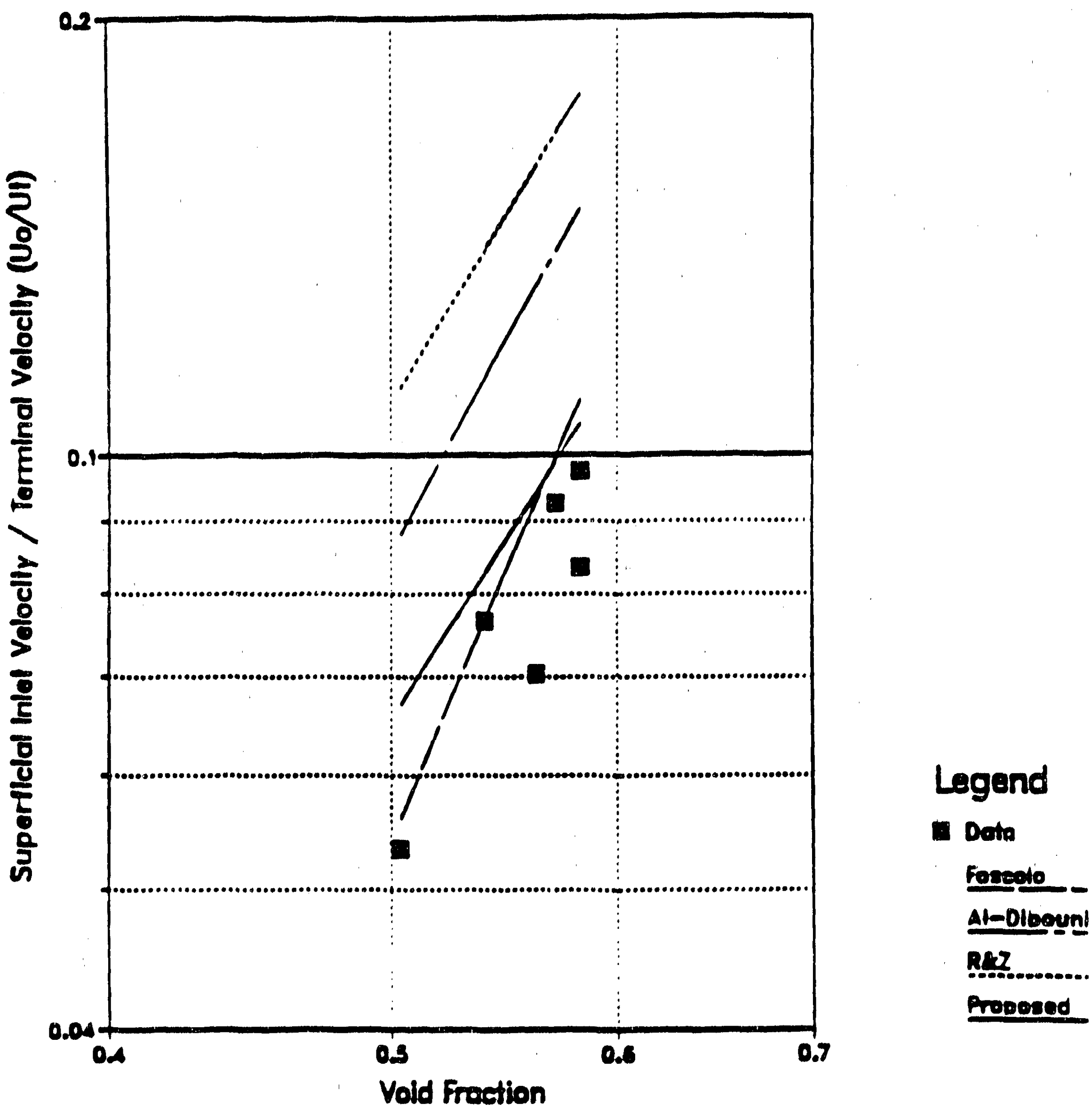

Figure 17. Jacob and Weimer data - carbon powder in gas,

P = 4140 kPa, D_p = 112 microns.

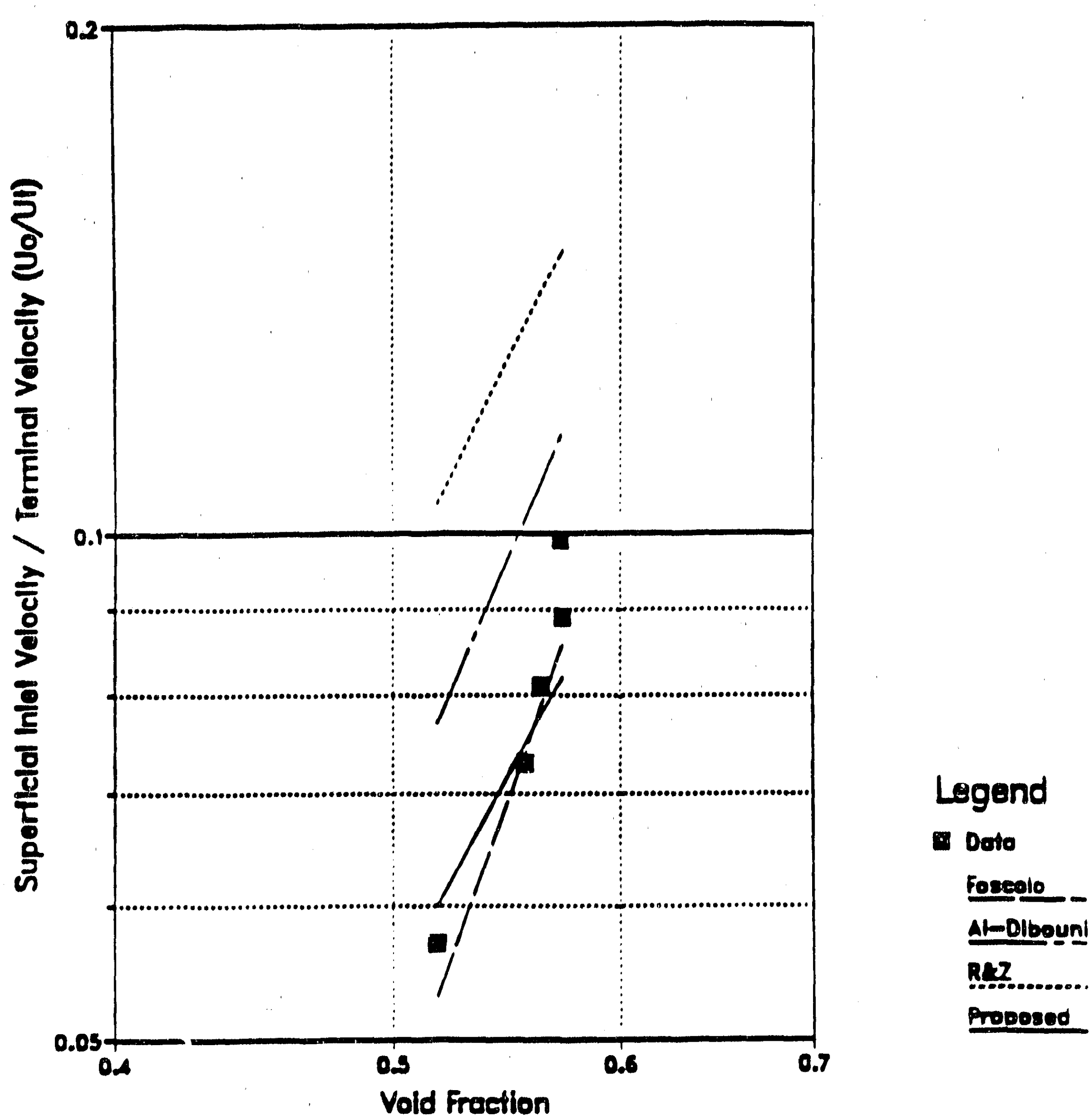

Figure 18. Jacob and Weimer data - carbon powder in gas, P = 2070 kPa, D_p = 112 microns.

are those developed by Richardson and Zaki. Richardson and Zaki performed sedimentation experiments and observed that the $\log(U_o/U_t)$ vs. $\log(\varepsilon)$ relationship was linear. As previously stated, most sedimentation data exist in the creeping flow or viscous region. Upon investigation of fluidization systems, they observed the same linearity; however, the fluidization systems investigated were all in the creeping flow and early transition regimes. Richardson and Zaki therefore concluded that the velocity relationship should be linear for fluidization as well as sedimentation. Consequently, the expansion index, n, should remain constant for any given system and that it should be a function of the terminal Reynold's number.

Richardson and Zaki, assuming that the exponent should remain constant for a given set of fluidization conditions, sought to determine an expression for defining the exponent. They determined the best value of the exponent that would satisfy the relationship for several individual data sets. As a result, one value of the expansion index represents the entire fluidization range for a given system, hence, a linear log - log relationship for each data set. This was a reasonably accurate assumption for the Richardson and Zaki data. The best value of the exponent for each data set was plotted against terminal Reynold's number. Equations 15 - 19 accurately represent the data.

An attempt was made in this study to determine the accuracy of the assumption that the expansion index should remain constant for a given flow regime and set of test conditions. Since the exponent selected by

Richardson and Zaki or those determined by Garside and Al-Dibouni may not be the optimum values over the entire range of conditions studied, the data from each set were examined to determine the exponent for each data point. Fluidization data collected for all three regions (creeping flow region, transition region, and inertial region) was applied to the classical Richardson and Zaki equation to calculate the exponent.

$$n = \log(U_o/U_t)/\log(\epsilon) \tag{57}$$

Values of the exponent were determined from this relationship for all data points. These exponents are plotted against terminal Reynold's number in Figure 19. Note the vertical alignment of data from each fluid particle system. This means that for a constant terminal Reynold's number (or given set of test conditions) the values of the exponent vary; however, the variation is not erratic. There is a tendency for the expansion index to decrease as the fluid velocity is increased. This indicates that the exponent is a function of the changing properties of the suspension and that the viscous and inertial forces are not constant for a given flow regime and set of test conditions.

PROPOSED EXPANSION INDEX

It is apparent from the data presented in the classical format that a single expansion index is not adequate for predicting

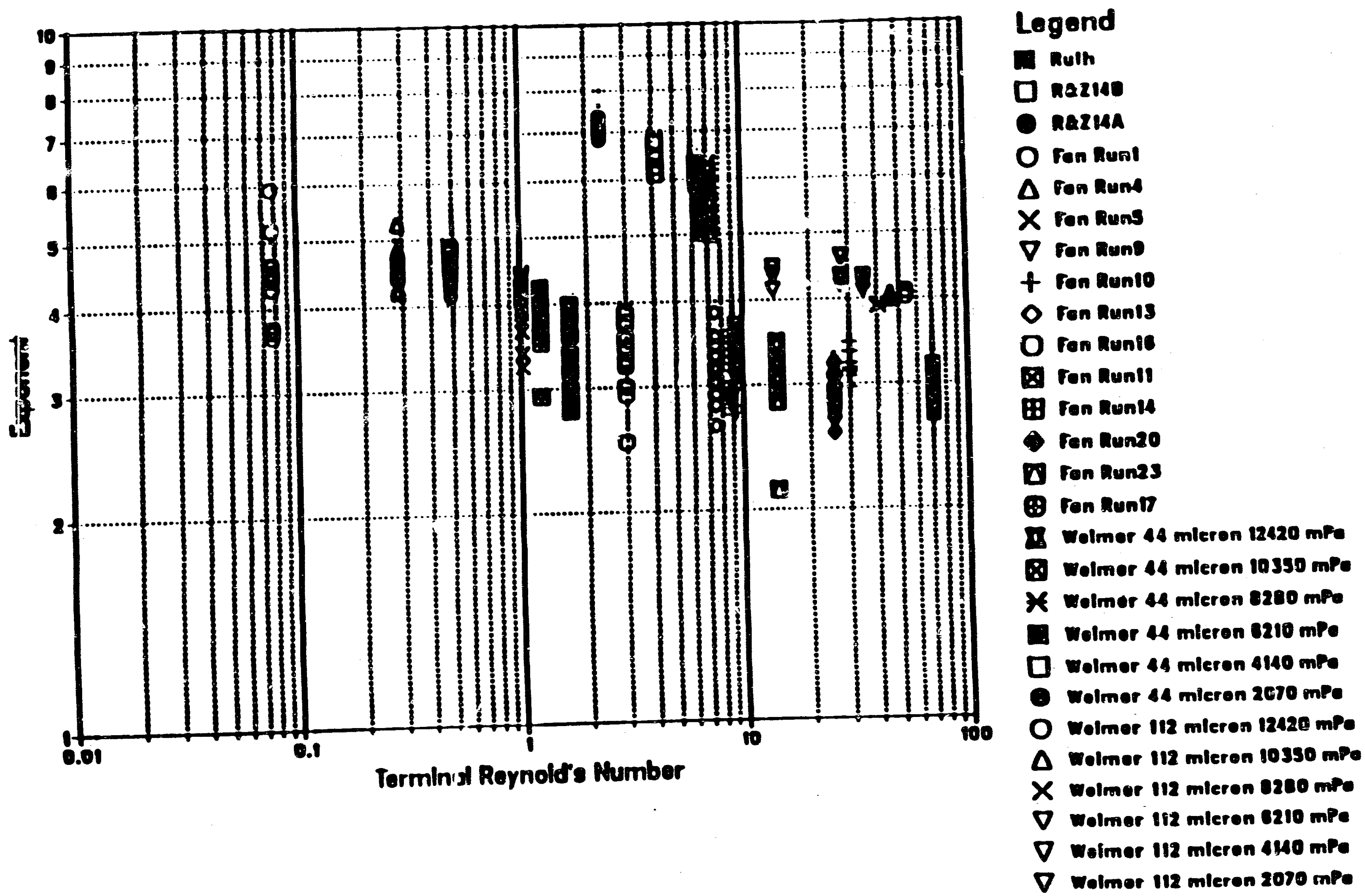

Figure 19. Classical fluidization exponent, $n = \log(U_o/U_t)/\log(\epsilon)$.

fluidization velocities. Therefore, it is proposed to develop a separate relationship for the exponent as a function of the changing characteristics of the suspension.

In order to characterize the suspension at incremental stages of fluidization, it is proposed to treat the exponent as being a function of the intermediate Reynold's number rather than the terminal Reynold's number. As a result, the Reynold's numbers may more realistically represent the viscous and inertial force contributions of the effective fluidizing media suspending the particles at each stage of fluidization. This becomes possible when the slurry viscosity and other slurry properties are used in the Reynold's number. The intermediate Reynold's number can therefore be defined as a function of the effective fluid density and viscosity and the effective terminal velocity of a particle falling through a slurry represented by these effective fluid properties.

$$Re = D_p U_{teff} \rho_{eff} / \mu_{eff} \qquad (58)$$

Most fluidization occurs in the transition region, and the terminal velocity used in the Reynold's number in this region should be corrected to account for the inertial and viscous effects in this region. Combining the drag coefficient equation for the transition region with the equation for terminal velocity for a single particle results in a relationship to describe the free falling velocity of a particle in the transition region (see equation 37). The proportionality of the fluid properties to the terminal velocity as indicated in this equation can be used to make this correction.

$$U_{teff} = U_t(\mu_f/\mu_{eff})^{0.4286}(\rho_f/\rho_{eff})^{0.2857}((\rho_p-\rho_{eff})/(\rho_p-\rho_f))^{0.7143} \qquad (59)$$

As with the Richardson and Zaki model, the expansion index in the proposed model was calculated to determine the values of the exponent that would yield accurate results for fluidization velocity dependence on voidage. Rearranging equation 59 and solving for the exponent gives the following expression for the expansion coefficient.

$$n = \log((\mu_f/\mu_{eff})^{-0.4286}(\rho_f/\rho_{eff})^{-0.2857}((\rho_p-\rho_{eff})/(\rho_p-\rho_f))^{-0.7143} (U_o/U_t)/\log(\epsilon)) + 0.7143 \qquad (60)$$

Values of log(n) are plotted against log(Re) as defined by equations 58 and 60 and are shown in Figure 20. Note that the expansion indexes within each data set, as well as expansion indexes of other data sets can be represented by a single relationship for each flow regime. Each data set is spread out over a common curve resulting in less deviation than with the classical Richardson and Zaki approach. In addition, the entire curve seems to have three distinct regions. At Reynold's numbers below 0.11 and above 10 the exponent remains constant. At Reynold's numbers between 0.11 and 10, the exponent changes; however, the dependence of log(n) appears linear with respect to log(Re). These three linear regions can be represented by the following equations.

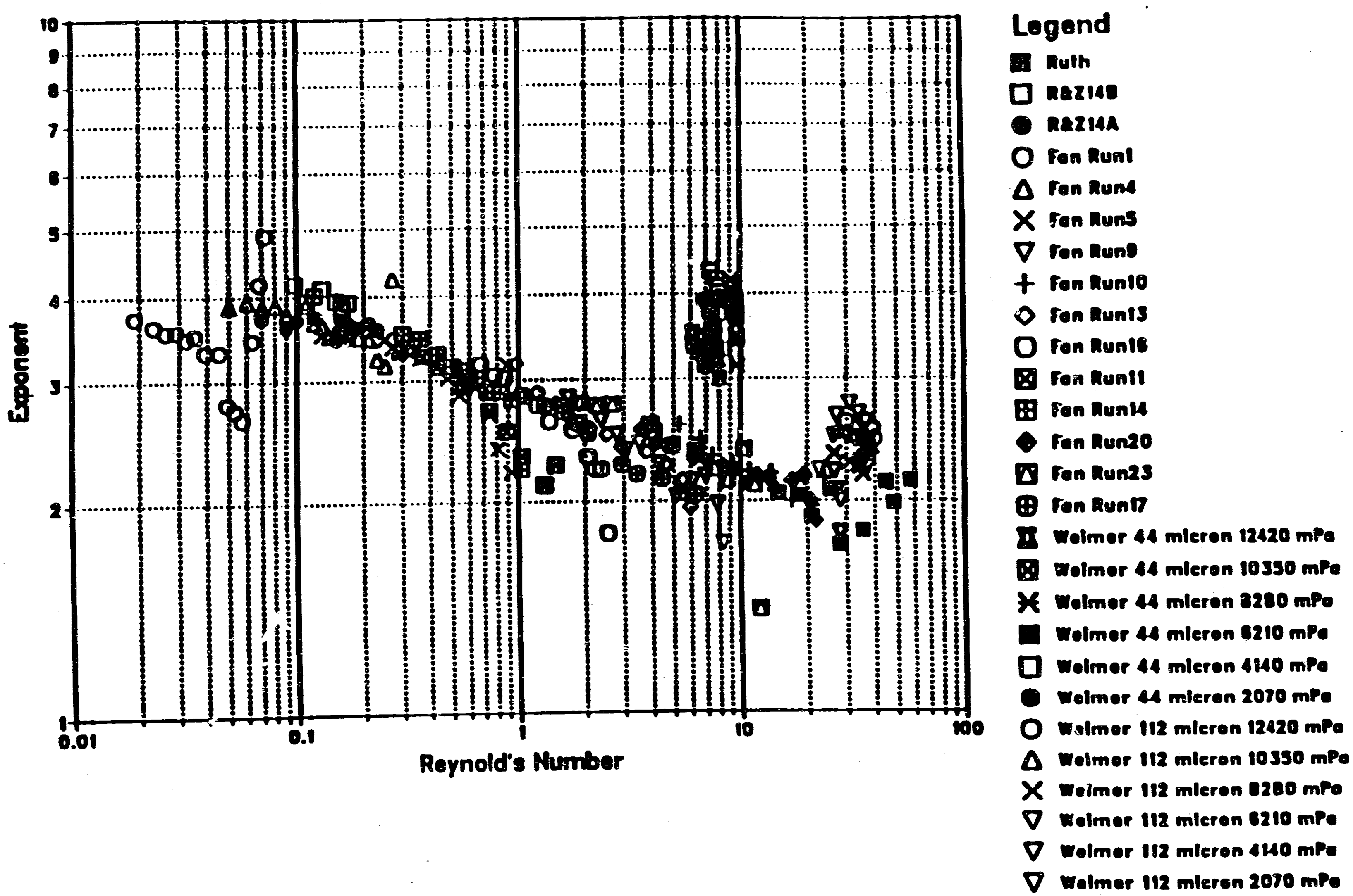

Figure 20. Modified fluidization exponent.

$$n = 3.75 \qquad Re < 0.11 \qquad (61)$$

$$n = 2.856Re^{-0.123} \qquad 0.11 < Re < 10 \qquad (62)$$

$$n = 2.15 \qquad 10 < Re \qquad (63)$$

These distinct regions of the curve are not unexpected; data on the drag coefficient at various Reynold's numbers also show three similar flow regimes and approximately the same region boundaries.

Richardson and Zaki developed relationships for the expansion index based on sedimentation data in the creeping flow regime and fluidization data in the creeping flow and early transition regimes. As previously stated, the expansion index is a measure of the extent to which inertial and viscous forces predominate; therefore, it can be expected that at very low Reynold's numbers, were viscous forces dominate, the exponent should approach a constant value. Similarly, at very high Reynold's number, where inertial forces dominate, the exponent should approach another limit. Consequently, because the Richardson and Zaki data fall in the viscous region, the exponent is justifiably constant for an entire data set. A single bed expansion data set may exhibit characteristics of both the viscous regime and inertial regime; hence a transition regime. Because the exponent is dependent on the extent to which viscous and inertial forces are present, it can be assumed that the exponent should be a function of the changing characteristics of the suspension. This would indicate that the exponent is not constant and would account for the nonlinearity exhibited by fluidization data in the transition flow regime.

Values of the expansion index shown in Figure 20 for the three regions are consistent with the exception of one batch of the Jacob and Weimer high pressure gas data, the data from 44 micron particles. There are several reasons why Jacob and Weimer data may not be as accurate as other presented data. As mentioned previously, gas - solid fluidization systems are prone to exhibit bubbling characteristics. Figure 21 illustrates the transition between uniform bed expansion and minimum bubbling. This is due primarily to the large ratio of particle density to fluid density. An attempt was made to avoid use of data when bubbles were forming, but there could be errors in the selection. Another factor contributing to the inaccuracy of gas fluidization are the presence of fines. Weimer indicated that the 44 micron particles contained a significant number of fines which aid in the fluidization of the larger particles.[20] Consequently, for a given fluidization velocity, predictions of bed voidage are consistently lower than actually observed. Therefore, the deviation of the Jacob and Weimer high pressure gas data can be attributed to the presence of bubbles and/or fines. If there were a significant fraction of fine particles among the nominal 44 micron particles, that alone could account for the higher expansion indexes observed with that material.

COMPARISON OF PROPOSED MODEL WITH PREVIOUS MODELS

The proposed definition of the expansion index as illustrated in Figure 20 suggests that this approach is superior to the classical

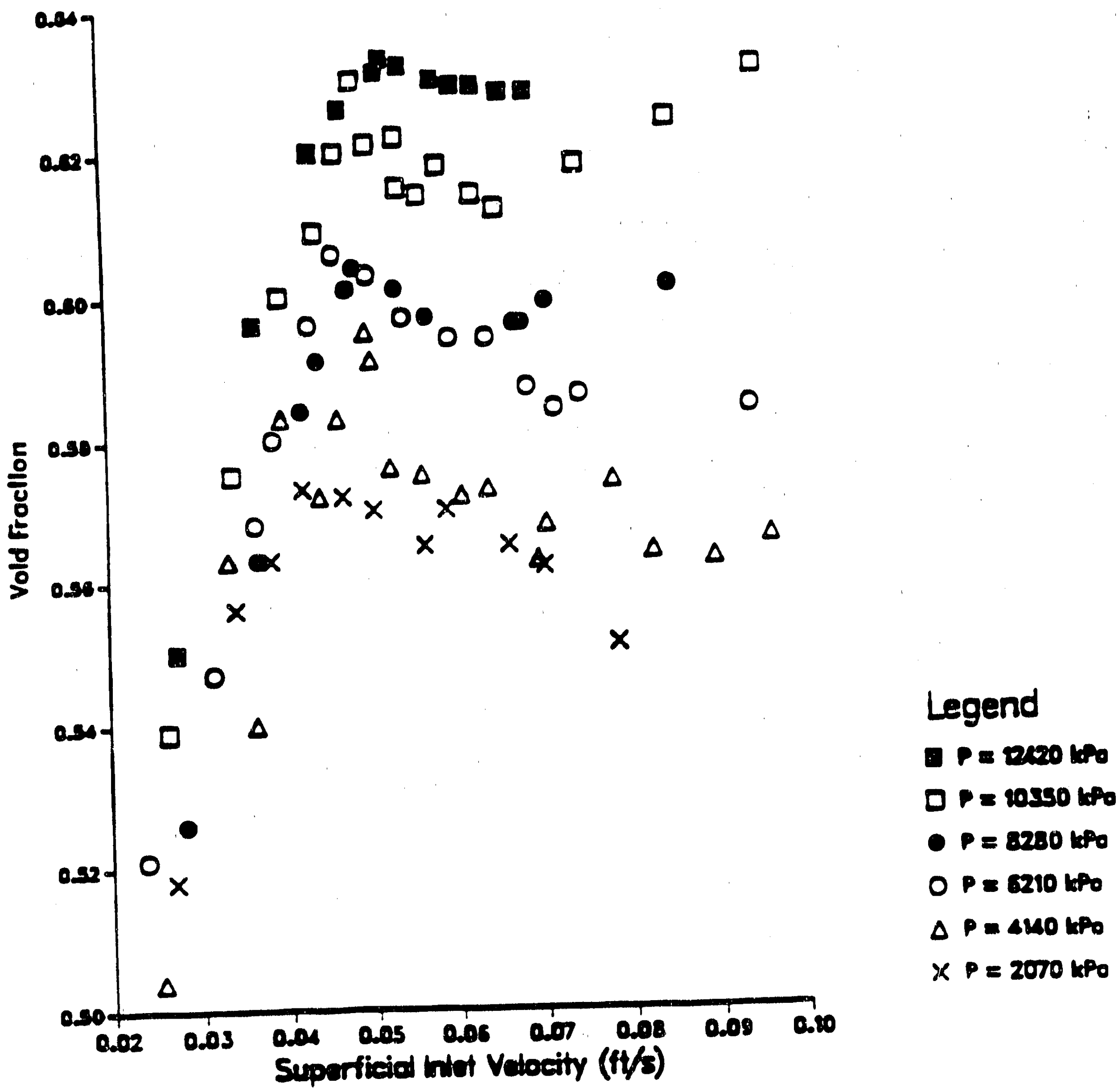

Figure 21. Jacob and Weimer bubbling fluidization data.

definition proposed by Richardson and Zaki. Because expansion indexes within a data set, and over a significant range of data sets, can be well represented by a common relationship, it is reasonable to assume that a resulting fluidization model incorporating this relationship for the index would also reflect this good agreement. Consequently, it is desired to compare the results of the proposed fluidization model with both relationships that can be placed in the Richardson and Zaki form and models that can only be expressed in other forms.

The proposed model is compared with relations developed by Al-Dibouni, Foscolo, and Richardson and Zaki. Although the previous investigators' models are accurate for a select collection of data, the proposed model results in a noticeable improvement over a much wider range of fluidization systems (gases and liquids), particularly in the transition region. Application of the three previous models to the liquid data of Zhang Fan, Ruth and Richardson and Zaki results in consistently low predictions of fluidization velocities for a given void fraction, while predictions of the proposed model yield improved results. This is primarily because the three previous models do not adequately account for the changing viscous and inertial forces during bed expansion.

The Foscolo relationship, as explained previously, was derived from the Ergun equation and expanded for flow through tubes of a constant tortuosity. Although this model accurately accounts for the tendency of the $\log(U_o/U_t)$ vs. $\log(\varepsilon)$ to be nonlinear, it does not adequately account for the different viscous and inertial effects exhibited by gas and liquid fluidization systems. This is evident as a results of the under-predictions of fluidization velocities for liquid systems and the over-prediction of fluidization velocities for gas systems required for given void fractions (see Figures 4, 5, 7, and 8). That is, it does not adequately describe the changing effective properties of the suspension as fluidization proceeds and the fluid bed expands.

The Richardson and Zaki equation, based on experimental data in the creeping flow and early transition regimes, accurately describes the fluid - particle dynamics in the viscous region. Consequently, these regions can be modeled with a straight forward linear expression. Unfortunately, most fluidization data exists in the transition region where inertial forces become significant. As a result, the Richardson and Zaki model breaks down and fluidization velocities are not accurately represented. As with the Foscolo model, gas fluidization velocities are over-predicted, while liquid fluidization velocities are under-predicted (see Figures 4, 5, 7, and 8). This again, is primarily due to failure to account for particle - particle interactions that contribute to the changing effective suspension properties such as viscosity and density. As discussed previously, the expansion index appears to be a function of these changing properties. Consequently, the constant exponent proposed by Richardson and Zaki is inconsistent with observation. This inconsistency was illustrated in Figure 19 by the tendency for the exponent to decrease as fluidization proceeds.

The Al-Dibouni equation originated from a predefined logistic equation for the expansion index in which parameters of the model correspond to limits of the logistic curve and is empirical. This model takes the form of the Richardson and Zaki equation with only a modification in the expansion index. Unfortunately, this modified expansion index is a function of only the terminal Reynold's number; therefore, it remains constant for a given fluidization system yielding a linear $\log(U_o/U_t)$ vs. $\log(\epsilon)$ relationship. Again, this is inconsistent with observations in the transition flow regime. Like the Foscolo and Richardson and Zaki relationships, fluidization velocities are under-predicted for liquid systems and over-predicted for gas systems (see Figures 4, 5, 7, and 8).

Although Richardson and Zaki and Garside and Al-Dibouni were able to predict bed expansions in the viscous region, they had to resort to empirical expressions for the expansion index as a function of Reynold's number. Note that when the slurry properties are used to correct the "terminal velocity" to slurry conditions (as in the proposed model), the expansion index becomes essentially a constant in the viscous region.

The proposed new model is derived to account for varying degrees of particle - particle interactions as fluidization proceeds. Suspended particles appear to be affected by an effective fluid in their environment, and the fluid changes with incremental variations in bed voidage. Therefore, the model describes the fluidizing media as a slurry with viscous properties that vary with fluid rate. This approach compensates for the changing viscous forces as fluidization proceeds and the fluid bed expands. The result is a relationship which adequately describes the tendency for the expansion index to be function of the changing suspension properties, and which accounts for the effective buoyancy and gravitational force contributions from the other surrounding particles. Consequent, this model more accurately predicts the fluidization velocities for a wider range of fluidization systems. To compare quantitatively the agreement of the correlations with the experimental results, the sum of the differences in predicted and observed void fractions squared (sum-of-the-squares), as well as the standard deviation was analyzed. Because the Fan data appeared to be the most reliable over a wide range of Reynold's number, they were used for the analysis. There were 152 data points and 12 different fluid / particle combinations to be analyzed. A summary of this quantitative comparison is listed in Table 2. The results indicate that the proposed model yields the best results. An overall sum-of-the-squares and standard deviation for the proposed model and the observed data are 0.0147 and 0.0098, respectively. This is significantly better than the values of 0.0712 and 0.0217 for the next best model, that of Richardson and Zaki.

APPLICATION OF MODEL TO BIMODAL FLUIDIZED BEDS

The proposed model predicts bed expansion of unimodal particles very well, and it is worthwhile to consider if it provides insight that

Table 2. Quantitative analysis of Fan data.

Run No.	No. of Points	Sum of the Squares: Richardson and Zaki	Sum of the Squares: Al-Dibouni	Sum of the Squares: Foscolo	Sum of the Squares: Proposed	Standard Deviation: Richardson and Zaki	Standard Deviation: Al-Dibouni	Standard Deviation: Foscolo	Standard Deviation: Proposed
1	14	0.0045	0.0148	0.0072	0.0053	0.0187	0.0337	0.0235	0.0201
4	17	0.0020	0.0057	0.0015	0.0006	0.0111	0.0189	0.0097	0.0063
5	18	0.0056	0.0250	0.0185	0.0009	0.0182	0.0383	0.0330	0.0071
9	12	0.0044	0.0254	0.0476	0.0009	0.0201	0.0480	0.0658	0.0090
10	11	0.0017	0.0069	0.0292	0.0011	0.0129	0.0262	0.0540	0.0107
11	9	0.0099	0.0265	0.0249	0.0012	0.0352	0.0575	0.0557	0.0124
13	11	0.0083	0.0332	0.0518	0.0008	0.0288	0.0576	0.0720	0.0026
14	11	0.0063	0.0186	0.0155	0.0006	0.0250	0.0431	0.0394	0.0076
16	13	0.0087	0.0305	0.0330	0.0008	0.0270	0.0504	0.0524	0.0081
17	10	0.0099	0.0390	0.0643	0.0012	0.0332	0.0659	0.0845	0.0118
20	15	0.0063	0.0261	0.0587	0.0002	0.0212	0.0432	0.0647	0.0014
23	11	0.0036	0.0196	0.0448	0.0011	0.0182	0.0422	0.0638	0.0101
Overall	152	0.0712	0.2713	0.3970	0.0147	0.0217	0.0424	0.0513	0.0098

is helpful in exploring other related problems. Particulate fluidization of different size and/or density particles will be considered next. Although the arguments can be expanded to describe any number of different particles, the current discussion will be limited to bimodal systems (two different particles). The model for unimodal suspensions suggests that in bimodal fluidization the small particles contribute to the fluidization of the large particles. Consequently, because the small particles influence the large particles to different extents during bed expansion, bimodal systems will be described by considering incremental increases in fluid velocity. At low superficial inlet velocities, neither large particles nor small particles would be fluidized. As the velocity is increased, the pressure gradient would increase as with any packed bed. When the velocity within the voidages between the large particles exceeds the minimum fluidization velocity of the small particles, the small particles would become fluidized. Within the volume of the unfluidized larger particles, however, wall effects are severe; in many cases the small particles would not be free to move and thus not be fluidized. At a somewhat higher velocity, the superficial velocity is high enough to fluidize the smaller particles (above the mixture), but not high enough to fluidize the larger particles. At this point some of the smaller particles may be "blown" through the bed of the larger particles and be fluidized at the top of the bed. Larger particles may be mixed (or dispersed) with the smaller particles, but they would not be stably fluidized. There would then be a profile of larger particles from the dispersion / settling in the fluidized bed, but the concentration of the large particles would approach zero at the top of the bed, and the concentration of fluidized small particles would be expected to approach zero at the bottom of the bed, which would contain settled large particles.

At a higher velocity, the larger particles would be fluidized by a fluid with a composition of the slurry of the fluidized smaller particles, not by pure fluid alone. At this velocity there could be two homogeneous regions of the bed. In the upper region, there will be only smaller particles fluidized. In the lower region, there will be a mixture of large and small particles. The larger particles can not necessarily reach the top of the fluidized smaller particles. The height of the region with large particles would depend upon the number of large particles present. This is primarily because the bed expansion of these larger particles is governed by the extent to which the slurry of smaller particles can fluidize the large particles. The size of each region will depend upon the initial mixture. There can be a transition between the two homogeneous regions because of the dispersion of the larger particles.

As the fluid velocity is increased further, the height of the lower fluidized bed region will increase as the bed height for the larger particles fluidized in the slurry of small particles increases. There can also be an expansion of the small particles on the top of the bimodal portion of the bed. Eventually, at very high velocities, both particles could be fluidized independently with a transition region between the two.

All of the above descriptions have assumed that the particles were initially arranged with both particles fractions well mixed. If the particles fractions were initially segregated, there may be no way for the small particles at the top of the bed to aid in the fluidization of the large particles at the bottom. Consequently, if the velocity were increased as described above and then decreased, different conditions would exist at the same flow rate because the particles would become segregated prior to decreasing the velocity.

The proposed model for unimodal fluidized beds was developed assuming no axial property variations; therefore, it is applicable for suspensions, or portions of suspension, that are homogeneous. Consequently, the region of a bimodal suspension for which the proposed model will apply is the lower portion where both small and large particles are present. In this region the large particles are fluidized by a slurry of smaller particles.

Dutta[21] presented data on fluidization of glass and chalcopyrite with water. His data exhibit distinct concentration profiles as the small particles migrate to the top of the suspension and the large particles to the bottom of the suspension. Figures 22 and 23 illustrate the concentration profiles. At low column heights, it is worth noting that the concentration of the smaller particles does not appear to approach zero at the bottom of the column, and complete segregation does not occur. Therefore, near the bottom of the column the larger particles appear to be suspended by a slurry of smaller particles.

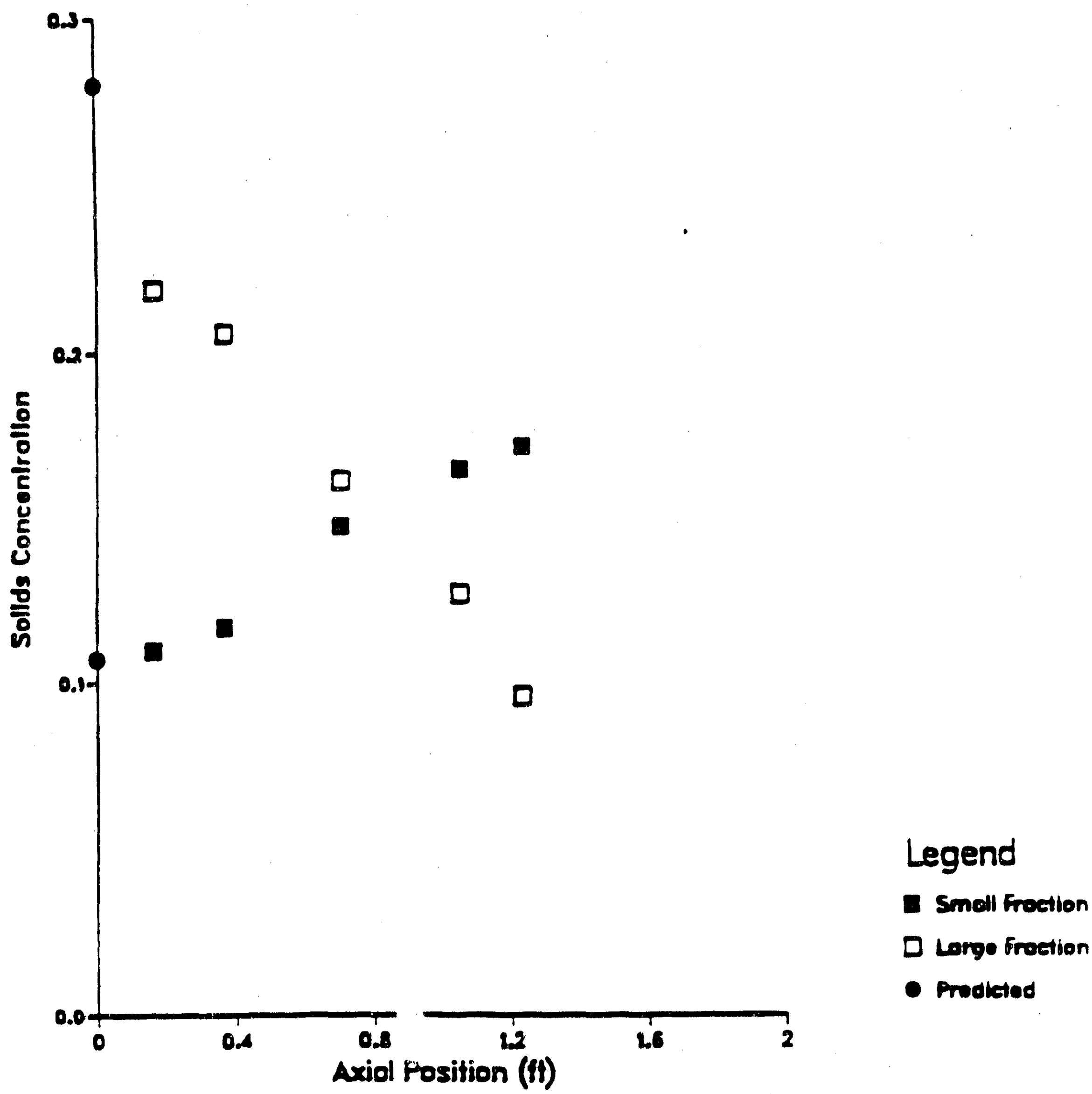

Figure 22. Dutta bimodal segregated data - Run 1, glass/chalcopyrite in water.

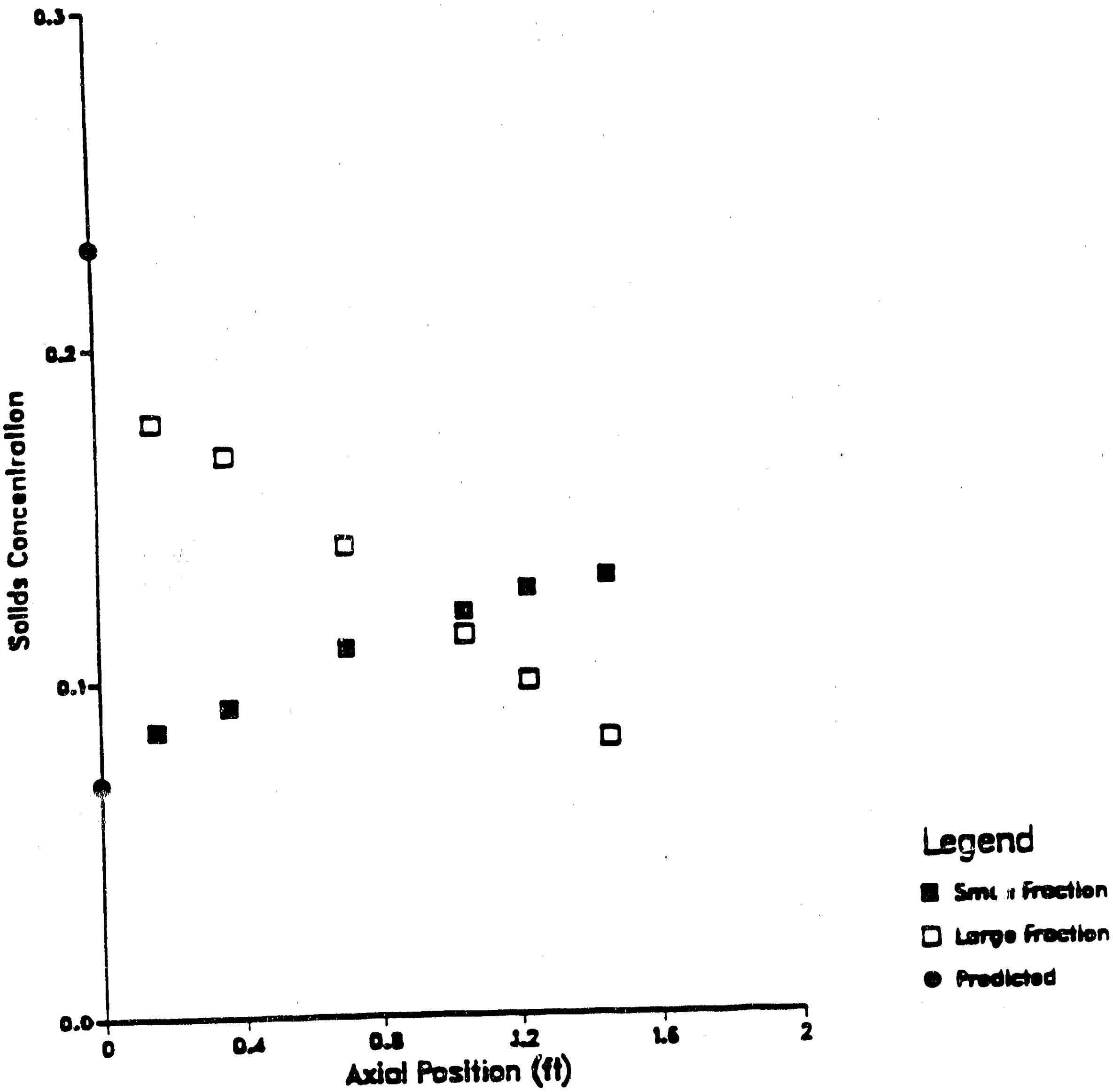

Figure 23. Dutta bimodal segregated data - Run 2, glass/chalcopyrite in water.

Then, according to the proposed model, this slurry has properties of a unimodal suspension of small particles. That is, the viscosity influencing the suspension of the large particles is the effective viscosity as determined by a unimodal suspension of the small particles. Similarly, the density influencing the suspension of the larger particles is the density as determined by a unimodal suspension of the small particles. As a result, the superficial inlet velocity is noticeably above the minimum fluidization velocity of the large particles in a suspension of small particles.

This phenomena can be analytically described by application of the proposed model. All particles and fluid properties, as well as the superficial inlet liquid velocity, are known; therefore, the solids concentration of the small particles can be calculated. Figure 24 indicates the solids concentrations and the effective slurry properties as "seen" by the larger particles. These effective fluid properties may further be used to determine the minimum fluidization velocity required to suspend the large particle with the slurry of small particles. Applying the following equation to the data of Figure 24 yields these minimum fluidization velocities, and the results are listed in Figure 25.

$$1.75/\varepsilon^3(d_pU_{mf}\rho/\mu)^2 + 150(1-\varepsilon_{mf})/\varepsilon_{mf}^3(d_pU_{mf}\rho/\mu) = d_p^3\rho(\rho_p-\rho)g/\mu^2 \quad (64)$$

where

U_{mf} = minimum fluidization velocity

ε_{mf} = minimum void fraction

SET NO	PARTICLE DIAMETER ft	PARTICLE DENSITY lb/cu ft	LIQUID VISCOSITY lb/(ft s)	LIQUID DENSITY lb/cu ft	TERMINAL VELOCITY ft/s	INLET FLOW ft/s	VOID FRACTION	SOLID FRACTION	EFFECTIVE VISCOSITY
1	0.00180	156.0705	0.000672	62.4300	0.2024	0.0709	0.7370	0.2630	0.0013
2	0.00180	156.0705	0.000672	62.4300	0.2024	0.1010	0.8100	0.1900	0.0011
3	0.00180	156.0705	0.000672	62.4300	0.2024	0.0817	0.7680	0.2320	0.0012
4	0.00180	156.0705	0.000672	62.4300	0.2024	0.1499	0.9170	0.0830	0.0008
5	0.00180	156.0705	0.000672	62.4300	0.2024	0.1591	0.9330	0.0670	0.0008
6	0.00180	162.3134	0.000672	62.4300	0.2323	0.1201	0.8270	0.1730	0.0010

Figure 24. Dutta bimodal segregated data applied to proposed model to determine effective slurry properties.

EFFECTIVE DENSITY	VISCOSITY RATIO	DENSITY RATIO	DEL DENSITY RATIO	EFFECTIVE REYNOLDS NUMBER	PROPOSED N
87.0575	0.7421	0.9094	0.8041	12.8014	2.1500
80.2217	0.8185	0.9309	0.8603	17.9118	2.1500
84.1546	0.7752	0.9182	0.8282	14.8852	2.1500
70.2022	0.9229	0.9670	0.9400	26.5484	2.1500
68.7039	0.9380	0.9730	0.9517	27.9353	2.1500
79.7098	0.8356	0.9326	0.8731	22.2472	2.1500

Figure 24. (Continued).

SET NO	PARTICLE DIAMETER ft	PARTICLE DENSITY lb/cu ft	SLURRY VISCOSITY lb/(ft s)	SLURRY DENSITY lb/cu ft	MINIMUM FLUIDIZATION VELOCITY	MINIMUM VOID FRACTION	LEFT SIDE EQ. 64	RIGHT SIDE EQ. 64
1	0.00180	187.2846	0.001348	87.0575	0.0063	0.4150	907.2574	907.8115
2	0.00180	187.2846	0.001072	80.2217	0.0083	0.4150	1411.6041	1412.0836
3	0.00180	168.5562	0.001217	84.1546	0.0058	0.4150	905.8236	906.0608
4	0.00180	168.5562	0.000810	70.2022	0.0100	0.4150	1987.3241	1987.8413
5	0.00180	168.5562	0.000780	68.7039	0.0106	0.4150	2130.9415	2130.0822
6	0.00180	187.2846	0.001022	79.7098	0.0088	0.4150	1552.9910	1552.5779

Figure 25. Dutta slurry data applied to minimum fluidization.

Because the minimum fluidization velocities are greater than the superficial inlet superficial velocities reported in Figure 24, the analysis above is consistent with observations.

The proposed model can also be applied to estimate the actual solids concentrations of both large and small particle fractions of a suspension; however, the model only predicts bed expansion for homogeneous suspension. For segregated beds, the model is applicable for the lower most region where both small and large particles are present. As previously described, this region is the most likely portion of a segregated suspension to have a homogeneous mixture of both the large and small particles. The unimodal expansion in the upper region can then be described by the proposed unimodal model. For well mixed bimodal systems, where no segregation is apparent, the model is applicable over the entire bed height.

To predict the expansion in a homogeneous bimodal region it is necessary to analyze the fluidization in two steps. The first step of the analysis considers the fluidization of the smaller particles as if the larger particles are not present. This step determines the effective properties of the fluid suspending the large particles. The second step involves fluidization of the larger particles by the slurry with properties determined in the first step.

For the first step, fluidization of the smaller particles, it is reasonable to assume that the smaller particles "see" the viscosity of a slurry as the fluidizing media consisting of the pure fluid and other smaller particles. The large particles have little direct influence. Consequently, it is proposed that only the small particles contribute to the effective viscosity of the slurry. That is, only the small particles are assumed to be present in the shear fields surrounding other small particles. As a result, the Ting and Luebbers equation for effective viscosity can be altered to account for the solids concentration of the smaller particles in the absence of the larger particles.

$$\mu_{eff}' = (0.464+0.21\varepsilon_s/(1-\varepsilon_L))/(0.464-0.78\varepsilon_s/(1-\varepsilon_L)) \qquad (65)$$

As stated previously, the density of the fluidizing media contributes to the viscous and inertial affects due to the fluid accelerating around the particles, as well as the buoyant forces acting on the particles. It is proposed that the effective fluid accelerating around the suspended smaller particles consists of the pure fluid and other smaller particles. Consequently, the effective density is a function of the pure fluid density and void fraction and the smaller particle density and solids concentration in the absence of the larger particles. Consequently, the relationship to be used in the density ratio of the proposed model to account for the affects of the accelerating fluid is as follows.

$$\rho_{eff}' = (\varepsilon\rho_f+\varepsilon_s\rho_s)/(1-\varepsilon_L) \qquad (66)$$

Because the pressure drop across a suspension is directly influenced by the total solids concentration of the system, and the buoyant forces are directly influenced by the pressure drop, it can be concluded that the buoyant forces should be a function of the total solids concentration of the system. Consequently, as in unimodal fluidization, all particles of the suspension, large and small, contribute to the buoyant forces of the suspension. Therefore, the density to be used in the density difference ratio must incorporate the total solids volume concentration.

$$\rho_{eff}' = \varepsilon_s \rho_s + \varepsilon_L \rho_L + \varepsilon \rho_f \tag{67}$$

With the exception of the density difference ratio, the effective properties of the suspension are functions of a corrected solids concentration based on the absence of the larger particles. Consequently, the void fraction must also be corrected for the absence of the larger particles.

$$\varepsilon' = (1-\varepsilon_s-\varepsilon_L)/(1-\varepsilon_L) \tag{68}$$

Similarly, the superficial inlet velocity must be corrected for the absence of the larger particles.

$$U_o' = U_o/(1-\varepsilon_L) \tag{69}$$

Incorporating the above effective fluid properties into the form of the proposed model results in the following relationship for fluidization of the small particle fraction.

$$U_o'/U_{ts} = \varepsilon'^{(n-0.7143)}(\mu_f/\mu_{eff}')^{0.4286}(\rho_f/\rho_{eff}')^{0.2857}((\rho_s-\rho_{eff}')/(\rho_s-\rho_f))^{0.7143} \quad (70)$$

The terminal velocity of the small particles, U_{ts}, is determined based on the particle falling through a media having properties of the pure fluid.

$$U_{ts} = (0.0721gD_{ps}^{1.6}(\rho_s-\rho_f)/(\mu_f^{0.6}\rho_f^{0.4}))^{0.7143} \quad (71)$$

The second step of the bimodal analysis involves the fluidization of the larger particles by a slurry of the fluid and the smaller particles. This step may be treated the same as unimodal fluidization. That is, the fluid phase may be considered to have properties of the slurry calculated in the first step and the total solids concentration may be considered to be the solids concentration of the large particles. Therefore, the effective viscosity of the slurry to be used for fluidization of the large particles is a function of the large particle solids concentration (total solids concentration for unimodal systems) and the slurry viscosity as calculated in the first step (pure fluid viscosity for unimodal systems).

$$\mu_{eff}'' = ((0.464+0.21\varepsilon_L)/(0.464-0.78\varepsilon_L))\mu_s, \quad (72)$$

The effective fluid accelerating around the larger particles is proposed to consist of the pure fluid, the smaller particles, and other larger particles. Therefore, the effective density to be used to describe the properties of the fluid accelerating around the suspended larger particles is a function of the total volume average concentration of all particles in the system.

$$\rho_{eff}'' = \varepsilon_s \rho_s + \varepsilon_L \rho_L + \varepsilon \rho_f \tag{73}$$

As in the first step of the analysis, all particles are proposed to contribute to the effective buoyant forces during fluidization of the larger particles. Consequently, the effective density to be used in the density difference ratio is a function of the total solids concentration of the system suspension.

$$\rho_{eff}'' = \varepsilon_s \rho_s + \varepsilon_L \rho_L + \varepsilon \rho_f \tag{73}$$

Because the total solids concentration is considered to be the large particle solids concentration, the void fraction to be used in the model is the volume occupied by the pure fluid and the smaller particles. Therefore, the void fraction is simply written as follows.

$$\varepsilon'' = (1-\varepsilon_L) \tag{74}$$

Substituting the effective fluid properties calculated from the first step for the pure fluid properties of the proposed model, and incorporating the effective fluid properties as described in the second step results in the following relationship for fluidization of the large particles.

$$U_o/U_{tL} = \varepsilon''^{(n-0.7143)}(\mu_{eff}'/\mu_{eff}'')^{0.4286}(\rho_{eff}'/\rho_{eff}'')^{0.2857} \\ ((\rho_s-\rho_{eff}'')/(\rho_s-\rho_{eff}'))^{0.7143} \tag{75}$$

The terminal velocity of the large particles, U_{tL}, is determined based on the settling of a particle through a media having properties of the slurry calculated in the first step of the analysis.

$$U_{tL} = (0.0721gD_{pL}^{1.6}(\rho_L-\rho_{eff}')/(\mu_{eff}'^{0.6}\rho_{eff}'^{0.4}))^{0.7143} \tag{76}$$

Data presented by Duijn[22] for bimodal studies of glass beads and ilmenite in water are applied to this two step process. Duijn reported results in the form of average void fraction at distances above the distributer plate. The total solids concentration axial profiles for the column appear relatively flat; therefore, it is assumed that the individual component solids concentration axial profiles are also flat. That is, the solids concentrations for the individual particle fractions are relatively constant from the bottom to the top of the column. All fluid and particle properties are known with the exception of the individual solid fractions. Therefore, because the two step process involves two equations and two unknowns, the relationship can be solved by trial and error. A summary of the results is listed in Table 3.

This method can be further applied to the segregated bed fluidization data of Dutta. As previously mentioned, his data exhibit

Table 3. Duijn bimodal data.

Superficial Inlet Velocity m/s	calculated ε_b	calculated ε_s	calculated ε_f	reported ε_f	% difference
0.0062	0.13	0.23	0.64	0.68	6.06
0.0032	0.10	0.33	0.57	0.60	4.60
0.0116	0.11	0.13	0.76	0.76	0.00

distinct concentration profiles for both the small and large particle fractions. Application of the two step analysis to this data yields individual solids fractions representative of the suspension near the bottom of the column. The two step method applies to homogeneous suspensions or portions of suspension; therefore, the results can be interpreted as the fraction of the individual components at the lower, homogeneous region of the suspension where both large and small particles are present. This portion of the suspension corresponds to the left most data of figures 22 and 23. The results may also be interpreted as the fraction of the individual components required to make the entire suspension homogeneous. A summary of the results for the model is listed in Table 4.

Because the proposed fluidization analysis of bimodal segregated suspension is new, existing data required to asses the merits and generalities of the model are difficult to obtain. Dutta presented data consisting of a fixed number of large and small particles. His data would have been more useful for testing the model if he had varied the number of large and small particles present. This would have provided additional insight into the various extents to which the small particles contribute to the fluidization of the larger particles as a function of axial position.

Table 4. Dutta bimodal data.

System	Inlet Velocity m/s	predicted average concentrations for bottom of column			extrapolated data to bottom of column			fluid fraction percent difference
		ε_b	ε_s	ε_f	ε_b	ε_s	ε_f	
glass/chalcopyrite	0.0216	0.28	0.11	0.61	0.22	0.10	0.67	9.4
glass/chalcopyrite	0.0308	0.23	0.07	0.70	0.18	0.08	0.74	5.5
glass/limestone	0.0249	0.21	0.13	0.66	0.21	0.08	0.71	7.3
glass/limestone	0.0485	0.11	0.05	0.84	0.07	0.05	0.88	4.6
sand/chalcopyrite	0.0366	0.19	0.07	0.74	0.19	0.05	0.76	2.7

CHAPTER V

CONCLUSIONS AND RECOMMENDATIONS

Although there are similarities in predictions between the proposed model and those developed by Richardson and Zaki, Foscolo, and Al-Dibouni for certain systems, the new model is more accurate over a wider range of flow regimes and systems types. In addition, the proposed relationship resulted from a more analytical approach to actual observed sedimentation and particulate fluidization phenomena.

Richardson and Zaki developed a linear log - log model based on data in the creeping flow and early transition regions. Because the data of the creeping flow region do not exhibit curvature, the linear model is adequate. Unfortunately, most fluidization data exists in the transition region where curvature is more evident and viscous as well as inertial forces are significant. Consequently, the Richardson and Zaki model is not accurate over a wide range of flow regimes and systems. The Al-Dibouni model uses different values for the expansion index but has the same problems outside the viscous region since it also assumes that the index is constant. The Foscolo et al relationship was developed from the Ergun equation for flow through packed beds. They accounted for tortuosity by incorporating a constant factor. The pressure drop then took the form of the Blake-Kozeny equation. Although their relationship accounts for the curvature during fluidization, it consistently under-predicts fluidization velocities for solid - liquid systems and over-predicts fluidization velocities for solid - gas systems.

One weakness of all previous models is their failure to account for the changing fluidization media as the bed expands. Suspended particles "see" a different fluid or slurry at incremental stages of bed expansion. Inclusion of these effects is the principal merit of the proposed new model. The effective properties of the proposed model appear to adequately correct for these changing slurry properties. In addition, the expansion index used in the model is a function of the intermediate Reynold's number, which in turn is a function of the changing fluid properties of the suspension; consequently, the curvature of the transition region, and the linearity of the creeping flow and inertial regions are well represented for a wide range of flow regimes and system types.

From this study the need for additional data, both unimodal and bimodal, has become more evident. Future work would involve extending the proposed model to various and different regions of segregated and mixed fluidized suspensions to describe the changing contributions of the smaller particles on the suspension of the larger particles at different column heights. As previously described, the proposed model suggests that a segregated bimodal suspension can have a homogeneous upper region of small particles and a homogeneous lower region of large and small particles with a transition region between the two. Further analysis of this type data would be useful in determining how the proposed model can be applied to the entire segregated suspension rather than only the lower homogeneous region. Hold-ups at various axial positions in the column would be predicted as a function of effective suspension properties and column height. Different scenarios of fluidization such as initial unfluidized packed bed conditions could be analyzed to determine how segregation proceeds. Three initial condition scenarios could be: (1) a lower packed region of large particle with an upper packed region of small particles; (2) a lower packed region of small particles with an upper packed region of larger particles; and (3) a well mixed region of large and small particle. Eventually, it would be useful to analyze the applicability of the model to multimodal systems.

Because gas fluidization data are difficult to obtain without the presence of bubbles, few data of this type are available for particulate fluid bed expansion. Consequently, efforts to obtain and apply gas particulate data, particularly high pressure gas data, would be useful for providing a better understanding of the differences in fluidization phenomena between gas and liquid systems. Because gas systems tend to be in the inertial region, additional gas data would be useful to extend the proposed model over a much wider range of flow regimes.

Finally, data analyzed in this study were selected based, in part, on negligible wall effects. Only small particle diameter to column diameters were used. It was obvious during the course of collecting the data that wall effects are significant for relatively small columns. Additional drag forces are imposed on the fluidized slurry from the walls of the container and velocity profiles are severely altered. As a result, bed expansion is a function of this diameter ratio. Consequently, liquid and gas fluidization data collected from various diameter columns would be useful for providing additional insight to a more encompassing bed expansion relationship.

BIBLIOGRAPHY

1. Robinson, C. E., "Improvement in Furnaces for Roasting Ores," United States Patent Office, Patent No. 212,508 (1879).

2. Ikeda, Y., "How to Apply Fluidized Bed to Catalytic Reactions," FLUIDIZATION '85 Science and Technology, Kwauk, Mooson and Kunii, Daizo, 1-2 (1985).

3. Shor, J. T. and Watson, J. S., "The Sedimentation of Bimodal Distributions of Unflocculated Microspheres," Oak Ridge National Laboratory (1987).

4. Richardson, J. F., and Zaki, W. N., "Sedimentation and Fluidization: Part I," Trans. Instn. Chem. Engrs., 32, 35-53 (1954).

5. Fan, Z., Xuanyu, Z., and Lichuang, X., "Particulate Fluidization of Uniformly Sized Spheres," FLUIDIZATION '85 Science and Technology, Kwauk, Mooson and Kunii, Diazo, 283-294 (1985).

6. Steinour, H. H., "Rate of Sedimentation of Nonflocculated Suspensions of Uniform Spheres," Industr. Engng. Chem., 36, 618-624 (1944).

7. Foscolo, P. U., Gibilaro, L. G., and Waldram, S. P., "A Unified Model for Particulate Expansion of Fluidized Beds and Flow in Fixed Porous Media," Chem. Engr. Sci., 38, 1251-1260 (1983).

8. Jacob, K. V. and Weimer, A. W., "High-pressure Particulate Expansion and Minimum Bubbling of Fine Carbon Powders," AIChE Journal, 33, 1698-1706 (1987).

9. Perry, R. H. and Green D., "Chemical Engineers' Handbook," 6th Ed., McGraw Hill, N. Y., 5-60 (1984).

10. Robinson, C. S., "Some Factors Influencing Sedimentation," Industr. Engng. Chem., 18, 869-871 (1926).

11. Stokes, G. G., Mathematical and Physics Papers, (1901).

12. Mirza, S. and Richardson, J. F., "Sedimentation of Suspension of Particles of Two or More Sizes," Chem. Eng. Sci., 34, 447 (1979).

13. Selim, M. S., Kothari, A. C., and Turian, R. M., "Sedimentation of Multisized Particles in Concentrated Suspensions," AIChE Journal 29 1029-1038 (1983).

14. Einstein, A., "Berichtigung zu Meiner Arbeit: Eine Neue Bestimmung der Molekuldimension," Ann. Phys. 34, 591-592 (1911).

15. Ting, A. P. and Luebbers, R. H., "Viscosity of Suspensions of Spherical and other Isodimensional Particles," AIChE Journal 3, 111-116 (1957).

16. Weiland, R. H., "A Low Reynold's Number Analysis of Gas Bubbles In Fluidized Beds," Fluidization Technology I, Kearns, D. L., 3 (1975).

17. Levenspiel, O., Chemical Reactor Engineering, 2nd Ed., Wiley, 357-400 (1972).

18. Garside, J. and Al-Dibouni, R., "Velocity-Voidage Relationships for Fluidization and Sedimentation in Solid-Liquid Systems," Ind. Eng. Chem., Process Des. Dev., 16, No. 2, 206-214 (1977).

19. Loeffler, A. L. and Ruth, B. F., "Particulate Fluidization and Sedimentation of Spheres," AIChE Journal, 5, No. 3, 310-314 (1959).

20. Weimer, J. V., Personal Communication (September 1990)

21. Dutta, B. K., Bhattacharya, Suman, Chaudhury, S. K., and Barman, B., "Mixing and Segregation in a Liquid Fluidized Bed of Particles with Different Size and Density," The Canadian Journal of Chemical Engineering, 66, 676-680, (1988).

22. Duijn, G. Van and Rietema, K., "Segregation of Liquid-Fluidized Solids," Chem. Eng. Sci., 37, No. 5, 727-733 (1982).

APPENDIX

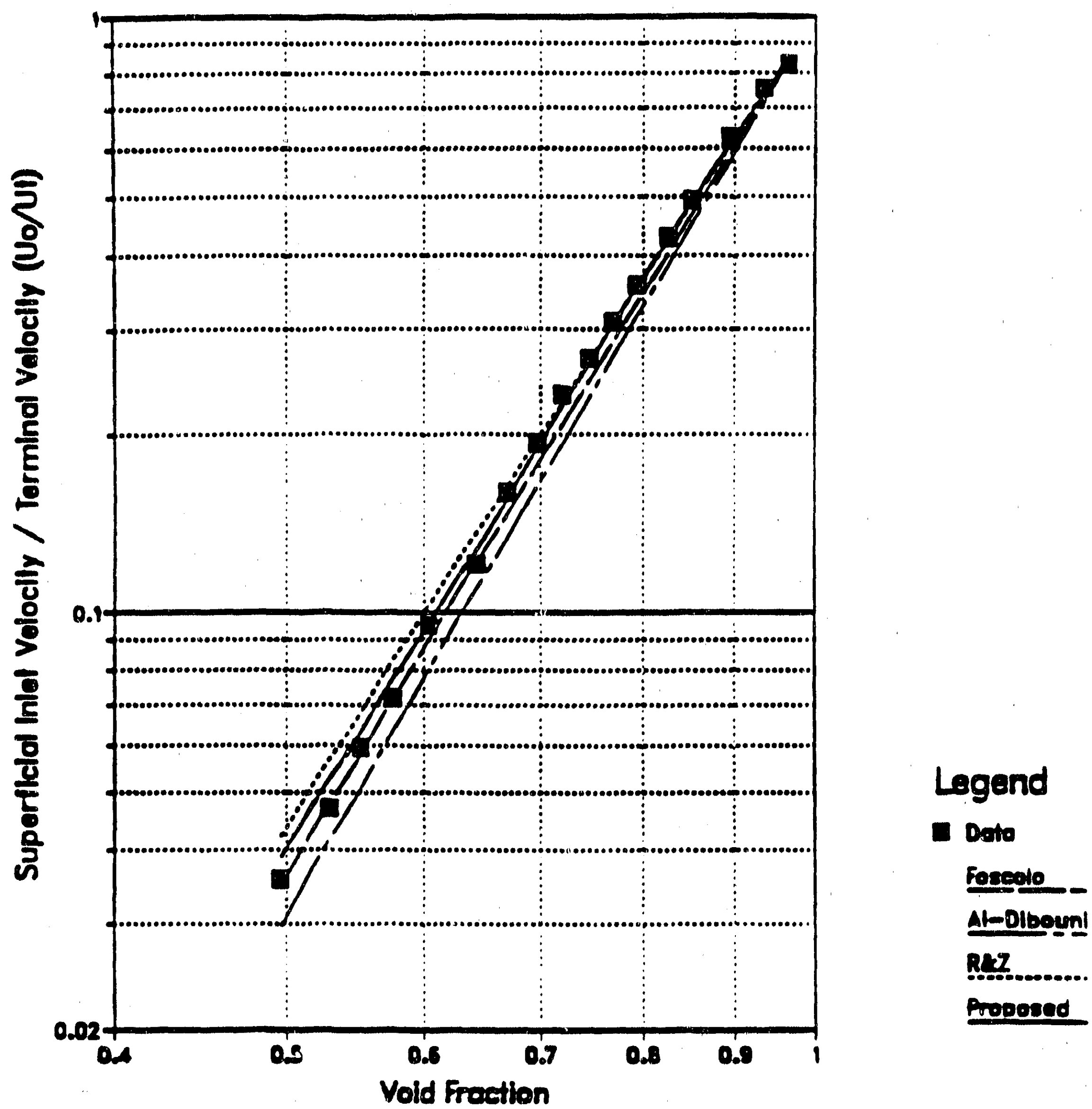

Figure 26. Fan data - Run 4, glass beads in water.

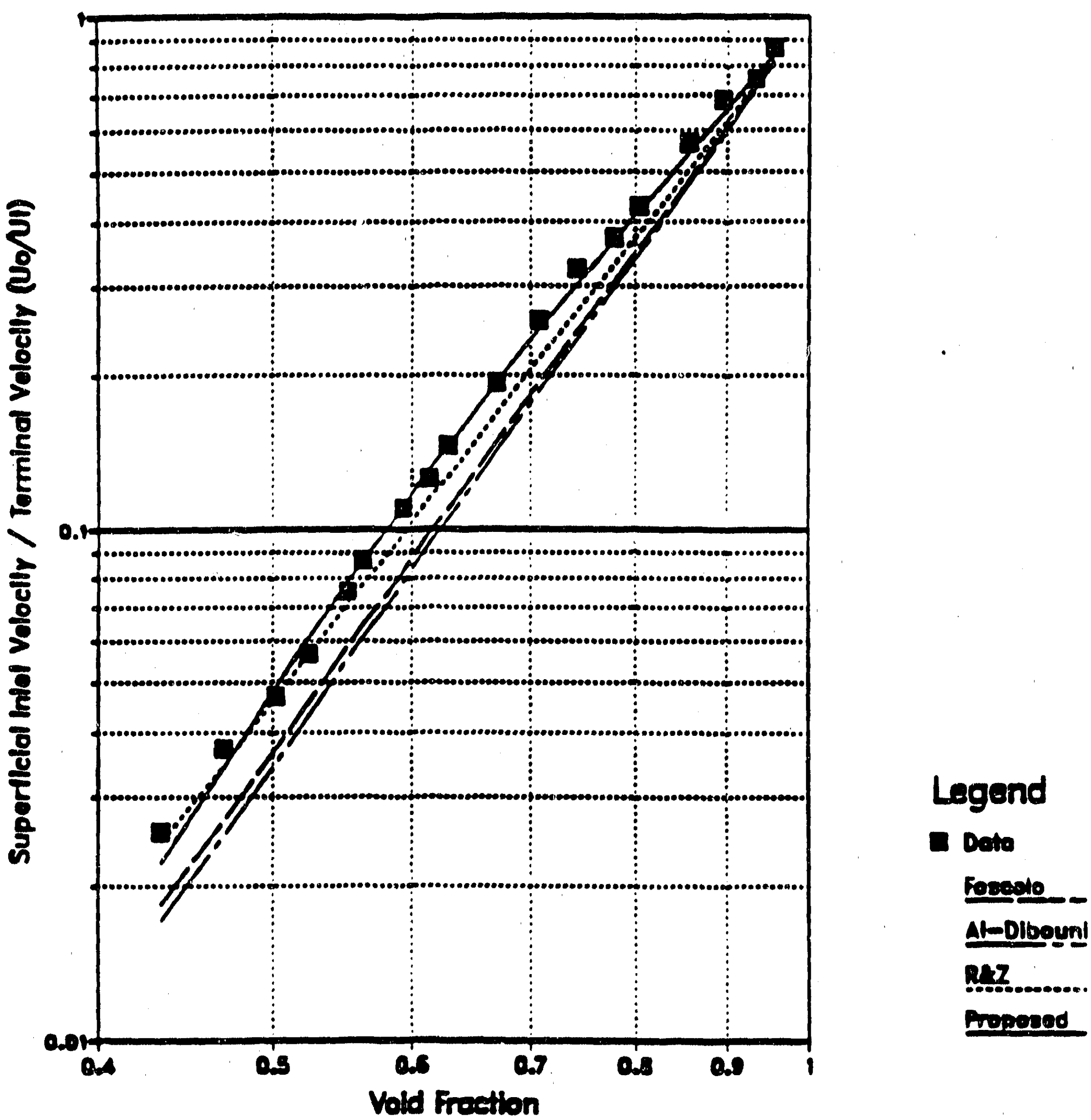

Figure 27. Fan data - Run 5, glass beads in water.

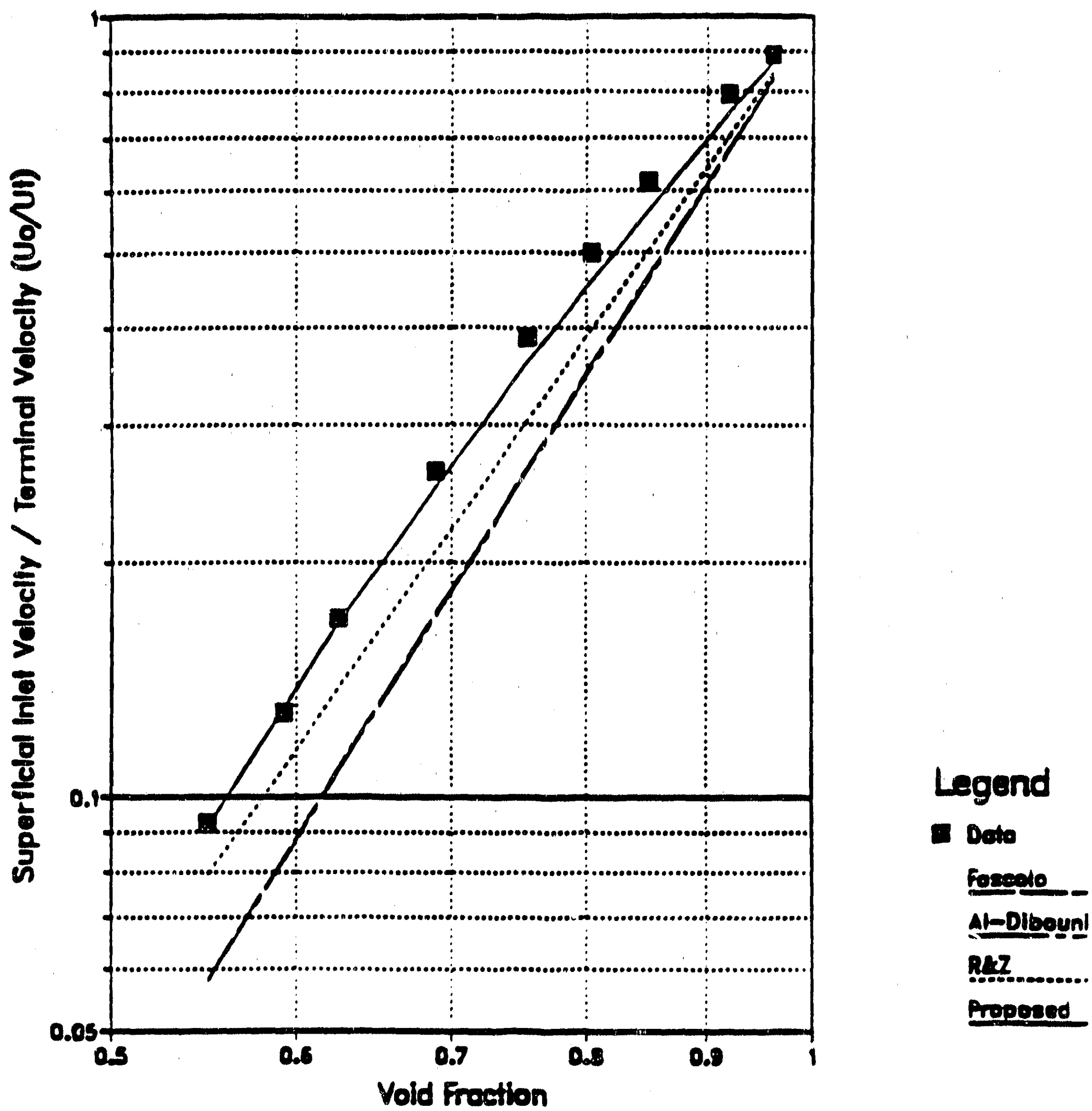

Figure 28. Fan data - Run 11, polystyrene spheres in water.

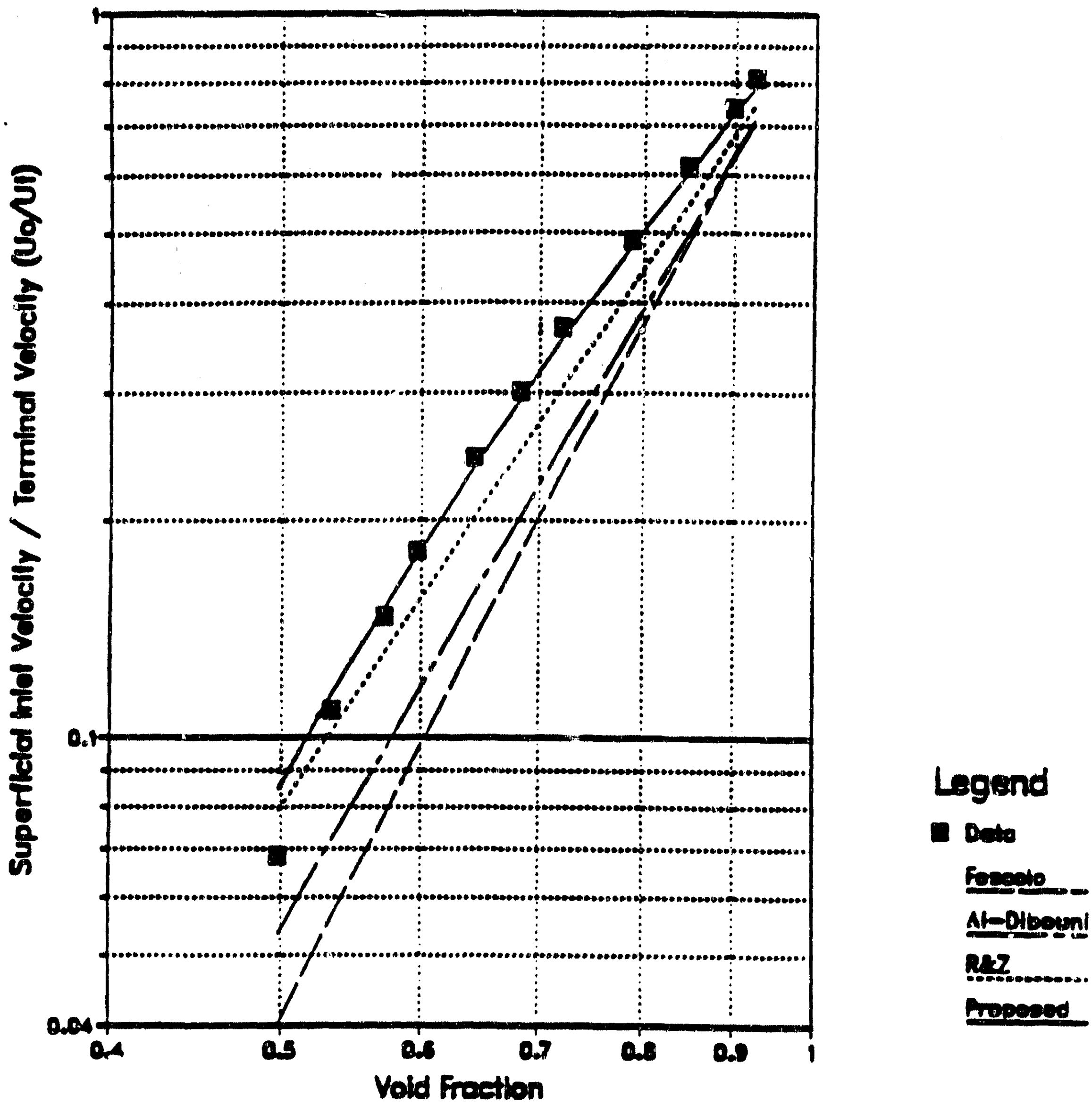

Figure 29. Fan data - Run 13, polystyrene spheres in water.

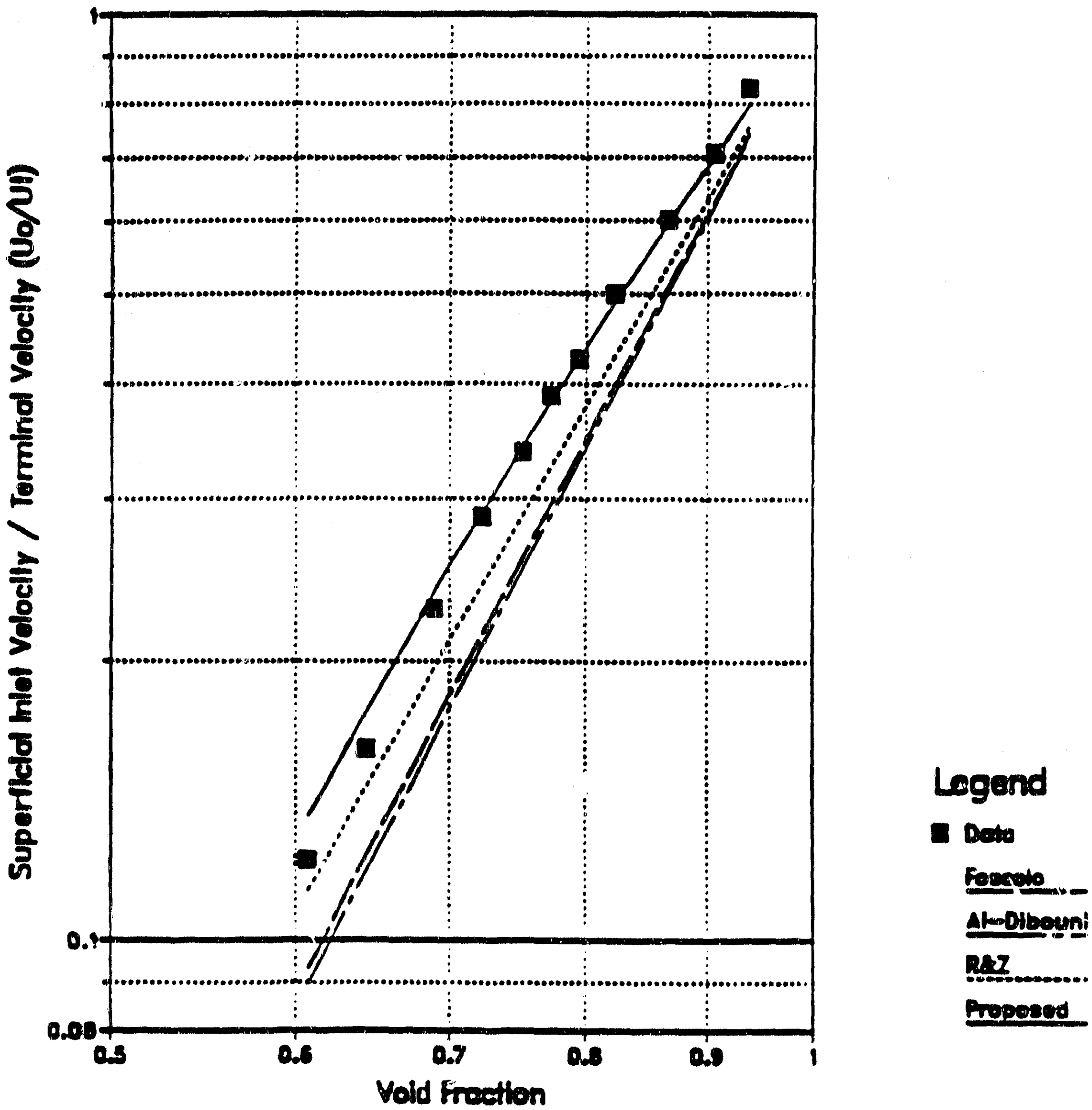

Figure 30. Fan data - Run 14, heavy polystyrene spheres in water.

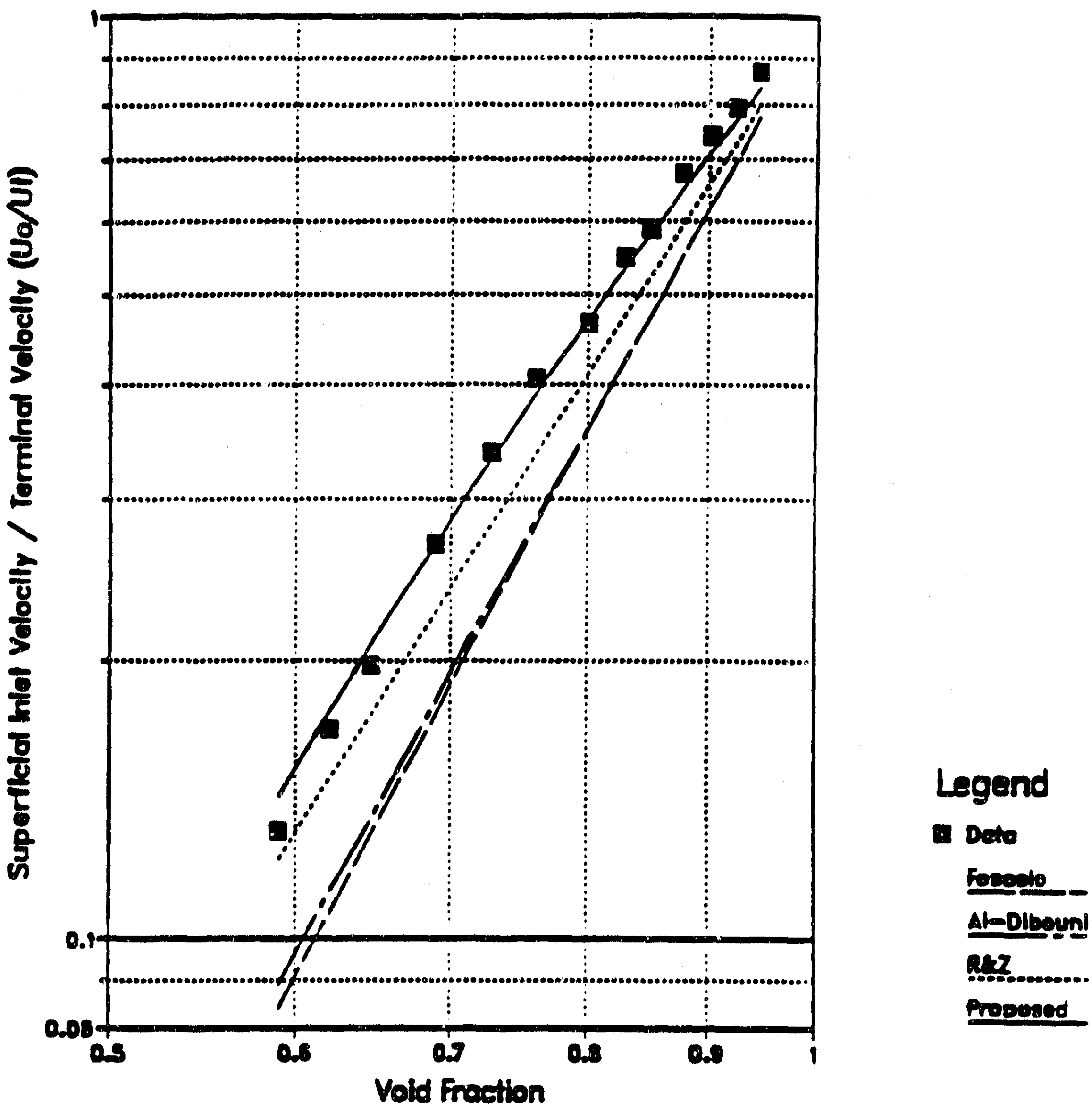

Figure 31. Fan data - Run 16, heavy polystyrene spheres in water.

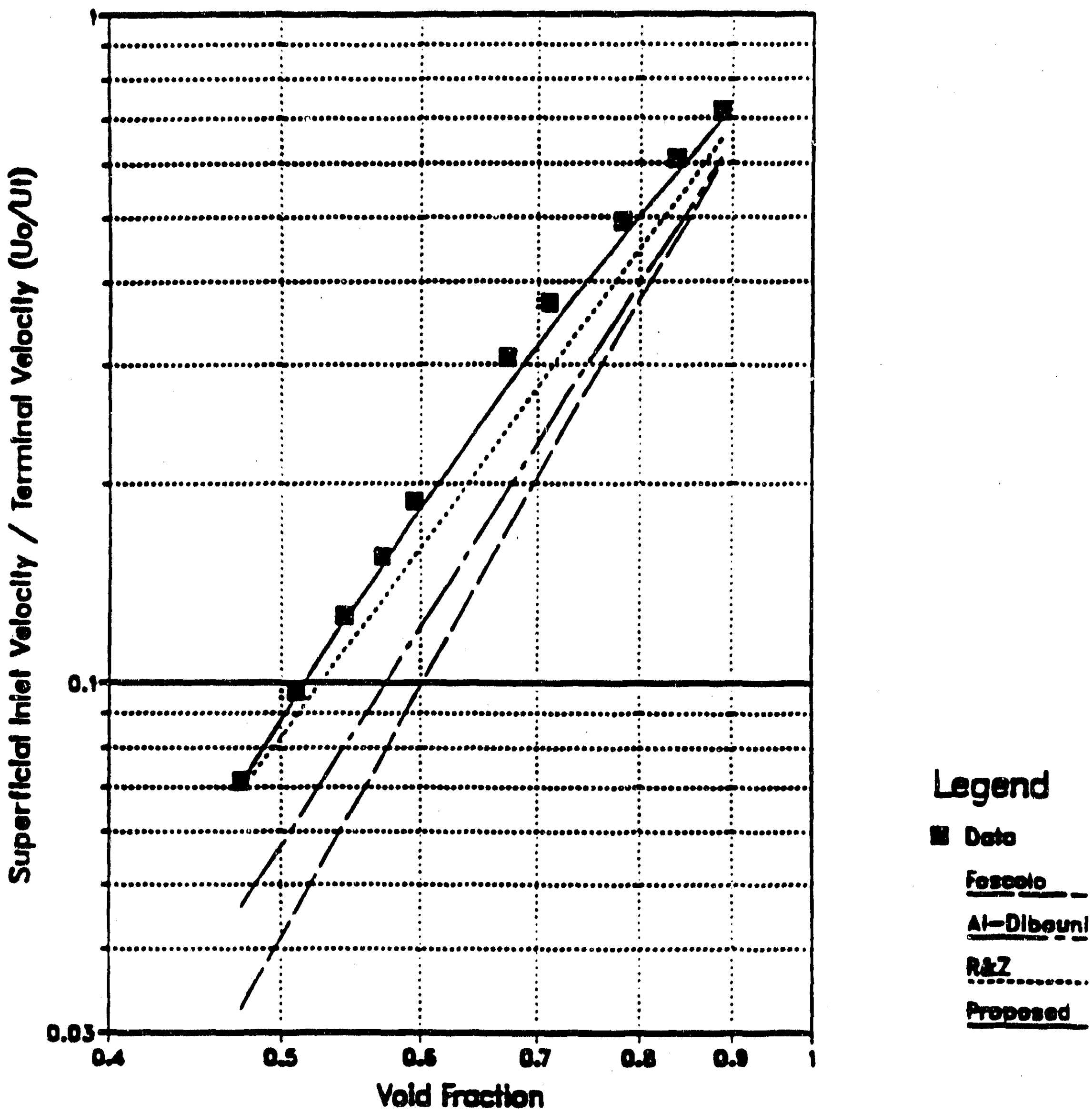

Figure 32. Fan data - Run 17, cation exchange resins in water.

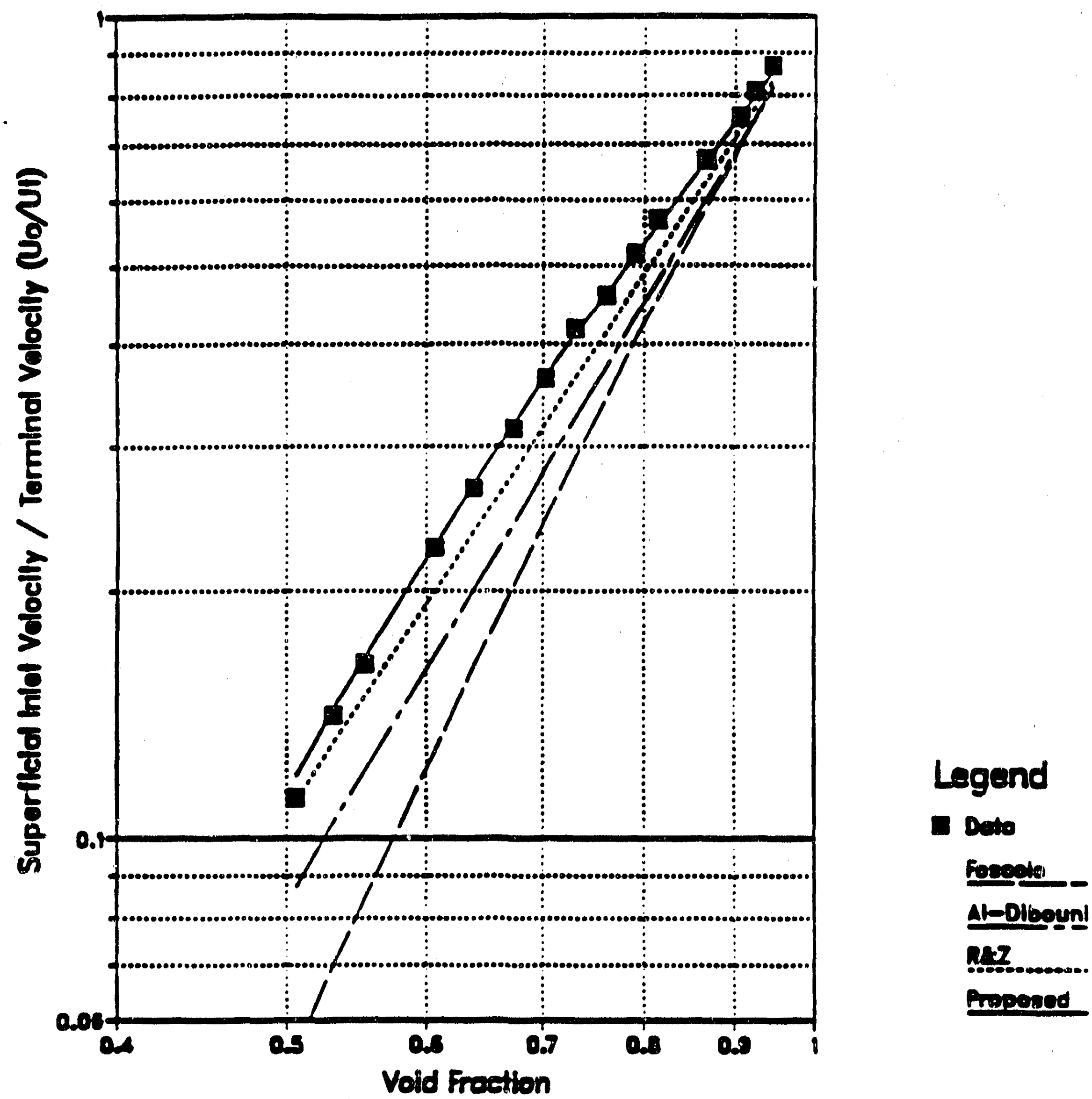

Figure 33. Fan data - Run 20, anion exchange resins in water.

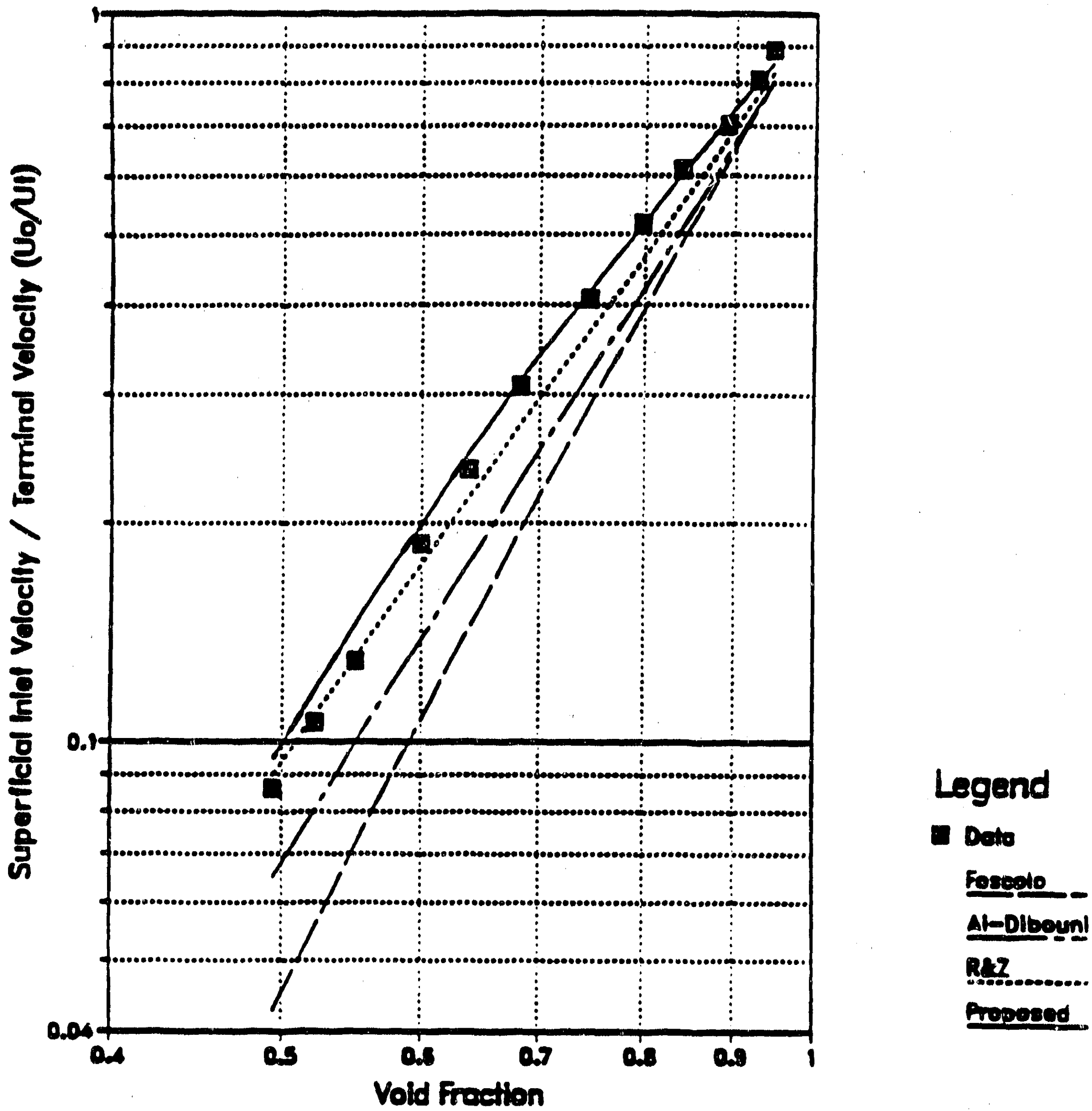

Figure 34. Fan data - Run 23, heavy exchange resins in water.

FAN DATA – RUN 1, GLASS BEADS IN WATER (1 of 3).

PARTICLE DIAMETER ft	PARTICLE DENSITY lb/cu ft	LIQUID VISCOSITY lb/(ft s)	LIQUID DENSITY lb/cu ft	VOID FRACTION	SOLID FRACTION	INTER. REYNOLD'S NUMBER	TERMINAL REYNOLD'S NUMBER	EFFECTIVE VISCOSITY
0.00018	148.1310	0.000672	62.2400	0.5541	0.4459	0.0050	0.0768	0.0017
0.00018	148.1310	0.000672	62.2400	0.5880	0.4120	0.0070	0.0768	0.0015
0.00018	148.1310	0.000672	62.2400	0.6215	0.3785	0.0093	0.0768	0.0014
0.00018	148.1310	0.000672	62.2400	0.6492	0.3508	0.0112	0.0768	0.0013
0.00018	148.1310	0.000672	62.2400	0.6728	0.3272	0.0135	0.0768	0.0012
0.00018	148.1310	0.000672	62.2400	0.6972	0.3028	0.0155	0.0768	0.0012
0.00018	148.1310	0.000672	62.2400	0.7341	0.2659	0.0206	0.0768	0.0011
0.00018	148.1310	0.000672	62.2400	0.7760	0.2240	0.0261	0.0768	0.0010
0.00018	148.1310	0.000672	62.2400	0.8073	0.1927	0.0345	0.0768	0.0009
0.00018	148.1310	0.000672	62.2400	0.8367	0.1633	0.0398	0.0768	0.0009
0.00018	148.1310	0.000672	62.2400	0.8670	0.1330	0.0458	0.0768	0.0008
0.00018	148.1310	0.000672	62.2400	0.9093	0.0907	0.0503	0.0768	0.0008
0.00018	148.1310	0.000672	62.2400	0.9386	0.0614	0.0553	0.0768	0.0007
0.00018	148.1310	0.000672	62.2400	0.9688	0.0312	0.0636	0.0768	0.0007

FAN DATA – RUN 1, GLASS BEADS IN WATER (2 of 3).

EFFECTIVE DENSITY	VISCOSITY RATIO	DENSITY RATIO	DEL DENSITY RATIO	EFFECTIVE REYNOLD'S NUMBER	REQUIRED CLASSICAL N	REQUIRED NEW N	PROPOSED N	PROPOSED Uo/Ut
100.5428	0.6775	0.8720	0.6559	0.0194	4.6156	3.7241	3.7500	0.0645
97.6282	0.7055	0.8793	0.6843	0.0227	4.5129	3.6139	3.7500	0.0847
94.7469	0.7324	0.8869	0.7120	0.0261	4.4465	3.5392	3.7500	0.1092
92.3683	0.7540	0.8933	0.7345	0.0292	4.4601	3.5453	3.7500	0.1333
90.3434	0.7720	0.8990	0.7535	0.0319	4.3872	3.4657	3.7500	0.1570
88.2451	0.7904	0.9051	0.7729	0.0348	4.4302	3.5013	3.7500	0.1850
85.0789	0.8175	0.9146	0.8019	0.0393	4.2565	3.3158	3.7500	0.2346
81.4818	0.8476	0.9259	0.8343	0.0448	4.2613	3.3061	3.7500	0.3032
78.7874	0.8698	0.9349	0.8582	0.0490	3.7329	2.7662	3.7500	0.3644
76.2694	0.8902	0.9436	0.8804	0.0530	3.6890	2.7110	3.7500	0.4303
73.6601	0.9111	0.9530	0.9031	0.0573	3.6231	2.6329	3.7500	0.5085
70.0329	0.9397	0.9669	0.9343	0.0634	4.4465	3.4383	3.7500	0.6360
67.5172	0.9593	0.9770	0.9557	0.0677	5.1876	4.1662	3.7500	0.7389
64.9204	0.9794	0.9880	0.9776	0.0722	5.9287	4.8931	3.7500	0.8592

FAN DATA - RUN 1, GLASS BEADS IN WATER (3 of 3).

R&Z N	R&Z Uo/Ut	AL-DIBOUNI N	AL-DIBOUNI Uo/Ut	FOSCOLO Uo/Ut	ACTUAL Uo/Ut
4.6500	0.0642	5.0644	0.0503	0.0589	0.0655
4.6500	0.0846	5.0644	0.0679	0.0784	0.0910
4.6500	0.1095	5.0644	0.0900	0.1023	0.1207
4.6500	0.1342	5.0644	0.1122	0.1261	0.1456
4.6500	0.1584	5.0644	0.1344	0.1496	0.1758
4.6500	0.1869	5.0644	0.1610	0.1775	0.2024
4.6500	0.2375	5.0644	0.2090	0.2273	0.2683
4.6500	0.3075	5.0644	0.2768	0.2967	0.3393
4.6500	0.3697	5.0644	0.3383	0.3588	0.4498
4.6500	0.4364	5.0644	0.4053	0.4258	0.5179
4.6500	0.5151	5.0644	0.4855	0.5052	0.5964
4.6500	0.6426	5.0644	0.6177	0.6346	0.6551
4.6500	0.7446	5.0644	0.7253	0.7388	0.7197
4.6500	0.8629	5.0644	0.8517	0.8601	0.8286

FAN DATA – RUN 4, GLASS BEADS IN WATER (1 of 3).

PARTICLE DIAMETER ft	PARTICLE DENSITY lb/cu ft	LIQUID VISCOSITY lb/(ft s)	LIQUID DENSITY lb/cu ft	VOID FRACTION	SOLID FRACTION	INTER. REYNOLD'S NUMBER	TERMINAL REYNOLD'S NUMBER	EFFECTIVE VISCOSITY
0.00027	148.1310	0.000672	62.2500	0.4959	0.5041	0.0102	0.2862	0.0020
0.00027	148.1310	0.000672	62.2500	0.5304	0.4696	0.0135	0.2862	0.0018
0.00027	148.1310	0.000672	62.2500	0.5519	0.4481	0.0171	0.2862	0.0017
0.00027	148.1310	0.000672	62.2500	0.5765	0.4235	0.0206	0.2862	0.0016
0.00027	148.1310	0.000672	62.2500	0.6045	0.3955	0.0273	0.2862	0.0015
0.00027	148.1310	0.000672	62.2500	0.6441	0.3559	0.0345	0.2862	0.0013
0.00027	148.1310	0.000672	62.2500	0.6701	0.3299	0.0458	0.2862	0.0012
0.00027	148.1310	0.000672	62.2500	0.6972	0.3028	0.0553	0.2862	0.0012
0.00027	148.1310	0.000672	62.2500	0.7197	0.2803	0.0667	0.2862	0.0011
0.00027	148.1310	0.000672	62.2500	0.7458	0.2542	0.0768	0.2862	0.0010
0.00027	148.1310	0.000672	62.2500	0.7698	0.2302	0.0884	0.2862	0.0010
0.00027	148.1310	0.000672	62.2500	0.7946	0.2054	0.1018	0.2862	0.0010
0.00027	148.1310	0.000672	62.2500	0.8268	0.1732	0.1228	0.2862	0.0009
0.00027	148.1310	0.000672	62.2500	0.8534	0.1466	0.1414	0.2862	0.0009
0.00027	148.1310	0.000672	62.2500	0.8950	0.1050	0.1789	0.2862	0.0008
0.00027	148.1310	0.000672	62.2500	0.9348	0.0652	0.2159	0.2862	0.0007
0.00027	148.1310	0.000672	62.2500	0.9650	0.0350	0.2372	0.2862	0.0007

FAN DATA – RUN 4, GLASS BEADS IN WATER (2 of 3).

EFFECTIVE DENSITY	VISCOSITY RATIO	DENSITY RATIO	DEL DENSITY RATIO	EFFECTIVE REYNOLD'S NUMBER	REQUIRED CLASSICAL N	REQUIRED NEW N	PROPOSED N	PROPOSED Uo/Ut
105.5460	0.6268	0.8600	0.6059	0.0533	4.7564	3.8753	3.7500	0.0388
102.5781	0.6573	0.8670	0.6358	0.0642	4.8171	3.9303	3.7500	0.0529
100.7366	0.6756	0.8715	0.6540	0.0714	4.7430	3.8520	3.7500	0.0634
98.6248	0.6961	0.8768	0.6747	0.0802	4.7771	3.8808	3.7500	0.0773
96.2136	0.7189	0.8830	0.6980	0.0908	4.6683	3.7653	3.7500	0.0961
92.8149	0.7500	0.8921	0.7304	0.1066	4.8071	3.8938	3.7500	0.1286
90.5787	0.7700	0.8984	0.7513	0.1176	4.5786	3.6579	3.7191	0.1561
88.2521	0.7904	0.9051	0.7729	0.1296	4.5605	3.6317	3.6750	0.1901
86.3232	0.8070	0.9108	0.7906	0.1398	4.4287	3.4927	3.6406	0.2219
84.0789	0.8260	0.9177	0.8110	0.1522	4.4866	3.5420	3.6029	0.2635
82.0156	0.8433	0.9242	0.8296	0.1638	4.4914	3.5385	3.5702	0.3063
79.8859	0.8609	0.9312	0.8486	0.1762	4.4976	3.5358	3.5384	0.3554
77.1270	0.8833	0.9406	0.8729	0.1926	4.4465	3.4725	3.4997	0.4270
74.8398	0.9017	0.9487	0.8929	0.2065	4.4465	3.4620	3.4697	0.4936
71.2701	0.9301	0.9621	0.9238	0.2287	4.2348	3.2329	3.4262	0.6118
67.8454	0.9569	0.9757	0.9530	0.2504	4.1850	3.1654	3.3881	0.7431
65.2592	0.9769	0.9866	0.9748	0.2670	5.2700	4.2363	3.3615	0.8549

FAN DATA – RUN 4, GLASS BEADS IN WATER (3 of 3).

R&Z N	R&Z Uo/Ut	AL-DIBOUNI N	AL-DIBOUNI Uo/Ut	FOSCOLO Uo/Ut	ACTUAL Uo/Ut
4.5164	0.0421	5.0108	0.0298	0.0347	0.0356
4.5164	0.0571	5.0108	0.0417	0.0480	0.0471
4.5164	0.0682	5.0108	0.0509	0.0580	0.0596
4.5164	0.0831	5.0108	0.0633	0.0715	0.0720
4.5164	0.1030	5.0108	0.0803	0.0899	0.0954
4.5164	0.1371	5.0108	0.1103	0.1218	0.1207
4.5164	0.1640	5.0108	0.1346	0.1473	0.1600
4.5164	0.1962	5.0108	0.1641	0.1781	0.1931
4.5164	0.2264	5.0108	0.1924	0.2074	0.2330
4.5164	0.2659	5.0108	0.2300	0.2461	0.2683
4.5164	0.3069	5.0108	0.2696	0.2864	0.3089
4.5164	0.3541	5.0108	0.3161	0.3334	0.3556
4.5164	0.4235	5.0108	0.3855	0.4031	0.4292
4.5164	0.4887	5.0108	0.4519	0.4692	0.4942
4.5164	0.6058	5.0108	0.5735	0.5891	0.6251
4.5164	0.7377	5.0108	0.7135	0.7257	0.7543
4.5164	0.8512	5.0108	0.8363	0.8445	0.8286

FAN DATA – RUN 5, GLASS BEADS IN WATER (1 of 3).

PARTICLE DIAMETER ft	PARTICLE DENSITY lb/cu ft	LIQUID VISCOSITY lb/(ft s)	LIQUID DENSITY lb/cu ft	VOID FRACTION	SOLID FRACTION	INTER. REYNOLD'S NUMBER	TERMINAL REYNOLD'S NUMBER	EFFECTIVE VISCOSITY
0.00034	148.1310	0.000672	62.2300	0.4334	0.5666	0.0261	1.0180	0.0025
0.00034	148.1310	0.000672	62.2300	0.4691	0.5309	0.0379	1.0180	0.0022
0.00034	148.1310	0.000672	62.2300	0.5018	0.4982	0.0480	1.0180	0.0020
0.00034	148.1310	0.000672	62.2300	0.5241	0.4759	0.0579	1.0180	0.0018
0.00034	148.1310	0.000672	62.2300	0.5519	0.4481	0.0768	1.0180	0.0017
0.00034	148.1310	0.000672	62.2300	0.5629	0.4371	0.0884	1.0180	0.0016
0.00034	148.1310	0.000672	62.2300	0.5927	0.4073	0.1118	1.0180	0.0015
0.00034	148.1310	0.000672	62.2300	0.6142	0.3858	0.1288	1.0180	0.0014
0.00034	148.1310	0.000672	62.2300	0.6290	0.3710	0.1483	1.0180	0.0014
0.00034	148.1310	0.000672	62.2300	0.6701	0.3299	0.1965	1.0180	0.0012
0.00034	148.1310	0.000672	62.2300	0.7084	0.2916	0.2606	1.0180	0.0011
0.00034	148.1310	0.000672	62.2300	0.7429	0.2571	0.3296	1.0180	0.0011
0.00034	148.1310	0.000672	62.2300	0.7791	0.2209	0.3795	1.0180	0.0010
0.00034	148.1310	0.000672	62.2300	0.8042	0.1958	0.4369	1.0180	0.0009
0.00034	148.1310	0.000672	62.2300	0.8568	0.1432	0.5792	1.0180	0.0009
0.00034	148.1310	0.000672	62.2300	0.8950	0.1050	0.6990	1.0180	0.0008
0.00034	148.1310	0.000672	62.2300	0.9348	0.0652	0.7679	1.0180	0.0007
0.00034	148.1310	0.000672	62.2300	0.9573	0.0427	0.8841	1.0180	0.0007

FAN DATA – RUN 5, GLASS BEADS IN WATER (2 of 3).

EFFECTIVE DENSITY	VISCOSITY RATIO	DENSITY RATIO	DEL DENSITY RATIO	EFFECTIVE REYNOLD'S NUMBER	REQUIRED CLASSICAL N	REQUIRED NEW N	PROPOSED N	PROPOSED Uo/Ut
110.9056	0.5675	0.8478	0.5503	0.1281	4.3833	3.5084	3.6802	0.0222
107.8350	0.6021	0.8546	0.5823	0.1618	4.3456	3.4679	3.5756	0.0344
105.0267	0.6321	0.8611	0.6111	0.1959	4.4295	3.5474	3.4922	0.0490
103.1060	0.6519	0.8657	0.6304	0.2211	4.4374	3.5517	3.4407	0.0611
100.7255	0.6756	0.8715	0.6540	0.2541	4.3477	3.4566	3.3820	0.0789
99.7766	0.6849	0.8738	0.6633	0.2679	4.2523	3.3589	3.3600	0.0868
97.2203	0.7093	0.8803	0.6882	0.3067	4.2220	3.3218	3.3045	0.1109
95.3717	0.7266	0.8852	0.7060	0.3362	4.2417	3.3362	3.2672	0.1308
94.1022	0.7382	0.8886	0.7181	0.3572	4.1552	3.2458	3.2430	0.1458
90.5653	0.7700	0.8983	0.7513	0.4184	4.1090	3.1882	3.1803	0.1937
87.2811	0.7986	0.9079	0.7817	0.4789	3.9525	3.0200	3.1277	0.2466
84.3174	0.8239	0.9169	0.8087	0.5362	3.7944	2.8506	3.0844	0.3020
81.2093	0.8498	0.9268	0.8367	0.5988	3.9525	2.9961	3.0427	0.3684
79.0536	0.8675	0.9339	0.8558	0.6437	3.8806	2.9151	3.0157	0.4199
74.5316	0.9041	0.9498	0.8955	0.7408	3.6484	2.6624	2.9639	0.5431
71.2522	0.9301	0.9621	0.9238	0.8135	3.3878	2.3858	2.9299	0.6464
67.8267	0.9569	0.9757	0.9530	0.8907	4.1850	3.1652	2.8973	0.7681
65.8943	0.9718	0.9838	0.9693	0.9346	3.2338	2.2036	2.8801	0.8433

FAN DATA – RUN 5, GLASS BEADS IN WATER (3 of 3).

R&Z N	R&Z Uo/Ut	AL-DIBOUNI N	AL-DIBOUNI Uo/Ut	FOSCOLO Uo/Ut	ACTUAL Uo/Ut
4.4421	0.0244	4.8646	0.0171	0.0184	0.0256
4.4421	0.0347	4.8646	0.0252	0.0270	0.0373
4.4421	0.0467	4.8646	0.03[illegible]	0.0373	0.0471
4.4421	0.0567	4.8646	0.0432	0.0459	0.0569
4.4421	0.0713	4.8646	0.0555	0.0588	0.0754
4.4421	0.0779	4.8646	0.0611	0.0647	0.0869
4.4421	0.0979	4.8646	0.0785	0.0828	0.1099
4.4421	0.1147	4.8646	0.0934	0.0982	0.1265
4.4421	0.1275	4.8646	0.1048	0.1100	0.1456
4.4421	0.1690	4.8646	0.1427	0.1491	0.1931
4.4421	0.2162	4.8646	0.1869	0.1944	0.2560
4.4421	0.2671	4.8646	0.2355	0.2440	0.3237
4.4421	0.3299	4.8646	0.2968	0.3062	0.3728
4.4421	0.3798	4.8646	0.3463	0.3561	0.4292
4.4421	0.5033	4.8646	0.4715	0.4817	0.5690
4.4421	0.6108	4.8646	0.5829	0.5925	0.6866
4.4421	0.7414	4.8646	0.7206	0.7285	0.7543
4.4421	0.8239	4.8646	0.8089	0.8152	0.8685

FAN DATA – RUN 9, GLASS BEADS IN WATER (1 of 3).

PARTICLE DIAMETER ft	PARTICLE DENSITY lb/cu ft	LIQUID VISCOSITY lb/(ft s)	LIQUID DENSITY lb/cu ft	VOID FRACTION	SOLID FRACTION	INTER. REYNOLD'S NUMBER	TERMINAL REYNOLD'S NUMBER	EFFECTIVE VISCOSITY
0.00107	141.2850	0.000672	62.3600	0.4959	0.5041	0.6990	9.2665	0.0020
0.00107	141.2850	0.000672	62.3600	0.5159	0.4841	0.8435	9.2665	0.0019
0.00107	141.2850	0.000672	62.3600	0.5607	0.4393	1.2285	9.2665	0.0016
0.00107	141.2850	0.000672	62.3600	0.5974	0.4026	1.6286	9.2665	0.0015
0.00107	141.2850	0.000672	62.3600	0.6215	0.3785	1.9654	9.2665	0.0014
0.00107	141.2850	0.000672	62.3600	0.6544	0.3456	2.2629	9.2665	0.0013
0.00107	141.2850	0.000672	62.3600	0.7112	0.2888	3.1443	9.2665	0.0011
0.00107	141.2850	0.000672	62.3600	0.7638	0.2362	4.1685	9.2665	0.0010
0.00107	141.2850	0.000672	62.3600	0.8202	0.1798	5.0305	9.2665	0.0009
0.00107	141.2850	0.000672	62.3600	0.8739	0.1261	6.0708	9.2665	0.0008
0.00107	141.2850	0.000672	62.3600	0.9238	0.0762	7.3262	9.2665	0.0008
0.00107	141.2850	0.000672	62.3600	0.9498	0.0502	8.0481	9.2665	0.0007

FAN DATA – RUN 9, GLASS BEADS IN WATER (2 of 3).

EFFECTIVE DENSITY	VISCOSITY RATIO	DENSITY RATIO	DEL DENSITY RATIO	EFFECTIVE REYNOLD'S NUMBER	REQUIRED CLASSICAL N	REQUIRED NEW N	PROPOSED N	PROPOSED Uo/Ut
102.1492	0.6268	0.8685	0.6059	1.6830	3.6845	2.8175	2.6786	0.0832
100.5671	0.6446	0.8724	0.6233	1.8804	3.6211	2.7514	2.6422	0.0979
97.0334	0.6830	0.8813	0.6615	2.3590	3.4922	2.6151	2.5693	0.1361
94.1366	0.7131	0.8890	0.6921	2.7891	3.3748	2.4902	2.5168	0.1734
92.2305	0.7324	0.8942	0.7120	3.0901	3.2608	2.3708	2.4851	0.2009
89.6370	0.7580	0.9015	0.7387	3.5220	3.3245	2.4265	2.4454	0.2423
85.1547	0.8007	0.9148	0.7839	4.3262	3.1712	2.2579	2.3841	0.3250
81.0044	0.8389	0.9280	0.8249	5.1312	2.9644	2.0353	2.3344	0.4150
76.5472	0.8788	0.9431	0.8680	6.0534	3.0829	2.1353	2.2873	0.5268
72.3093	0.9158	0.9586	0.9082	6.9771	3.1387	2.1719	2.2476	0.6485
68.3742	0.9495	0.9740	0.9450	7.8673	2.9644	1.9782	2.2146	0.7759
66.3232	0.9668	0.9826	0.9639	8.3406	2.7363	1.7396	2.1987	0.8482

FAN DATA – RUN 9, GLASS BEADS IN WATER (3 of 3).

R&Z N	R&Z Uo/Ut	AL-DIBOUNI N	AL-DIBOUNI Uo/Ut	FOSCOLO Uo/Ut	ACTUAL Uo/Ut
3.5618	0.0822	4.0922	0.0567	0.0405	0.0754
3.5618	0.0947	4.0922	0.0666	0.0489	0.0910
3.5618	0.1273	4.0922	0.0937	0.0725	0.1326
3.5618	0.1596	4.0922	0.1214	0.0979	0.1758
3.5618	0.1838	4.0922	0.1428	0.1180	0.2121
3.5618	0.2208	4.0922	0.1763	0.1502	0.2442
3.5618	0.2970	4.0922	0.2479	0.2213	0.3393
3.5618	0.3829	4.0922	0.3319	0.3071	0.4498
3.5618	0.4937	4.0922	0.4445	0.4240	0.5429
3.5618	0.6188	4.0922	0.5761	0.5619	0.6551
3.5618	0.7540	4.0922	0.7230	0.7155	0.7906
3.5618	0.8323	4.0922	0.8099	0.8058	0.8685

FAN DATA – RUN 10, GLASS BEADS IN WATER (1 of 3).

PARTICLE DIAMETER ft	PARTICLE DENSITY lb/cu ft	LIQUID VISCOSITY lb/(ft s)	LIQUID DENSITY lb/cu ft	VOID FRACTION	SOLID FRACTION	INTER. REYNOLD'S NUMBER	TERMINAL REYNOLD'S NUMBER	EFFECTIVE VISCOSITY
0.00164	151.2430	0.000672	62.3200	0.4861	0.5139	2.4859	30.0000	0.0021
0.00164	151.2430	0.000672	62.3200	0.5241	0.4759	3.4542	30.0000	0.0018
0.00164	151.2430	0.000672	62.3200	0.5497	0.4503	4.3690	30.0000	0.0017
0.00164	151.2430	0.000672	62.3200	0.5950	0.4050	5.7921	30.0000	0.0015
0.00164	151.2430	0.000672	62.3200	0.6365	0.3635	7.3262	30.0000	0.0013
0.00164	151.2430	0.000672	62.3200	0.6622	0.3378	8.4353	30.0000	0.0013
0.00164	151.2430	0.000672	62.3200	0.6972	0.3028	9.7124	30.0000	0.0012
0.00164	151.2430	0.000672	62.3200	0.7638	0.2362	13.4953	30.0000	0.0010
0.00164	151.2430	0.000672	62.3200	0.8106	0.1894	15.5384	30.0000	0.0009
0.00164	151.2430	0.000672	62.3200	0.8400	0.1600	17.8909	30.0000	0.0009
0.00164	151.2430	0.000672	62.3200	0.8879	0.1121	20.5995	30.0000	0.0008

FAN DATA – RUN 10, GLASS BEADS IN WATER (2 of 3).

EFFECTIVE DENSITY	VISCOSITY RATIO	DENSITY RATIO	DEL DENSITY RATIO	EFFECTIVE REYNOLD'S NUMBER	REQUIRED CLASSICAL N	REQUIRED NEW N	PROPOSED N	PROPOSED Uo/Ut
108.0147	0.6179	0.8546	0.5974	5.3342	3.4530	2.5677	2.3233	0.0988
104.6340	0.6519	0.8624	0.6304	6.5767	3.3463	2.4546	2.2641	0.1302
102.3639	0.6738	0.8678	0.6522	7.4787	3.2196	2.3228	2.2284	0.1541
98.3320	0.7112	0.8778	0.6902	9.2105	3.1680	2.2607	2.1719	0.2022
94.6445	0.7441	0.8875	0.7242	10.9334	3.1204	2.2020	2.1500	0.2500
92.3564	0.7640	0.8937	0.7450	12.0658	3.0784	2.1525	2.1500	0.2815
89.2431	0.7904	0.9025	0.7729	13.6798	3.1272	2.1904	2.1500	0.3285
83.3262	0.8389	0.9204	0.8249	16.9586	2.9644	2.0047	2.1500	0.4326
79.1664	0.8720	0.9339	0.8607	19.4070	3.1321	2.1547	2.1500	0.5185
76.5493	0.8925	0.9429	0.8829	20.9971	2.9644	1.9751	2.1500	0.5784
72.2879	0.9253	0.9585	0.9186	23.6501	3.1620	2.1521	2.1500	0.6868

FAN DATA – RUN 10, GLASS BEADS IN WATER (3 of 3).

R&Z N	R&Z Uo/Ut	AL-DIBOUNI N	AL-DIBOUNI Uo/Ut	FOSCOLO Uo/Ut	ACTUAL Uo/Ut
3.1670	0.1018	3.5034	0.0799	0.0483	0.0829
3.1670	0.1293	3.5034	0.1040	0.0686	0.1151
3.1670	0.1503	3.5034	0.1229	0.0854	0.1456
3.1670	0.1932	3.5034	0.1622	0.1224	0.1931
3.1670	0.2391	3.5034	0.2054	0.1652	0.2442
3.1670	0.2711	3.5034	0.2360	0.1966	0.2812
3.1670	0.3191	3.5034	0.2827	0.2455	0.3237
3.1670	0.4259	3.5034	0.3890	0.3593	0.4498
3.1670	0.5142	3.5034	0.4791	0.4566	0.5179
3.1670	0.5757	3.5034	0.5429	0.5253	0.5964
3.1670	0.6862	3.5034	0.6593	0.6496	0.6866

FAN DATA – RUN 11, POLYSTYRENE SPHERES IN WATER (1 of 3).

PARTICLE DIAMETER ft	PARTICLE DENSITY lb/cu ft	LIQUID VISCOSITY lb/(ft s)	LIQUID DENSITY lb/cu ft	VOID FRACTION	SOLID FRACTION	INTER. REYNOLD'S NUMBER	TERMINAL REYNOLD'S NUMBER	EFFECTIVE VISCOSITY
0.00172	65.0408	0.000672	62.3720	0.5497	0.4503	0.1539	1.6625	0.0017
0.00172	65.0408	0.000672	62.3720	0.5927	0.4073	0.2127	1.6625	0.0015
0.00172	65.0408	0.000672	62.3720	0.6265	0.3735	0.2806	1.6625	0.0014
0.00172	65.0408	0.000672	62.3720	0.6890	0.3110	0.4353	1.6625	0.0012
0.00172	65.0408	0.000672	62.3720	0.7547	0.2453	0.6447	1.6625	0.0010
0.00172	65.0408	0.000672	62.3720	0.8042	0.1958	0.8312	1.6625	0.0009
0.00172	65.0408	0.000672	62.3720	0.8500	0.1500	1.0234	1.6625	0.0009
0.00172	65.0408	0.000672	62.3720	0.9201	0.0799	1.3195	1.6625	0.0008
0.00172	65.0408	0.000672	62.3720	0.9611	0.0389	1.4811	1.6625	0.0007

FAN DATA – RUN 11, POLYSTYRENE SPHERES IN WATER (2 of 3).

EFFECTIVE DENSITY	VISCOSITY RATIO	DENSITY RATIO	DEL DENSITY RATIO	EFFECTIVE REYNOLD'S NUMBER	REQUIRED CLASSICAL N	REQUIRED NEW N	PROPOSED N	PROPOSED Uo/Ut
63.5738	0.6738	0.9946	0.6522	0.2947	3.9768	3.3078	3.3207	0.0919
63.4591	0.7093	0.9951	0.6882	0.3687	3.9309	3.2649	3.2303	0.1303
63.3689	0.7363	0.9955	0.7160	0.4340	3.8044	3.1401	3.1660	0.1668
63.2020	0.7842	0.9962	0.7664	0.5720	3.5973	2.9346	3.0599	0.2499
63.0265	0.8324	0.9970	0.8179	0.7434	3.3667	2.7043	2.9626	0.3606
62.8947	0.8675	0.9976	0.8558	0.8913	3.1800	2.5172	2.8970	0.4603
62.7722	0.8994	0.9982	0.8904	1.0444	2.9861	2.3224	2.8409	0.5658
62.5851	0.9470	0.9990	0.9423	1.3098	2.7762	2.1104	2.7627	0.7518
62.4757	0.9744	0.9995	0.9721	1.4838	2.9150	2.2476	2.7205	0.8744

FAN DATA – RUN 11, POLYSTYRENE SPHERES IN WATER (3 of 3).

R&Z N	R&Z Uo/Ut	AL-DIBOUNI N	AL-DIBOUNI Uo/Ut	FOSCOLO Uo/Ut	ACTUAL Uo/Ut
4.2295	0.0796	4.7604	0.0579	0.0584	0.0926
4.2295	0.1094	4.7604	0.0829	0.0837	0.1279
4.2295	0.1384	4.7604	0.1079	0.1091	0.1688
4.2295	0.2069	4.7604	0.1698	0.1719	0.2618
4.2295	0.3042	4.7604	0.2620	0.2655	0.3878
4.2295	0.3978	4.7604	0.3543	0.3589	0.5000
4.2295	0.5030	4.7604	0.4614	0.4668	0.6156
4.2295	0.7033	4.7604	0.6729	0.6784	0.7937
4.2295	0.8457	4.7604	0.8281	0.8322	0.8909

FAN DATA – RUN 13, POLYSTYRENE SPHERES IN WATER (1 of 3).

PARTICLE DIAMETER ft	PARTICLE DENSITY lb/cu ft	LIQUID VISCOSITY lb/(ft s)	LIQUID DENSITY lb/cu ft	VOID FRACTION	SOLID FRACTION	INTER. REYNOLD'S NUMBER	TERMINAL REYNOLD'S NUMBER	EFFECTIVE VISCOSITY
0.00335	65.0408	0.000672	62.3670	0.4978	0.5022	0.5117	7.4643	0.0020
0.00335	65.0408	0.000672	62.3670	0.5346	0.4654	0.8123	7.4643	0.0018
0.00335	65.0408	0.000672	62.3670	0.5719	0.4281	1.0968	7.4643	0.0016
0.00335	65.0408	0.000672	62.3670	0.5974	0.4026	1.3503	7.4643	0.0015
0.00335	65.0408	0.000672	62.3670	0.6441	0.3559	1.8234	7.4643	0.0013
0.00335	65.0408	0.000672	62.3670	0.6836	0.3164	2.2449	7.4643	0.0012
0.00335	65.0408	0.000672	62.3670	0.7225	0.2775	2.7638	7.4643	0.0011
0.00335	65.0408	0.000672	62.3670	0.7884	0.2116	3.6469	7.4643	0.0010
0.00335	65.0408	0.000672	62.3670	0.8467	0.1533	4.5948	7.4643	0.0009
0.00335	65.0408	0.000672	62.3670	0.8985	0.1015	5.5277	7.4643	0.0008
0.00335	65.0408	0.000672	62.3670	0.9238	0.0762	6.0629	7.4643	0.0008

FAN DATA – RUN 13, POLYSTYRENE SPHERES IN WATER (2 of 3).

EFFECTIVE DENSITY	VISCOSITY RATIO	DENSITY RATIO	DEL DENSITY RATIO	EFFECTIVE REYNOLD'S NUMBER	REQUIRED CLASSICAL N	REQUIRED NEW N	PROPOSED N	PROPOSED Uo/Ut
63.7097	0.6285	0.9939	0.6076	0.9795	3.8425	3.1681	2.8635	0.0848
63.6113	0.6609	0.9944	0.6394	1.2174	3.5423	2.8720	2.7877	0.1147
63.5117	0.6923	0.9948	0.6709	1.4896	3.4319	2.7646	2.7192	0.1507
63.4435	0.7131	0.9951	0.6921	1.6947	3.3187	2.6530	2.6763	0.1787
63.3186	0.7500	0.9957	0.73[illegible]	2.1127	3.2039	2.5402	2.6045	0.2375
63.2131	0.7801	0.9962	0.7620	2.5102	3.1580	2.4952	2.5497	0.2946
63.1088	0.8091	0.9966	0.7928	2.9454	3.0572	2.3949	2.4999	0.3579
62.9328	0.8564	0.9974	0.8438	3.7816	3.0122	2.3496	2.4240	0.4800
62.7770	0.8971	0.9981	0.8879	4.6364	2.9150	2.2513	2.3638	0.6042
62.6383	0.9325	0.9988	0.9264	5.4942	2.8071	2.1419	2.3148	0.7270
62.5707	0.9495	0.9991	0.9450	5.9476	2.6235	1.9575	2.2923	0.7910

FAN DATA – RUN 13, POLYSTYRENE SPHERES IN WATER (3 of 3).

R&Z N	R&Z Uo/Ut	AL–DIBOUNI N	AL–DIBOUNI Uo/Ut	FOSCOLO Uo/Ut	ACTUAL Uo/Ut
3.6397	0.0790	4.1996	0.0534	0.0401	0.0686
3.6397	0.1024	4.1996	0.0721	0.0563	0.1088
3.6397	0.1308	4.1996	0.0957	0.0775	0.1469
3.6397	0.1533	4.1996	0.1149	0.0954	0.1809
3.6397	0.2017	4.1996	0.1576	0.1361	0.2443
3.6397	0.2504	4.1996	0.2024	0.1799	0.3008
3.6397	0.3064	4.1996	0.2554	0.2330	0.3703
3.6397	0.4209	4.1996	0.3684	0.3485	0.4886
3.6397	0.5456	4.1996	0.4971	0.4820	0.6156
3.6397	0.6774	4.1996	0.6380	0.6286	0.7405
3.6397	0.7494	4.1996	0.7169	0.7105	0.8123

FAN DATA – RUN 14, HEAVY POLYSTYRENE SPHERES IN WATER (1 of 3).

PARTICLE DIAMETER ft	PARTICLE DENSITY lb/cu ft	LIQUID VISCOSITY lb/(ft s)	LIQUID DENSITY lb/cu ft	VOID FRACTION	SOLID FRACTION	INTER. REYNOLD'S NUMBER	TERMINAL REYNOLD'S NUMBER	EFFECTIVE VISCOSITY
0.00115	72.1984	0.000672	62.4100	0.6069	0.3931	0.1504	1.2311	0.0014
0.00115	72.1984	0.000672	62.4100	0.6441	0.3559	0.1984	1.2311	0.0013
0.00115	72.1984	0.000672	62.4100	0.6890	0.3110	0.2806	1.2311	0.0012
0.00115	72.1984	0.000672	62.4100	0.7225	0.2775	0.3536	1.2311	0.0011
0.00115	72.1984	0.000672	62.4100	0.7518	0.2482	0.4156	1.2311	0.0010
0.00115	72.1984	0.000672	62.4100	0.7729	0.2271	0.4774	1.2311	0.0010
0.00115	72.1984	0.000672	62.4100	0.7946	0.2054	0.5236	1.2311	0.0010
0.00115	72.1984	0.000672	62.4100	0.8235	0.1765	0.6156	1.2311	0.0009
0.00115	72.1984	0.000672	62.4100	0.8670	0.1330	0.7405	1.2311	0.0008
0.00115	72.1984	0.000672	62.4100	0.9057	0.0943	0.8706	1.2311	0.0008
0.00115	72.1984	0.000672	62.4100	0.9386	0.0614	1.0234	1.2311	0.0007

FAN DATA – RUN 14, HEAVY POLYSTYRENE SPHERES IN WATER (2 of 3).

EFFECTIVE DENSITY	VISCOSITY RATIO	DENSITY RATIO	DEL DENSITY RATIO	EFFECTIVE REYNOLD'S NUMBER	REQUIRED CLASSICAL N	REQUIRED NEW N	PROPOSED N	PROPOSED Uo/Ut
66.2575	0.7208	0.9831	0.7000	0.3020	4.2106	3.5207	3.3107	0.1356
65.8937	0.7500	0.9846	0.7304	0.3584	4.1493	3.4602	3.2416	0.1774
65.4543	0.7842	0.9865	0.7664	0.4342	3.9694	3.2804	3.1658	0.2379
65.1258	0.8091	0.9879	0.7928	0.4966	3.8393	3.1499	3.1138	0.2906
64.8399	0.8303	0.9891	0.8156	0.5552	3.8057	3.1157	3.0712	0.3419
64.6329	0.8455	0.9901	0.8319	0.6001	3.6774	2.9869	3.0419	0.3823
64.4201	0.8609	0.9910	0.8486	0.6486	3.7192	3.0280	3.0129	0.4268
64.1376	0.8811	0.9922	0.8705	0.7165	3.5694	2.8772	2.9761	0.4905
63.7115	0.9111	0.9941	0.9031	0.8272	3.5628	2.8687	2.9238	0.5968
63.3333	0.9373	0.9958	0.9317	0.9340	3.4980	2.8020	2.8803	0.7016
63.0114	0.9593	0.9973	0.9557	1.0316	2.9150	2.2171	2.8452	0.7988

FAN DATA – RUN 14, HEAVY POLYSTYRENE SPHERES IN WATER (3 of 3).

R&Z N	R&Z Uo/Ut	AL-DIBOUNI N	AL-DIBOUNI Uo/Ut	FOSCOLO Uo/Ut	ACTUAL Uo/Ut
4.3584	0.1135	4.8282	0.0897	0.0931	0.1221
4.3584	0.1470	4.8282	0.1196	0.1237	0.1612
4.3584	0.1972	4.8282	0.1655	0.1708	0.2279
4.3584	0.2426	4.8282	0.2082	0.2144	0.2872
4.3584	0.2883	4.8282	0.2522	0.2590	0.3376
4.3584	0.3254	4.8282	0.2883	0.2956	0.3878
4.3584	0.3672	4.8282	0.3296	0.3374	0.4253
4.3584	0.4290	4.8282	0.3916	0.3998	0.5000
4.3584	0.5370	4.8282	0.5022	0.5107	0.6015
4.3584	0.6493	4.8282	0.6198	0.6278	0.7071
4.3584	0.7585	4.8282	0.7363	0.7430	0.8312

FAN DATA – RUN 16, HEAVY POLYSTYRENE SPHERES IN WATER (1 of 3).

PARTICLE DIAMETER ft	PARTICLE DENSITY lb/cu ft	LIQUID VISCOSITY lb/(ft s)	LIQUID DENSITY lb/cu ft	VOID FRACTION	SOLID FRACTION	INTER. REYNOLD'S NUMBER	TERMINAL REYNOLD'S NUMBER	EFFECTIVE VISCOSITY
0.00160	72.1984	0.000672	62.4150	0.5903	0.4097	0.3878	2.9622	0.0015
0.00160	72.1984	0.000672	62.4150	0.6215	0.3785	0.5000	2.9622	0.0014
0.00160	72.1984	0.000672	62.4150	0.6467	0.3533	0.5878	2.9622	0.0013
0.00160	72.1984	0.000672	62.4150	0.6890	0.3110	0.7937	2.9622	0.0012
0.00160	72.1984	0.000672	62.4150	0.7283	0.2717	1.0000	2.9622	0.0011
0.00160	72.1984	0.000672	62.4150	0.7607	0.2393	1.2030	2.9622	0.0010
0.00160	72.1984	0.000672	62.4150	0.8010	0.1990	1.3819	2.9622	0.0009
0.00160	72.1984	0.000672	62.4150	0.8301	0.1699	1.6245	2.9622	0.0009
0.00160	72.1984	0.000672	62.4150	0.8500	0.1500	1.7411	2.9622	0.0009
0.00160	72.1984	0.000672	62.4150	0.8774	0.1226	2.0000	2.9622	0.0008
0.00160	72.1984	0.000672	62.4150	0.9021	0.0979	2.1936	2.9622	0.0008
0.00160	72.1984	0.000672	62.4150	0.9238	0.0762	2.3511	2.9622	0.0008
0.00160	72.1984	0.000672	62.4150	0.9460	0.0540	2.5787	2.9622	0.0007

FAN DATA – RUN 16, HEAVY POLYSTYRENE SPHERES IN WATER (2 of 3).

EFFECTIVE DENSITY	VISCOSITY RATIO	DENSITY RATIO	DEL DENSITY RATIO	EFFECTIVE REYNOLD'S NUMBER	REQUIRED CLASSICAL N	REQUIRED NEW N	PROPOSED N	PROPOSED Uo/Ut
66.4230	0.7074	0.9824	0.6863	0.6705	3.8575	3.1671	3.0006	0.1429
66.1177	0.7324	0.9837	0.7120	0.7783	3.7410	3.0515	2.9459	0.1775
65.8719	0.7520	0.9847	0.7324	0.8720	3.7100	3.0209	2.9048	0.2087
65.4577	0.7842	0.9865	0.7664	1.0446	3.5353	2.8462	2.8409	0.2685
65.0732	0.8133	0.9882	0.7973	1.2218	3.4252	2.7357	2.7865	0.3322
64.7557	0.8368	0.9895	0.8226	1.3811	3.2953	2.6051	2.7447	0.3909
64.3622	0.8653	0.9913	0.8534	1.5954	3.4356	2.7442	2.6963	0.4715
64.0776	0.8856	0.9925	0.8754	1.7625	3.2251	2.5326	2.6633	0.5352
63.8822	0.8994	0.9934	0.8904	1.8834	3.2705	2.5772	2.6416	0.5816
63.6143	0.9181	0.9946	0.9108	2.0574	3.0034	2.3087	2.6130	0.6488
63.3729	0.9349	0.9957	0.9290	2.2227	2.9150	2.2192	2.5882	0.7129
63.1605	0.9495	0.9966	0.9450	2.3749	2.9150	2.2180	2.5672	0.7720
62.9430	0.9643	0.9976	0.9611	2.5376	2.4986	1.8003	2.5463	0.8353

FAN DATA - RUN 16, HEAVY POLYSTYRENE SPHERES IN WATER (3 of 3).

R&Z N	R&Z Uo/Ut	AL-DIBOUNI N	AL-DIBOUNI Uo/Ut	FOSCOLO Uo/Ut	ACTUAL Uo/Ut
3.9921	0.1219	4.5891	0.0890	0.0839	0.1309
3.9921	0.1498	4.5891	0.1128	0.1073	0.1688
3.9921	0.1755	4.5891	0.1353	0.1297	0.1984
3.9921	0.2260	4.5891	0.1809	0.1753	0.2679
3.9921	0.2821	4.5891	0.2334	0.2282	0.3376
3.9921	0.3357	4.5891	0.2851	0.2804	0.4061
3.9921	0.4123	4.5891	0.3612	0.3576	0.4665
3.9921	0.4754	4.5891	0.4254	0.4228	0.5484
3.9921	0.5227	4.5891	0.4744	0.4726	0.5878
3.9921	0.5933	4.5891	0.5487	0.5479	0.6752
3.9921	0.6628	4.5891	0.6232	0.6234	0.7405
3.9921	0.7288	4.5891	0.6951	0.6959	0.7937
3.9921	0.8013	4.5891	0.7752	0.7766	0.8706

FAN DATA – RUN 17, CATION EXCHANGE RESINS IN WATER (1 of 3).

PARTICLE DIAMETER ft	PARTICLE DENSITY lb/cu ft	LIQUID VISCOSITY lb/(ft s)	LIQUID DENSITY lb/cu ft	VOID FRACTION	SOLID FRACTION	INTER. REYNOLD'S NUMBER	TERMINAL REYNOLD'S NUMBER	EFFECTIVE VISCOSITY
0.00181	80.6010	0.000672	62.3620	0.4747	0.5253	0.6173	8.6457	0.0022
0.00181	80.6010	0.000672	62.3620	0.5098	0.4902	0.8386	8.6457	0.0019
0.00181	80.6010	0.000672	62.3620	0.5432	0.4568	1.0868	8.6457	0.0017
0.00181	80.6010	0.000672	62.3620	0.5696	0.4304	1.3436	8.6457	0.0016
0.00181	80.6010	0.000672	62.3620	0.5950	0.4050	1.6223	8.6457	0.0015
0.00181	80.6010	0.000672	62.3620	0.6728	0.3272	2.6311	8.6457	0.0012
0.00181	80.6010	0.000672	62.3620	0.7112	0.2888	3.2132	8.6457	0.0011
0.00181	80.6010	0.000672	62.3620	0.7821	0.2179	4.2634	8.6457	0.0010
0.00181	80.6010	0.000672	62.3620	0.8367	0.1633	5.2707	8.6457	0.0009
0.00181	80.6010	0.000672	62.3620	0.8879	0.1121	6.2160	8.6457	0.0008

FAN DATA – RUN 17, CATION EXCHANGE RESINS IN WATER (2 of 3).

EFFECTIVE DENSITY	VISCOSITY RATIO	DENSITY RATIO	DEL DENSITY RATIO	EFFECTIVE REYNOLD'S NUMBER	REQUIRED CLASSICAL N	REQUIRED NEW N	PROPOSED N	PROPOSED Uo/Ut
71.9428	0.6073	0.9600	0.5873	1.0670	3.5426	2.8185	2.8334	0.0706
71.3026	0.6392	0.9624	0.6180	1.3232	3.4630	2.7420	2.7592	0.0959
70.6939	0.6683	0.9648	0.6467	1.5954	3.3980	2.6788	2.6963	0.1244
70.2114	0.6905	0.9667	0.6690	1.8317	3.3083	2.5899	2.6507	0.1502
69.7484	0.7112	0.9685	0.6902	2.0759	3.2229	2.5050	2.6101	0.1777
68.3298	0.7720	0.9742	0.7535	2.9352	2.9733	2.2545	2.5009	0.2792
67.6297	0.8007	0.9771	0.7839	3.4237	2.9041	2.1840	2.4539	0.3390
66.3354	0.8520	0.9825	0.8390	4.4455	2.8774	2.1538	2.3761	0.4669
65.3412	0.8902	0.9868	0.8804	5.3402	2.7750	2.0480	2.3230	0.5805
64.4065	0.9253	0.9908	0.9186	6.2732	2.7750	2.0442	2.2773	0.6993

FAN DATA – RUN 17, CATION EXCHANGE RESINS IN WATER (3 of 3).

R&Z N	R&Z Uo/Ut	AL-DIBOUNI N	AL-DIBOUNI Uo/Ut	FOSCOLO Uo/Ut	ACTUAL Uo/Ut
3.5866	0.0691	4.1271	0.0462	0.0325	0.0714
3.5866	0.0892	4.1271	0.0620	0.0457	0.0970
3.5866	0.1120	4.1271	0.0806	0.0618	0.1257
3.5866	0.1329	4.1271	0.0980	0.0775	0.1554
3.5866	0.1554	4.1271	0.1173	0.0952	0.1876
3.5866	0.2414	4.1271	0.1948	0.1697	0.3078
3.5866	0.2945	4.1271	0.2450	0.2196	0.3717
3.5866	0.4143	4.1271	0.3627	0.3401	0.4931
3.5866	0.5275	4.1271	0.4790	0.4611	0.6096
3.5866	0.6528	4.1271	0.6122	0.6003	0.7190

FAN DATA – RUN 20, ANION EXCHANGE RESINS IN WATER (1 of 3).

PARTICLE DIAMETER ft	PARTICLE DENSITY lb/cu ft	LIQUID VISCOSITY lb/(ft s)	LIQUID DENSITY lb/cu ft	VOID FRACTION	SOLID FRACTION	INTER. REYNOLD'S NUMBER	TERMINAL REYNOLD'S NUMBER	EFFECTIVE VISCOSITY
0.00387	68.1528	0.000672	62.3160	0.5058	0.4942	2.8561	25.5623	0.0019
0.00387	68.1528	0.000672	62.3160	0.5325	0.4675	3.6151	25.5623	0.0018
0.00387	68.1528	0.000672	62.3160	0.5541	0.4459	4.1641	25.5623	0.0017
0.00387	68.1528	0.000672	62.3160	0.6069	0.3931	5.7917	25.5623	0.0014
0.00387	68.1528	0.000672	62.3160	0.6390	0.3610	6.8305	25.5623	0.0013
0.00387	68.1528	0.000672	62.3160	0.6728	0.3272	8.0556	25.5623	0.0012
0.00387	68.1528	0.000672	62.3160	0.7028	0.2972	9.2791	25.5623	0.0011
0.00387	68.1528	0.000672	62.3160	0.7312	0.2688	10.6884	25.5623	0.0011
0.00387	68.1528	0.000672	62.3160	0.7607	0.2393	11.7450	25.5623	0.0010
0.00387	68.1528	0.000672	62.3160	0.7915	0.2085	13.2138	25.5623	0.0010
0.00387	68.1528	0.000672	62.3160	0.8138	0.1862	14.5200	25.5623	0.0009
0.00387	68.1528	0.000672	62.3160	0.8670	0.1330	17.1241	25.5623	0.0008
0.00387	68.1528	0.000672	62.3160	0.9057	0.0943	19.2656	25.5623	0.0008
0.00387	68.1528	0.000672	62.3160	0.9238	0.0762	20.6770	25.5623	0.0008
0.00387	68.1528	0.000672	62.3160	0.9460	0.0540	22.1917	25.5623	0.0007

FAN DATA – RUN 20, ANION EXCHANGE RESINS IN WATER (2 of 3).

EFFECTIVE DENSITY	VISCOSITY RATIO	DENSITY RATIO	DEL DENSITY RATIO	EFFECTIVE REYNOLD'S NUMBER	REQUIRED CLASSICAL N	REQUIRED NEW N	PROPOSED N	PROPOSED Uo/Ut
65.2006	0.6357	0.9872	0.6145	3.5834	3.2153	2.5316	2.4401	0.1189
65.0446	0.6591	0.9878	0.6376	4.1878	3.1042	2.4232	2.3937	0.1441
64.9189	0.6775	0.9884	0.6559	4.7144	3.0730	2.3938	2.3590	0.1663
64.6103	0.7208	0.9897	0.7000	6.1658	2.9733	2.2969	2.2821	0.2283
64.4230	0.7461	0.9905	0.7262	7.1611	2.9470	2.2717	2.2404	0.2710
64.2258	0.7720	0.9914	0.7535	8.3072	2.9138	2.2391	2.1998	0.3201
64.0508	0.7945	0.9922	0.7773	9.4119	2.8730	2.1[illegible]6	2.1661	0.3672
63.8850	0.8154	0.9929	0.7996	10.5379	2.7851	2.1105	2.1500	0.4130
63.7125	0.8368	0.9937	0.8226	11.7941	2.8440	2.1691	2.1500	0.4619
63.5329	0.8586	0.9945	0.8462	13.1961	2.8221	2.1466	2.1500	0.5165
63.4030	0.8743	0.9951	0.8631	14.2736	2.7445	2.0686	2.1500	0.5586
63.0921	0.9111	0.9965	0.9031	17.0747	2.8081	2.1305	2.1500	0.6680
62.8666	0.9373	0.9975	0.9317	19.3123	2.8543	2.1752	2.1500	0.7556
62.7608	0.9495	0.9980	0.9450	20.4245	2.6759	1.9961	2.1500	0.7991
62.6310	0.9643	0.9986	0.9611	21.8450	2.5485	1.8676	2.1500	0.8546

FAN DATA – RUN 20, ANION EXCHANGE RESINS IN WATER (3 of 3).

R&Z N	R&Z Uo/Ut	AL-DIBOUNI N	AL-DIBOUNI Uo/Ut	FOSCOLO Uo/Ut	ACTUAL Uo/Ut
3.2181	0.1115	3.5781	0.0873	0.0553	0.1117
3.2181	0.1316	3.5781	0.1049	0.0703	0.1414
3.2181	0.1495	3.5781	0.1209	0.0845	0.1629
3.2181	0.2005	3.5781	0.1675	0.1282	0.2266
3.2181	0.2367	3.5781	0.2014	0.1616	0.2672
3.2181	0.2793	3.5781	0.2422	0.2031	0.3151
3.2181	0.3214	3.5781	0.2831	0.2456	0.3630
3.2181	0.3651	3.5781	0.3262	0.2912	0.4181
3.2181	0.4148	3.5781	0.3759	0.3443	0.4595
3.2181	0.4712	3.5781	0.4332	0.4059	0.5169
3.2181	0.5152	3.5781	0.4784	0.4546	0.5680
3.2181	0.6318	3.5781	0.6002	0.5853	0.6699
3.2181	0.7270	3.5781	0.7015	0.6929	0.7537
3.2181	0.7749	3.5781	0.7531	0.7471	0.8089
3.2181	0.8365	3.5781	0.8199	0.8168	0.8681

FAN DATA – RUN 23, HEAVY EXCHANGE RESINS IN WATER (1 of 3).

PARTICLE DIAMETER ft	PARTICLE DENSITY lb/cu ft	LIQUID VISCOSITY lb/(ft s)	LIQUID DENSITY lb/cu ft	VOID FRACTION	SOLID FRACTION	INTER. REYNOLD'S NUMBER	TERMINAL REYNOLD'S NUMBER	EFFECTIVE VISCOSITY
0.00244	74.3770	0.000672	62.3600	0.4939	0.5061	1.2227	14.1818	0.0020
0.00244	74.3770	0.000672	62.3600	0.5221	0.4779	1.5116	14.1818	0.0018
0.00244	74.3770	0.000672	62.3600	0.5519	0.4481	1.8252	14.1818	0.0017
0.00244	74.3770	0.000672	62.3600	0.5998	0.4002	2.6611	14.1818	0.0015
0.00244	74.3770	0.000672	62.3600	0.6390	0.3610	3.3683	14.1818	0.0013
0.00244	74.3770	0.000672	62.3600	0.6836	0.3164	4.3651	14.1818	0.0012
0.00244	74.3770	0.000672	62.3600	0.7458	0.2542	5.7917	14.1818	0.0010
0.00244	74.3770	0.000672	62.3600	0.7978	0.2022	7.3309	14.1818	0.0009
0.00244	74.3770	0.000672	62.3600	0.8400	0.1600	8.6457	14.1818	0.0009
0.00244	74.3770	0.000672	62.3600	0.8914	0.1086	9.9589	14.1818	0.0008
0.00244	74.3770	0.000672	62.3600	0.9275	0.0725	11.4714	14.1818	0.0008
0.00244	74.3770	0.000672	62.3600	0.9460	0.0540	12.6054	14.1818	0.0007

FAN DATA – RUN 23, HEAVY EXCHANGE RESINS IN WATER (2 of 3).

EFFECTIVE DENSITY	VISCOSITY RATIO	DENSITY RATIO	DEL DENSITY RATIO	EFFECTIVE REYNOLD'S NUMBER	REQUIRED CLASSICAL N	REQUIRED NEW N	PROPOSED N	PROPOSED Uo/Ut
68.4418	0.6250	0.9738	0.6042	1.9113	3.4744	2.7704	2.6368	0.0947
68.1032	0.6500	0.9751	0.6286	2.2591	3.4446	2.7432	2.5830	0.1183
67.7453	0.6756	0.9766	0.6540	2.6630	3.4490	2.7495	2.5312	0.1465
67.1697	0.7151	0.9790	0.6941	3.3937	3.2729	2.5753	2.4566	0.1994
66.6979	0.7461	0.9810	0.7262	4.0706	3.2101	2.5131	2.4021	0.2496
66.1628	0.7801	0.9832	0.7620	4.9276	3.0971	2.4001	2.3461	0.3142
65.4144	0.8260	0.9864	0.8110	6.2935	3.0536	2.3553	2.2764	0.4180
64.7898	0.8631	0.9891	0.8510	7.5920	2.9211	2.2209	2.2243	0.5165
64.2829	0.8925	0.9914	0.8829	8.7578	2.8381	2.1360	2.1855	0.6044
63.6647	0.9277	0.9941	0.9212	10.3229	3.0758	2.3709	2.1500	0.7203
63.2316	0.9519	0.9960	0.9476	11.5174	2.8168	2.1098	2.1500	0.8064
63.0086	0.9643	0.9970	0.9611	12.1655	2.1238	1.4156	2.1500	0.8534

FAN DATA – RUN 23, HEAVY EXCHANGE RESINS IN WATER (3 of 3).

R&Z N	R&Z Uo/Ut	AL-DIBOUNI N	AL-DIBOUNI Uo/Ut	FOSCOLO Uo/Ut	ACTUAL Uo/Ut
3.4134	0.0900	3.8736	0.0651	0.0427	0.0862
3.4134	0.1088	3.8736	0.0807	0.0555	0.1066
3.4134	0.1315	3.8736	0.1000	0.0722	0.1287
3.4134	0.1746	3.8736	0.1380	0.1066	0.1876
3.4134	0.2168	3.8736	0.1765	0.1432	0.2375
3.4134	0.2729	3.8736	0.2291	0.1951	0.3078
3.4134	0.3675	3.8736	0.3211	0.2894	0.4084
3.4134	0.4625	3.8736	0.4169	0.3899	0.5169
3.4134	0.5514	3.8736	0.5089	0.4875	0.6096
3.4134	0.6755	3.8736	0.6407	0.6272	0.7022
3.4134	0.7734	3.8736	0.7470	0.7392	0.8089
3.4134	0.8275	3.8736	0.8066	0.8015	0.8888

RICHARDSON AND ZAKI DATA – DIVINYL BENZENE PARTICLES IN WATER, SMALL COLUMN (1 of 3).

PARTICLES DIAMETER ft	PARTICLE DENSITY lb/cu ft	LIQUID VISCOSITY lb/(ft s)	LIQUID DENSITY lb/cu ft	VOID FRACTION	SOLID FRACTION	INLET FLOW ft/s	TERMINAL VELOCITY ft/s	TERMINAL REYNOLD'S NUMBER
0.00083	66.1700	0.000672	62.4300	0.5720	0.4280	0.0004	0.0064	0.4908
0.00083	66.1700	0.000672	62.4300	0.5970	0.4030	0.0006	0.0064	0.4908
0.00083	66.1700	0.000672	62.4300	0.6090	0.3910	0.0006	0.0064	0.4908
0.00083	66.1700	0.000672	62.4300	0.6280	0.3720	0.0007	0.0064	0.4908
0.00083	66.1700	0.000672	62.4300	0.6670	0.3330	0.0010	0.0064	0.4908
0.00083	66.1700	0.000672	62.4300	0.6720	0.3280	0.0010	0.0064	0.4908
0.00083	66.1700	0.000672	62.4300	0.6790	0.3210	0.0011	0.0064	0.4908
0.00083	66.1700	0.000672	62.4300	0.6970	0.3030	0.0012	0.0064	0.4908

RICHARDSON AND ZAKI DATA – DIVINYL BENZENE PARTICLES IN WATER, SMALL COLUMN (2 of 3).

EFFECTIVE VISCOSITY	EFFECTIVE DENSITY	VISCOSITY RATIO	DENSITY RATIO	DEL DENSITY RATIO	EFFECTIVE REYNOLD'S NUMBER	REQUIRED CLASSICAL N	REQUIRED NEW N	PROPOSED N
0.0016	64.0307	0.6924	0.9928	0.6710	0.0985	4.8386	4.1677	3.7500
0.0015	63.9372	0.7128	0.9932	0.6918	0.1118	4.6090	3.9395	3.7500
0.0014	63.8923	0.7225	0.9934	0.7017	0.1185	4.6849	4.0160	3.7500
0.0014	63.8213	0.7375	0.9937	0.7173	0.1296	4.7792	4.1111	3.7500
0.0012	63.6754	0.7676	0.9944	0.7488	0.1544	4.6094	3.9424	3.7500
0.0012	63.6567	0.7714	0.9945	0.7528	0.1577	4.5337	3.8667	3.7500
0.0012	63.6305	0.7767	0.9946	0.7584	0.1625	4.4984	3.8316	3.7500
0.0012	63.5632	0.7902	0.9949	0.7727	0.1752	4.5902	3.9237	3.7500

RICHARDSON AND ZAKI DATA – DIVINYL BENZENE PARTICLES IN WATER, SMALL COLUMN (3 of 3).

PROPOSED Uo/Ut	R&Z N	R&Z Uo/Ut	AL-DIBOUNI N	AL-DIBOUNI Uo/Ut	FOSCOLO Uo/Ut	ACTUAL Uo/Ut
0.0846	4.5626	0.0782	4.9655	0.0624	0.0692	0.0670
0.1023	4.5626	0.0950	4.9655	0.0772	0.0849	0.0928
0.1118	4.5626	0.1041	4.9655	0.0852	0.0934	0.0979
0.1280	4.5626	0.1197	4.9655	0.0993	0.1083	0.1082
0.1672	4.5626	0.1576	4.9655	0.1339	0.1445	0.1546
0.1728	4.5626	0.1631	4.9655	0.1389	0.1498	0.1649
0.1809	4.5626	0.1710	4.9655	0.1463	0.1574	0.1753
0.2031	4.5626	0.1926	4.9655	0.1666	0.1784	0.1907

RICHARDSON AND ZAKI DATA – DIVINYL BENZENE PARTICLES IN WATER, LARGE COLUMN (1 of 3).

PARTICLE DIAMETER ft	PARTICLE DENSITY lb/cu ft	LIQUID VISCOSITY lb/(ft s)	LIQUID DENSITY lb/cu ft	VOID FRACTION	SOLID FRACTION	INLET FLOW ft/s	TERMINAL VELOCITY ft/s	TERMINAL REYNOLD'S NUMBER
0.00083	66.1700	0.000672	62.4300	0.5210	0.4790	0.0004	0.0064	0.4908
0.00083	66.1700	0.000672	62.4300	0.5540	0.4460	0.0005	0.0064	0.4908
0.00083	66.1700	0.000672	62.4300	0.5770	0.4230	0.0006	0.0064	0.4908
0.00083	66.1700	0.000672	62.4300	0.6140	0.3860	0.0007	0.0064	0.4908
0.00083	66.1700	0.000672	62.4300	0.6640	0.3360	0.0012	0.0064	0.4908
0.00083	66.1700	0.000672	62.4300	0.6720	0.3280	0.0011	0.0064	0.4908
0.00083	66.1700	0.000672	62.4300	0.6930	0.3070	0.0013	0.0064	0.4908
0.00083	66.1700	0.000672	62.4300	0.7150	0.2850	0.0015	0.0064	0.4908
0.00083	66.1700	0.000672	62.4300	0.7440	0.2560	0.0018	0.0064	0.4908
0.00083	66.1700	0.000672	62.4300	0.7670	0.2330	0.0021	0.0064	0.4908

RICHARDSON AND ZAKI DATA – DIVINYL BENZENE PARTICLES IN WATER, LARGE COLUMN (2 of 3).

EFFECTIVE VISCOSITY	EFFECTIVE DENSITY	VISCOSITY RATIO	DENSITY RATIO	DEL DENSITY RATIO	EFFECTIVE REYNOLD'S NUMBER	REQUIRED CLASSICAL N	REQUIRED NEW N	PROPOSED N
0.0018	64.2215	0.6491	0.9919	0.6277	0.0744	4.3879	3.7126	3.7500
0.0017	64.0980	0.6774	0.9925	0.6558	0.0896	4.2679	3.5957	3.7500
0.0016	64.0120	0.6966	0.9929	0.6752	0.1011	4.3643	3.6937	3.7500
0.0014	63.8736	0.7264	0.9935	0.7058	0.1213	4.3987	3.7300	3.7500
0.0013	63.6866	0.7653	0.9943	0.7464	0.1524	4.1202	3.4531	3.7500
0.0012	63.6567	0.7714	0.9945	0.7528	0.1577	4.3738	3.7068	3.7500
0.0012	63.5782	0.7872	0.9948	0.7695	0.1724	4.3193	3.6527	3.7500
0.0011	63.4959	0.8035	0.9952	0.7869	0.1885	4.2643	3.5978	3.7500
0.0011	63.3874	0.8247	0.9957	0.8096	0.2113	4.3184	3.6520	3.7500
0.0010	63.3014	0.8412	0.9960	0.8274	0.2305	4.2340	3.5673	3.7500

RICHARDSON AND ZAKI DATA – DIVINYL BENZENE PARTICLES IN WATER, LARGE COLUMN (3 of 3).

PROPOSED Uo/Ut	R&Z N	R&Z Uo/Ut	AL-DIBOUNI N	AL-DIBOUNI Uo/Ut	FOSCOLO U/Ut	ACTUAL U/Ut
0.0558	4.5169	0.0526	4.9655	0.0393	0.0442	0.0572
0.0734	4.5169	0.0694	4.9655	0.0533	0.0593	0.0804
0.0880	4.5169	0.0834	4.9655	0.0652	0.0721	0.0907
0.1159	4.5169	0.1105	4.9655	0.0887	0.0972	0.1170
0.1639	4.5169	0.1573	4.9655	0.1309	0.1414	0.1851
0.1728	4.5169	0.1661	4.9655	0.1389	0.1498	0.1758
0.1980	4.5169	0.1908	4.9655	0.1619	0.1736	0.2052
0.2273	4.5169	0.2197	4.9655	0.1890	0.2016	0.2392
0.2709	4.5169	0.2630	4.9655	0.2303	0.2439	0.2789
0.3099	4.5169	0.3017	4.9655	0.2679	0.2822	0.3253

LOEFFLER AND RUTH DATA – GLASS BEADS IN WATER (1 of 3).

PARTICLE DIAMETER ft	PARTICLE DENSITY lb/cu ft	LIQUID VISCOSITY lb/(ft s)	LIQUID DENSITY lb/cu ft	VOID FRACTION	SOLID FRACTION	INTER. REYNOLD'S NUMBER	TERMINAL REYNOLD'S NUMBER	EFFECTIVE VISCOSITY
0.00216	164.1909	0.000672	62.4300	0.5100	0.4900	9.5000	70.0000	1.9077E-03
0.00216	164.1909	0.000672	62.4300	0.5500	0.4500	12.0000	70.0000	1.6868E-03
0.00216	164.1909	0.000672	62.4300	0.5800	0.4200	15.0000	70.0000	1.5496E-03
0.00216	164.1909	0.000672	62.4300	0.6250	0.3750	17.0000	70.0000	1.3777E-03
0.00216	164.1909	0.000672	62.4300	0.6500	0.3500	22.0000	70.0000	1.2963E-03
0.00216	164.1909	0.000672	62.4300	0.7200	0.2800	28.0000	70.0000	1.1076E-03
0.00216	164.1909	0.000672	62.4300	0.7980	0.2020	34.5000	70.0000	9.4713E-04
0.00216	164.1909	0.000672	62.4300	0.8300	0.1700	40.0000	70.0000	8.9229E-04
0.00216	164.1909	0.000672	62.4300	0.9000	0.1000	50.0000	70.0000	7.8913E-04

LOEFFLER AND RUTH DATA – GLASS BEADS IN WATER (2 of 3).

EFFECITVE DENSITY	VISCOSITY RATIO	DENSITY RATIO	DEL DENSITY RATIO	EFFECTIVE REYNOLD'S NUMBER	REQUIRED CLASSICAL N	REQUIRED NEW N	PROPOSED N	PROPOSED Uo/Ut
112.2928	0.6394	0.8456	0.6182	14.8239	2.9661	2.0528	2.1500	0.1271
108.2224	0.6740	0.8546	0.6524	18.1671	2.9499	2.0272	2.1500	0.1593
105.1696	0.6990	0.8616	0.6777	20.8711	2.8279	1.8970	2.1500	0.1867
100.5903	0.7351	0.8726	0.7148	25.2253	3.0112	2.0666	2.1500	0.2335
98.0463	0.7546	0.8790	0.7351	27.7895	2.6869	1.7338	2.1500	0.2627
90.9231	0.8072	0.8982	0.7908	35.4630	2.7893	1.8103	2.1500	0.3578
82.9857	0.8632	0.9219	0.8511	44.7169	3.1356	2.1234	2.1500	0.4899
79.7294	0.8856	0.9325	0.8754	48.6696	3.0034	1.9761	2.1500	0.5532
72.6061	0.9335	0.9578	0.9275	57.4874	3.1935	2.1305	2.1500	0.7128

LOEFFLER AND RUTH DATA – GLASS BEADS IN WATER (3 of 3).

R&Z N	R&Z Uo/Ut	AL-DIBOUNI N	AL-DIBOUNI Uo/Ut	FOSCOLO Uo/Ut	ACTUAL Uo/Ut
3.2070	0.1154	3.1745	0.1179	0.0837	0.1357
3.2070	0.1470	3.1745	0.1499	0.1157	0.1714
3.2070	0.1743	3.1745	0.1774	0.1445	0.2143
3.2070	0.2215	3.1745	0.2249	0.1955	0.2429
3.2070	0.2512	3.1745	0.2547	0.2260	0.3143
3.2070	0.3487	3.1745	0.3525	0.3352	0.4000
3.2070	0.4850	3.1745	0.4886	0.4828	0.4929
3.2070	0.5502	3.1745	0.5535	0.5518	0.5714
3.2070	0.7133	3.1745	0.7157	0.7200	0.7143

JACOB AND WEIMER DATA – CARBON POWDER IN GAS, P = 12420 kPa, Dp = 44 MICRONS (1 of 3).

PARTICLE DIAMETER ft	PARTICLE DENSITY lb/cu ft	GAS VISCOSITY lb/(ft s)	GAS DENSITY lb/cu ft	VOID FRACTION	SOLID FRACTION	INLET FLOW ft/s	TERMINAL VELOCITY ft/s	TERMINAL REYNOLD'S NUMBER
1.4436E-04	53.0656	1.1155E-05	5.3203	0.6660	0.3340	0.0132	0.1063	7.3187
1.4436E-04	53.0658	1.1155E-05	5.3203	0.7050	0.2950	0.0175	0.1063	7.3187
1.4436E-04	53.0656	1.1155E-05	5.3203	0.7390	0.2610	0.0222	0.1063	7.3187
1.4436E-04	53.0656	1.1155E-05	5.3203	0.7590	0.2410	0.0231	0.1063	7.3187
1.4436E-04	53.0656	1.1155E-05	5.3203	0.7730	0.2270	0.0269	0.1063	7.3187
1.4436E-04	53.0656	1.1155E-05	5.3203	0.7850	0.2150	0.0307	0.1063	7.3187
1.4436E-04	53.0656	1.1155E-05	5.3203	0.8030	0.1970	0.0357	0.1063	7.3187

JACOB AND WEIMER DATA – CARBON POWDER IN GAS, P = 12420 kPa, Dp = 44 MICRONS (2 of 3).

EFFECTIVE VISCOSITY	EFFECTIVE DENSITY	VISCOSITY RATIO	DENSITY RATIO	DEL DENSITY RATIO	EFFECTIVE REYNOLD'S NUMBER	REQUIRED CLASSICAL N	REQUIRED NEW N	PROFOSED N
2.0724E-05	21.2672	0.7668	0.6731	0.7460	6.0799	5.1281	3.5011	2.2861
1.8988E-05	19.4052	0.7961	0.6909	0.7790	6.7203	5.1578	3.4480	2.2580
1.7670E-05	17.7818	0.8211	0.7084	0.8057	7.2367	5.1765	3.3849	2.2375
1.6966E-05	16.8269	0.8355	0.7197	0.8212	7.5150	5.5360	3.6913	2.2271
1.6501E-05	16.1585	0.8455	0.7280	0.8320	7.6961	5.3366	3.4522	2.2206
1.6119E-05	15.5855	0.8540	0.7356	0.8412	7.8410	5.1252	3.2049	2.2155
1.5574E-05	14.7261	0.8667	0.7476	0.8549	8.0382	4.9780	3.0003	2.2087

JACOB AND WEIMER DATA – CARBON POWDER IN GAS, P = 12420 kPa, Dp = 44 MICRONS (3 of 3).

PROPOSED Uo/Ut	R&Z N	R&Z Uo/Ut	AL-DIBOUNI N	AL-DIBOUNI Uo/Ut	FOSCOLO Uo/Ut	ACTUAL Uo/Ut
0.2038	3.6535	0.2265	4.2091	0.1807	0.1589	0.1244
0.2498	3.6535	0.2788	4.2091	0.2296	0.2075	0.1648
0.2956	3.6535	0.3312	4.2091	0.2800	0.2583	0.2089
0.3254	3.6535	0.3651	4.2091	0.3133	0.2922	0.2173
0.3475	3.6535	0.3904	4.2091	0.3383	0.3179	0.2531
0.3675	3.6535	0.4130	4.2091	0.3610	0.3412	0.2892
0.3991	3.6535	0.4486	4.2091	0.3971	0.3785	0.3355

JACOB AND WEIMER DATA – CARBON POWDER IN GAS, P = 10350 kPa, Dp = 44 MICRONS (1 of 3).

PARTICLE DIAMETER ft	PARTICLE DENSITY lb/cu ft	GAS VISCOSITY lb/(ft s)	GAS DENSITY lb/cu ft	VOID FRACTION	SOLID FRACTION	INLET FLOW ft/s	TERMINAL VELOCITY ft/s	TERMINAL REYNOLD'S NUMBER
1.4436E–04	53.0656	1.1155E–05	4.4332	0.6710	0.3290	0.0151	0.1145	6.5688
1.4436E–04	53.0656	1.1155E–05	4.4332	0.7000	0.3000	0.0187	0.1145	6.5688
1.4436E–04	53.0656	1.1155E–05	4.4332	0.7460	0.2540	0.0215	0.1145	6.5688
1.4436E–04	53.0656	1.1155E–05	4.4332	0.7220	0.2780	0.0224	0.1145	6.5688
1.4436E–04	53.0656	1.1155E–05	4.4332	0.7690	0.2310	0.0265	0.1145	6.5688
1.4436E–04	53.0656	1.1155E–05	4.4332	0.7810	0.2190	0.0305	0.1145	6.5688

JACOB AND WEIMER DATA – CARBON POWDER IN GAS, P = 10350 kPa, Dp = 44 MICRONS (2 of 3).

EFFECTIVE VISCOSITY	EFFECTIVE DENSITY	VISCOSITY RATIO	DENSITY RATIO	DEL DENSITY RATIO	EFFECTIVE REYNOLD'S NUMBER	REQUIRED CLASSICAL N	REQUIRED NEW N	PROPOSED N
2.0486E-05	20.4333	0.7706	0.6463	0.7520	6.1745	5.0844	3.3373	2.2817
1.9196E-05	19.0229	0.7924	0.6596	0.7751	6.6357	5.0803	3.2613	2.2616
1.7418E-05	16.7858	0.8261	0.6836	0.8111	7.2969	5.7094	3.7595	2.2352
1.8309E-05	17.9530	0.8087	0.6706	0.7924	6.9647	5.0122	3.1335	2.2481
1.6631E-05	15.6673	0.8427	0.6972	0.8289	7.5828	5.5655	3.5406	2.2246
1.6245E-05	15.0837	0.8512	0.7048	0.8381	7.7171	5.3546	3.2875	2.2198

JACOB AND WEIMER DATA – CARBON POWDER IN GAS, P = 10350 kPa, Dp = 44 MICRONS (3 of 3).

PROPOSED Uo/Ut	R&Z N	R&Z Uo/Ut	AL-DIBOUNI N	AL-DIBOUNI Uo/Ut	FOSCOLO Uo/Ut	ACTUAL Uo/Ut
0.2004	3.6932	0.2291	4.2608	0.1827	0.1629	0.1315
0.2333	3.6932	0.2679	4.2608	0.2188	0.1987	0.1633
0.2934	3.6932	0.3388	4.2608	0.2869	0.2674	0.1877
0.2607	3.6932	0.3003	4.2608	0.2496	0.2297	0.1954
0.3275	3.6932	0.3791	4.2608	0.3266	0.3079	0.2318
0.3466	3.6932	0.4014	4.2608	0.3488	0.3307	0.2662

JACOB AND WEIMER DATA – CARBON POWDER IN GAS, P = 8280 kPa, Dp = 44 MICRONS (1 of 3).

PARTICLE DIAMETER ft	PARTICLE DENSITY lb/cu ft	GAS VISCOSITY lb/(ft s)	GAS DENSITY lb/cu ft	VOID FRACTION	SOLID FRACTION	INLET FLOW ft/s	TERMINAL VELOCITY ft/s	TERMINAL REYNOLD'S NUMBER
1.4436E-04	53.0656	1.1155E-05	3.5466	0.6810	0.3190	0.0167	0.1568	7.1965
1.4436E-04	53.0656	1.1155E-05	3.5466	0.7130	0.2870	0.0211	0.1568	7.1965
1.4436E-04	53.0656	1.1155E-05	3.5466	0.7430	0.2570	0.0241	0.1568	7.1965
1.4436E-04	53.0656	1.1155E-05	3.5466	0.7320	0.2680	0.0256	0.1568	7.1965
1.4436E-04	53.0656	1.1155E-05	3.5466	0.7620	0.2380	0.0298	0.1568	7.1965
1.4436E-04	53.0656	1.1155E-05	3.5466	0.7760	0.2240	0.0342	0.1568	7.1965
1.4436E-04	53.0656	1.1155E-05	3.5466	0.7830	0.2170	0.0371	0.1568	7.1965
1.4436E-04	53.0656	1.1155E-05	3.5466	0.7890	0.2110	0.0400	0.1568	7.1965
1.4436E-04	53.0656	1.1155E-05	3.5466	0.7880	0.2120	0.0429	0.1568	7.1965

JACOB AND WEIMER DATA - CARBON POWDER IN GAS, P = 8280 kPa, Dp = 44 MICRONS (2 of 3).

EFFECTIVE VISCOSITY	EFFECTIVE DENSITY	VISCOSITY RATIO	DENSITY RATIO	DEL DENSITY RATIO	EFFECTIVE REYNOLD'S NUMBER	REQUIRED CLASSICAL N	REQUIRED NEW N	PROPOSED N
2.0025E-05	19.3432	0.7782	0.6159	0.7600	7.9647	5.8345	3.9203	2.2112
1.8663E-05	17.7586	0.8021	0.6311	0.7853	8.5623	5.9344	3.9218	2.1916
1.7525E-05	16.2730	0.8240	0.6471	0.8088	9.0637	6.3024	4.1853	2.1762
1.7928E-05	16.8177	0.8160	0.6410	0.8002	8.8876	5.8065	3.7293	2.1815
1.6864E-05	15.3321	0.8377	0.6582	0.8235	9.3436	6.1102	3.9197	2.1681
1.6404E-05	14.6389	0.8477	0.6670	0.8343	9.5275	6.0061	3.7572	2.1629
1.6182E-05	14.2922	0.8526	0.6715	0.8397	9.6116	5.8951	3.6156	2.1605
1.5995E-05	13.9951	0.8569	0.6756	0.8443	9.6792	5.7651	3.4584	2.1587
1.6026E-05	14.0446	0.8562	0.6749	0.8435	9.6682	5.4355	3.1334	2.1590

JACOB AND WEIMER DATA – CARBON POWDER IN GAS, P = 8280 kPa, Dp = 44 MICRONS (3 of 3).

PROPOSED Uo/Ut	R&Z N	R&Z Uo/Ut	AL-DIBOUNI N	AL-DIBOUNI Uo/Ut	FOSCOLO Uo/Ut	ACTUAL Uo/Ut
0.2050	3.6597	0.2451	4.2173	0.1979	0.1761	0.1063
0.2412	3.6597	0.2900	4.2173	0.2401	0.2183	0.1343
0.2793	3.6597	0.3372	4.2173	0.2857	0.2644	0.1538
0.2648	3.6597	0.3193	4.2173	0.2683	0.2468	0.1634
0.3058	3.6597	0.3698	4.2173	0.3178	0.2972	0.1900
0.3267	3.6597	0.3953	4.2173	0.3432	0.3232	0.2180
0.3375	3.6597	0.4085	4.2173	0.3564	0.3368	0.2364
0.3471	3.6597	0.4201	4.2173	0.3681	0.3488	0.2551
0.3455	3.6597	0.4181	4.2173	0.3661	0.3468	0.2739

JACOB AND WEIMER DATA – CARBON POWDER IN GAS, P = 6210 kPa, Dp = 44 MICRONS (1 of 3).

PARTICLE DIAMETER ft	PARTICLE DENSITY lb/cu ft	GAS VISCOSITY lb/(ft s)	GAS DENSITY lb/cu ft	VOID FRACTION	SOLID FRACTION	INLET FLOW ft/s	TERMINAL VELOCITY ft/s	TERMINAL REYNOLD'S NUMBER
1.4436E-04	53.0656	1.1155E-05	2.6601	0.6800	0.3200	0.0175	0.1811	6.2342
1.4436E-04	53.0656	1.1155E-05	2.6601	0.7030	0.2970	0.0210	0.1811	6.2342
1.4436E-04	53.0656	1.1155E-05	2.6601	0.7340	0.2660	0.0257	0.1811	6.2342
1.4436E-04	53.0656	1.1155E-05	2.6601	0.7310	0.2690	0.0259	0.1811	6.2342
1.4436E-04	53.0656	1.1155E-05	2.6601	0.7560	0.2440	0.0309	0.1811	6.2342
1.4436E-04	53.0656	1.1155E-05	2.6601	0.7660	0.2340	0.0347	0.1811	6.2342
1.4436E-04	53.0656	1.1155E-05	2.6601	0.7670	0.2330	0.0380	0.1811	6.2342

JACOB AND WEIMER DATA – CARBON POWDER IN GAS, P = 6210 kPa, Dp = 44 MICRONS (2 of 3).

EFFECTIVE VISCOSITY	EFFECTIVE DENSITY	VISCOSITY RATIO	DENSITY RATIO	DEL DENSITY RATIO	EFFECTIVE REYNOLD'S NUMBER	REQUIRED CLASSICAL N	REQUIRED NEW N	PROPOSED N
2.0070E-05	18.7899	0.7775	0.5720	0.7592	8.2641	6.0662	3.9652	2.2012
1.9071E-05	17.6305	0.7947	0.5826	0.7775	8.6983	6.1099	3.9243	2.1873
1.7854E-05	16.0680	0.8174	0.5982	0.8018	9.2247	6.3195	4.0061	2.1715
1.7966E-05	16.2192	0.8152	0.5966	0.7995	9.1772	6.2084	3.9082	2.1729
1.7068E-05	14.9590	0.8334	0.6106	0.8189	9.5464	6.3174	3.9018	2.1623
1.6731E-05	14.4550	0.8405	0.6166	0.8266	9.6758	6.1936	3.7278	2.1588
1.6697E-05	14.4046	0.8412	0.6172	0.8274	9.6881	5.8872	3.4162	2.1584

JACOB AND WEIMER DATA – CARBON POWDER IN GAS, P = 6210 kPa, Dp = 44 MICRONS (3 of 3).

PROPOSED Uo/Ut	R&Z N	R&Z Uo/Ut	AL-DIBOUNI N	AL-DIBOUNI Uo/Ut	FOSCOLO Uo/Ut	ACTUAL Uo/Ut
0.1903	3.7126	0.2389	4.2853	0.1915	0.1727	0.0964
0.2142	3.7126	0.2703	4.2853	0.2209	0.2019	0.1161
0.2498	3.7126	0.3172	4.2853	0.2657	0.2470	0.1417
0.2462	3.7126	0.3124	4.2853	0.2611	0.2423	0.1429
0.2779	3.7126	0.3540	4.2853	0.3016	0.2834	0.1708
0.2915	3.7126	0.3717	4.2853	0.3191	0.3012	0.1918
0.2928	3.7126	0.3735	4.2853	0.3209	0.3031	0.2098

JACOB AND WEIMER DATA – CARBON POWDER IN GAS, P = 4140 kPa, Dp = 44 MICRONS (1 of 3).

PARTICLE DIAMETER ft	PARTICLE DENSITY lb/cu ft	GAS VISCOSITY lb/(ft s)	GAS DENSITY lb/cu ft	VOID FRACTION	SOLID FRACTION	INLET FLOW ft/s	TERMINAL VELOCITY ft/s	TERMINAL REYNOLD'S NUMBER
1.4436E-04	53.0656	1.1155E-05	1.7736	0.6880	0.3120	0.0146	0.1811	4.1566
1.4436E-04	53.0656	1.1155E-05	1.7736	0.6840	0.3160	0.0168	0.1811	4.1566
1.4436E-04	53.0656	1.1155E-05	1.7736	0.7200	0.2800	0.0196	0.1811	4.1566
1.4436E-04	53.0656	1.1155E-05	1.7736	0.7360	0.2640	0.0229	0.1811	4.1566
1.4436E-04	53.0656	1.1155E-05	1.7736	0.7510	0.2490	0.0283	0.1811	4.1566
1.4436E-04	53.0656	1.1155E-05	1.7736	0.7570	0.2430	0.0331	0.1811	4.1566

JACOB AND WEIMER DATA – CARBON POWDER IN GAS, P = 4140 kPa, Dp = 44 MICRONS (2 of 3).

EFFECTIVE VISCOSITY	EFFECTIVE DENSITY	VISCOSITY RATIO	DENSITY RATIO	DEL DENSITY RATIO	EFFECTIVE REYNOLD'S NUMBER	REQUIRED CLASSICAL N	REQUIRED NEW N	PROPOSED N
1.9712E-05	17.7767	0.7835	0.5176	0.7656	7.3196	6.7274	4.3140	2.2344
1.9890E-05	17.9819	0.7805	0.5159	0.7624	7.2557	6.2556	3.8605	2.2368
1.8386E-05	16.1354	0.8072	0.5322	0.7908	7.7937	6.7707	4.1984	2.2171
1.7780E-05	15.3147	0.8189	0.5401	0.8034	8.0017	6.7510	4.0898	2.2099
1.7242E-05	14.5453	0.8298	0.5482	0.8150	8.1756	6.4806	3.7294	2.2041
1.7034E-05	14.2376	0.8341	0.5515	0.8197	8.2389	6.1044	3.3151	2.2020

JACOB AND WEIMER DATA – CARBON POWDER IN GAS, P = 4140 kPa, Dp = 44 MICRONS (3 of 3).

PROPOSED Uo/Ut	R&Z N	R&Z Uo/Ut	AL-DIBOUNI N	AL-DIBOUNI Uo/Ut	FOSCOLO Uo/Ut	ACTUAL Uo/Ut
0.1759	3.8662	0.2356	4.4619	0.1885	0.1772	0.0808
0.1722	3.8662	0.2303	4.4619	0.1837	0.1724	0.0929
0.2074	3.8662	0.2808	4.4619	0.2309	0.2197	0.1082
0.2247	3.8662	0.3057	4.4619	0.2547	0.2437	0.1263
0.2420	3.8662	0.3305	4.4619	0.2787	0.2679	0.1563
0.2492	3.8662	0.3406	4.4619	0.2888	0.2781	0.1828

JACOB AND WEIMER DATA – CARBON POWDER IN GAS, P = 2070 kPa, Dp = 44 MICRONS (1 of 3).

PARTICLE DIAMETER ft	PARTICLE DENSITY lb/cu ft	GAS VISCOSITY lb/(ft s)	GAS DENSITY lb/cu ft	VOID FRACTION	SOLID FRACTION	INLET FLOW ft/s	TERMINAL VELOCITY ft/s	TERMINAL REYNOLD'S NUMBER
1.4436E-04	53.0656	1.1155E-05	0.8865	0.7040	0.2960	0.0177	0.2027	2.3254
1.4436E-04	53.0656	1.1155E-05	0.8865	0.7480	0.2520	0.0243	0.2027	2.3254
1.4436E-04	53.0656	1.1155E-05	0.8865	0.7670	0.2330	0.0307	0.2027	2.3254
1.4436E-04	53.0656	1.1155E-05	0.8865	0.7650	0.2350	0.0324	0.2027	2.3254

JACOB AND WEIMER DATA – CARBON POWDER IN GAS, P = 2070 kPa, Dp = 44 MICRONS (2 of 3).

EFFECTIVE VISCOSITY	EFFECTIVE DENSITY	VISCOSITY RATIO	DENSITY RATIO	DEL DENSITY RATIO	EFFECTIVE REYNOLD'S NUMBER	REQUIRED CLASSICAL N	REQUIRED NEW N	PROPOSED N
1.9029E-05	16.3315	0.7954	0.4350	0.7783	6.7621	6.9389	3.9150	2.2563
1.7347E-05	14.0356	0.8276	0.4542	0.8127	7.2330	7.3089	3.9393	2.2376
1.6697E-05	13.0442	0.8412	0.4638	0.8274	7.3800	7.1143	3.5666	2.2321
1.6764E-05	13.1486	0.8398	0.4628	0.8258	7.3664	6.8393	3.3114	2.2326

JACOB AND WEIMER DATA – CARBON POWDER IN GAS, P = 2070 kPa, Dp = 44 MICRONS (3 of 3).

PROPOSED Uo/Ut	R&Z N	R&Z Uo/Ut	AL-DIBOUNI N	AL-DIBOUNI Uo/Ut	FOSCOLO Uo/Ut	ACTUAL Uo/Ut
0.1567	4.0974	0.2374	4.6677	0.1943	0.1924	0.0876
0.1963	4.0974	0.3043	4.6677	0.2579	0.2567	0.1198
0.2158	4.0974	0.3373	4.6677	0.2899	0.2891	0.1515
0.2137	4.0974	0.3337	4.6677	0.2864	0.2856	0.1601

JACOB AND WEIMER DATA – CARBON POWDER IN GAS, P = 12420 kPa, Dp = 112 MICRONS (1 of 3).

PARTICLE DIAMETER ft	PARTICLE DENSITY lb/cu ft	GAS VISCOSITY lb/(ft s)	GAS DENSITY lb/cu ft	VOID FRACTION	SOLID FRACTION	INLET FLOW ft/s	TERMINAL VELOCITY ft/s	TERMINAL REYNOLD'S NUMBER
3.6745E-04	53.0656	1.1155E-05	5.3203	0.5500	0.4500	0.0276	0.3067	53.7500
3.6745E-04	53.0656	1.1155E-05	5.3203	0.5960	0.4040	0.0368	0.3067	53.7500
3.6745E-04	53.0656	1.1155E-05	5.3203	0.6200	0.3800	0.0437	0.3067	53.7500
3.6745E-04	53.0656	1.1155E-05	5.3203	0.6270	0.3730	0.0474	0.3067	53.7500

JACOB AND WEIMER DATA – CARBON POWDER IN GAS, P = 12420 kPa, Dp = 112 MICRONS (2 of 3).

EFFECTIVE VISCOSITY	EFFECTIVE DENSITY	VISCOSITY RATIO	DENSITY RATIO	DEL DENSITY RATIO	EFFECTIVE REYNOLD'S NUMBER	REQUIRED CLASSICAL N	REQUIRED NEW N	PROPOSED N
2.[illegible]001E-05	26.8057	0.6740	0.6300	0.6524	29.8917	4.0285	2.5959	2.1500
2.4639E-05	24.6094	0.7120	0.6456	0.6910	35.7527	4.0984	2.5966	2.1500
2.3159E-05	23.4635	0.7312	0.6545	0.7107	38.8331	4.0777	2.5358	2.1500
2.2756E-05	23.1293	0.7367	0.6571	0.7165	39.7290	3.9997	2.4457	2.1500

JACOB AND WEIMER DATA – CARBON POWDER IN GAS, P = 12420 kPa, Dp = 112 MICRONS (3 of 3).

PROPOSED Uo/Ut	R&Z N	R&Z Uo/Ut	AL-DIBOUNI N	AL-DIBOUNI Uo/Ut	FOSCOLO Uo/Ut	ACTUAL Uo/Ut
0.1174	3.0016	0.1662	3.2640	0.1421	0.1046	0.0900
0.1511	3.0016	0.2115	3.2640	0.1847	0.1478	0.1199
0.1712	3.0016	0.2382	3.2640	0.2101	0.1745	0.1424
0.1774	3.0016	0.2463	3.2640	0.2179	0.1828	0.1546

JACOB AND WEIMER DATA – CARBON POWDER IN GAS, P = 10350 kPa, Dp = 112 MICRONS (1 of 3).

PARTICLE DIAMETER ft	PARTICLE DENSITY lb/cu ft	GAS VISCOSITY lb/(ft s)	GAS DENSITY lb/cu ft	VOID FRACTION	SOLID FRACTION	INLET FLOW ft/s	TERMINAL VELOCITY ft/s	TERMINAL REYNOLD'S NUMBER
3.6745E-04	53.0656	1.1155E-05	4.4332	0.5390	0.4610	0.0265	0.3159	46.1313
3.6745E-04	53.0656	1.1155E-05	4.4332	0.5750	0.4250	0.0341	0.3159	46.1313
3.6745E-04	53.0656	1.1155E-05	4.4332	0.6000	0.4000	0.0399	0.3159	46.1313
3.6745E-04	53.0656	1.1155E-05	4.4332	0.6090	0.3910	0.0441	0.3159	46.1313
3.6745E-04	53.0656	1.1155E-05	4.4332	0.6200	0.3800	0.0467	0.3159	46.1313
3.6745E-04	53.0656	1.1155E-05	4.4332	0.6300	0.3700	0.0489	0.3159	46.1313

JACOB AND WEIMER DATA – CARBON POWDER IN GAS, P = 10350 kPa, Dp = 112 MICRONS (2 of 3).

EFFECTIVE VISCOSITY	EFFECTIVE DENSITY	VISCOSITY RATIO	DENSITY RATIO	DEL DENSITY RATIO	EFFECTIVE REYNOLD'S NUMBER	REQUIRED CLASSICAL N	REQUIRED NEW N	PROPOSED N
2.8930E-05	26.8527	0.6647	0.5977	0.6431	27.5286	4.0074	2.5138	2.1500
2.6079E-05	25.1020	0.6949	0.6094	0.6735	31.8639	4.0217	2.4688	2.1500
2.4381E-05	23.8862	0.7152	0.6181	0.6943	34.9036	4.0523	2.4543	2.1500
2.3817E-05	23.4485	0.7225	0.6213	0.7017	35.9969	3.9690	2.3539	2.1500
2.3159E-05	22.9135	0.7312	0.6254	0.7107	37.3291	3.9997	2.3630	2.1500
2.2588E-05	22.4272	0.7391	0.6293	0.7189	38.5340	4.0371	2.3802	2.1500

JACOB AND WEIMER DATA – CARBON POWDER IN GAS, P = 10350 kPa, Dp = 112 MICRONS (3 of 3).

PROPOSED Uo/Ut	R&Z N	R&Z Uo/Ut	AL-DIBOUNI N	AL-DIBOUNI Uo/Ut	FOSCOLO Uo/Ut	ACTUAL Uo/Ut
0.1052	3.0478	0.1520	3.3214	0.1284	0.0904	0.0840
0.1288	3.0478	0.1851	3.3214	0.1591	0.1203	0.1080
0.1474	3.0478	0.2108	3.3214	0.1833	0.1447	0.1262
0.1545	3.0478	0.2206	3.3214	0.1926	0.1542	0.1397
0.1636	3.0478	0.2329	3.3214	0.2044	0.1665	0.1478
0.1722	3.0478	0.2446	3.3214	0.2155	0.1781	0.1548

JACOB AND WEIMER DATA – CARBON POWDER IN GAS, P = 8280 kPa, Dp = 112 MICRONS (1 of 3).

PARTICLE DIAMETER ft	PARTICLE DENSITY lb/cu ft	GAS VISCOSITY lb/(ft s)	GAS DENSITY lb/cu ft	VOID FRACTION	SOLID FRACTION	INLET FLOW ft/s	TERMINAL VELOCITY ft/s	TERMINAL REYNOLD'S NUMBER
3.6745E-04	53.0656	1.1155E-05	3.5466	0.5260	0.4740	0.0284	0.3461	40.4336
3.6745E-04	53.0656	1.1155E-05	3.5466	0.5630	0.4370	0.0369	0.3461	40.4336
3.6745E-04	53.0656	1.1155E-05	3.5466	0.5840	0.4160	0.0422	0.3461	40.4336
3.6745E-04	53.0656	1.1155E-05	3.5466	0.5910	0.4090	0.0442	0.3461	40.4335
3.6745E-04	53.0656	1.1155E-05	3.5466	0.6010	0.3990	0.0477	0.3461	40.4336
3.6745E-04	53.0656	1.1155E-05	3.5466	0.6010	0.3990	0.0479	0.3461	40.4336

JACOB AND WEIMER DATA – CARBON POWDER IN GAS, P = 8280 kPa, Dp = 112 MICRONS (2 of 3).

EFFECTIVE VISCOSITY	EFFECTIVE DENSITY	VISCOSITY RATIO	DENSITY RATIO	DEL DENSITY RATIO	EFFECTIVE REYNOLD'S NUMBER	REQUIRED CLASSICAL N	REQUIRED NEW N	PROPOSED N
3.0102E-05	27.0186	0.6535	0.5598	0.6320	26.3305	3.8930	2.3278	2.1500
2.6971E-05	25.1864	0.6850	0.5712	0.6634	30.8245	3.8977	2.2642	2.1500
2.5444E-05	24.1465	0.7023	0.5781	0.6810	33.3686	3.9143	2.2383	2.1500
2.4969E-05	23.7999	0.7080	0.5805	0.6868	34.2170	3.9147	2.2240	2.1500
2.4317E-05	23.3047	0.7161	0.5840	0.6951	35.4269	3.8935	2.1811	2.1500
2.4317E-05	23.3047	0.7161	0.5840	0.6951	35.4269	3.8841	2.1717	2.1500

JACOB AND WEIMER DATA - CARBON POWDER IN GAS, P = 8280 kPa, Dp = 112 MICRONS (3 of 3).

PROPOSED Uo/Ut	R&Z N	R&Z Uo/Ut	AL-DIBOUNI N	AL-DIBOUNI Uo/Ut	FOSCOLO Uo/Ut	ACTUAL Uo/Ut
0.0919	3.0882	0.1375	3.3740	0.1144	0.0771	0.0820
0.1138	3.0882	0.1696	3.3740	0.1440	0.1048	0.1065
0.1277	3.0882	0.1899	3.3740	0.1629	0.1232	0.1218
0.1327	3.0882	0.1971	3.3740	0.1696	0.1299	0.1276
0.1399	3.0882	0.2075	3.3740	0.1794	0.1398	0.1377
0.1399	3.0882	0.2075	3.3740	0.1794	0.1398	0.1384

JACOB AND WEIMER DATA – CARBON POWDER IN GAS, P = 6210 kPa, Dp = 112 MICRONS (1 of 3).

PARTICLE DIAMETER ft	PARTICLE DENSITY lb/cu ft	GAS VISCOSITY lb/(ft s)	GAS DENSITY lb/cu ft	VOID FRACTION	SOLID FRACTION	INLET FLOW ft/s	TERMINAL VELOCITY ft/s	TERMINAL REYNOLD'S NUMBER
3.6745E-04	53.0656	1.1155E-05	2.6601	0.5210	0.4790	0.0239	0.3983	34.9009
3.6745E-04	53.0656	1.1155E-05	2.6601	0.5470	0.4530	0.0317	0.3983	34.9009
3.6745E-04	53.0656	1.1155E-05	2.6601	0.5680	0.4320	0.0366	0.3983	34.9009
3.6745E-04	53.0656	1.1155E-05	2.6601	0.5800	0.4200	0.0389	0.3983	34.9009
3.6745E-04	53.0656	1.1155E-05	2.6601	0.5960	0.4040	0.0432	0.3983	34.9009
3.6745E-04	53.0656	1.1155E-05	2.6601	0.6060	0.3940	0.0462	0.3983	34.9009
3.6745E-04	53.0656	1.1155E-05	2.6601	0.6030	0.3970	0.0502	0.3983	34.9009

JACOB AND WEIMER DATA - CARBON POWDER IN GAS, P = 6210 kPa, Dp = 112 MICRONS (2 of 3).

EFFECTIVE VISCOSITY	EFFECTIVE DENSITY	VISCOSITY RATIO	DENSITY RATIO	DEL DENSITY RATIO	EFFECTIVE REYNOLD'S NUMBER	REQUIRED CLASSICAL N	REQUIRED NEW N	PROPOSED N
3.0576E-05	26.8[illegible]43	[illegible]	0.5168	0.6277	27.0173	4.3117	2.6366	2.1500
2.8249E-05	25.4938	0.6715	0.5243	0.6499	30.2210	4.1937	2.4633	2.1500
2.6592E-05	24.4353	0.6891	0.5307	0.6676	32.8345	4.2212	2.4428	2.1500
2.5722E-05	23.8304	0.6990	0.5345	0.6777	34.3304	4.2715	2.4641	2.1500
2.4639E-05	23.0239	0.7120	0.5398	0.6910	36.3195	4.2905	2.4428	2.1500
2.4002E-05	22.5199	0.7201	0.5432	0.6992	37.5557	4.3026	2.4285	2.1500
2.4190E-05	22.6711	0.7177	0.5422	0.6968	37.1856	4.0947	2.2286	2.1500

JACOB AND WEIMER DATA – CARBON POWDER IN GAS, P = 6210 kPa, Dp = 112 MICRONS (3 of 3).

PROPOSED Uo/Ut	R&Z N	R&Z Uo/Ut	AL-DIBOUNI N	AL-DIBOUNI Uo/Ut	FOSCOLO Uo/Ut	ACTUAL Uo/Ut
0.0826	3.1340	0.1296	3.4361	0.1064	0.0701	0.0601
0.0962	3.1340	0.1510	3.4361	0.1258	0.0876	0.0797
0.1084	3.1340	0.1699	3.4361	0.1432	0.1039	0.0918
0.1158	3.1340	0.1814	3.4361	0.1539	0.1141	0.0976
0.1263	3.1340	0.1975	3.4361	0.1689	0.1288	0.1086
0.1332	3.1340	0.2081	3.4361	0.1789	0.1387	0.1159
0.1311	3.1340	0.2049	3.4361	0.1759	0.1357	0.1260

JACOB AND WEIMER DATA – CARBON POWDER IN GAS, P = 4140 kPa, Dp = 112 MICRONS (1 of 3).

PARTICLE DIAMETER ft	PARTICLE DENSITY lb/cu ft	GAS VISCOSITY lb/(ft s)	GAS DENSITY lb/cu ft	VOID FRACTION	SOLID FRACTION	INLET FLOW ft/s	TERMINAL VELOCITY ft/s	TERMINAL REYNOLD'S NUMBER
3.6745E-04	53.0656	1.1155E-05	1.7736	0.5040	0.4960	0.0255	0.4767	27.8503
3.6745E-04	53.0656	1.1155E-05	1.7736	0.5630	0.4370	0.0335	0.4767	27.8503
3.6745E-04	53.0656	1.1155E-05	1.7736	0.5400	0.4600	0.0365	0.4767	27.8503
3.6745E-04	53.0656	1.1155E-05	1.7736	0.5830	0.4170	0.0399	0.4767	27.8503
3.6745E-04	53.0656	1.1155E-05	1.7736	0.5720	0.4280	0.0442	0.4767	27.8503
3.6745E-04	53.0656	1.1155E-05	1.7736	0.5830	0.4170	0.0465	0.4767	27.8503

JACOB AND WEIMER DATA – CARBON POWDER IN GAS, P = 4140 kPa, Dp = 112 MICRONS (2 of 3).

EFFECTIVE VISCOSITY	EFFECTIVE DENSITY	VISCOSITY RATIO	DENSITY RATIO	DEL DENSITY RATIO	EFFECTIVE REYNOLD'S NUMBER	REQUIRED CLASSICAL N	REQUIRED NEW N	PROPOSED N
3.2294E-05	27.2144	0.6341	0.4583	0.6130	26.2953	4.2760	2.4724	2.1500
2.6971E-05	24.1882	0.6850	0.4740	0.6634	33.8385	4.6207	2.6625	2.1500
2.8843E-05	25.3679	0.6655	0.4676	0.6439	30.8747	4.1694	2.2751	2.1500
2.5513E-05	23.1624	0.7015	0.4799	0.6802	36.4145	4.5990	2.5813	2.1500
2.6297E-05	23.7266	0.6924	0.4766	0.6710	34.9991	4.2589	2.2744	2.1500
2.5513E-05	23.1624	0.7015	0.4799	0.6802	36.4145	4.3153	2.2976	2.1500

JACOB AND WEIMER DATA – CARBON POWDER IN GAS, P = 4140 kPa, Dp = 112 MICRONS (3 of 3).

PROPOSED Uo/Ut	R&Z N	R&Z Uo/Ut	AL-DIBOUNI N	AL-DIBOUNI Uo/Ut	FOSCOLO Uo/Ut	ACTUAL Uo/Ut
0.0666	3.2055	0.1112	3.5377	0.0886	0.0558	0.0534
0.0944	3.2055	0.1586	3.5377	0.1310	0.0932	0.0703
0.0827	3.2055	0.1387	3.5377	0.1131	0.0769	0.0766
0.1055	3.2055	0.1774	3.5377	0.1483	0.1093	0.0836
0.0993	3.2055	0.1668	3.5377	0.1386	0.1002	0.0926
0.1055	3.2055	0.1774	3.5377	0.1483	0.1093	0.0975

JACOB AND WEIMER DATA – CARBON POWDER IN GAS, P = 2070 kPa, Dp = 112 MICRONS (1 of 3).

PARTICLE DIAMETER ft	PARTICLE DENSITY lb/cu ft	GAS VISCOSITY lb/(ft s)	GAS DENSITY lb/cu ft	VOID FRACTION	SOLID FRACTION	INLET FLOW ft/s	TERMINAL VELOCITY ft/s	TERMINAL REYNOLD'S NUMBER
3.6745E-04	53.0656	1.1155E-05	0.8865	0.5180	0.4820	0.0271	0.4724	13.7949
3.6745E-04	53.0656	1.1155E-05	0.8865	0.5560	0.4440	0.0343	0.4724	13.7949
3.6745E-04	53.0656	1.1155E-05	0.8865	0.5630	0.4370	0.0385	0.4724	13.7949
3.6745E-04	53.0656	1.1155E-05	0.8865	0.5730	0.4270	0.0422	0.4724	13.7949
3.6745E-04	53.0656	1.1155E-05	0.8865	0.5720	0.4280	0.0470	0.4724	13.7949

JACOB AND WEIMER DATA – CARBON POWDER IN GAS, P = 2070 kPa, Dp = 112 MICRONS (2 of 3).

EFFECTIVE VISCOSITY	EFFECTIVE DENSITY	VISCOSITY RATIO	DENSITY RATIO	DEL DENSITY RATIO	EFFECTIVE REYNOLD'S NUMBER	REQUIRED CLASSICAL N	REQUIRED NEW N	PROPOSED N
3.0867E-05	26.0368	0.6465	0.3807	0.6251	22.5279	4.3436	2.2123	2.1500
2.7517E-05	24.0540	0.6791	0.3894	0.6575	26.3868	4.4656	2.1997	2.1500
2.6971E-05	23.6888	0.6850	0.3912	0.6634	27.0993	4.3665	2.0739	2.1500
2.6224E-05	23.1670	0.6933	0.3936	0.6718	28.1150	4.3379	2.0058	2.1500
2.6297E-05	23.2192	0.6924	0.3934	0.6710	28.0136	4.1318	1.8037	2.1500

JACOB AND WEIMER DATA – CARBON POWDER IN GAS, P = 2070 kPa, Dp = 112 MICRONS (3 of 3).

PROPOSED Uo/Ut	R&Z N	R&Z Uo/Ut	AL-DIBOUNI N	AL-DIBOUNI Uo/Ut	FOSCOLO Uo/Ut	ACTUAL Uo/Ut
0.0598	3.4388	0.1041	3.8879	0.0775	0.0532	0.0574
0.0749	3.4388	0.1328	3.8879	0.1021	0.0744	0.0727
0.0779	3.4388	0.1387	3.8879	0.1072	0.0789	0.0814
0.0824	3.4388	0.1473	3.8879	0.1147	0.0857	0.0893
0.0820	3.4388	0.1465	3.8879	0.1140	0.0850	0.0995

END

DATE FILMED

02 / 20 / 91